International
Progress Report

IPR-08-16

Äspö Hard Rock Laboratory

Temperature Buffer Test

Sensors data report
(Period 030326-080101)
Report No:11

Reza Goudarzi
Mattias Åkesson
Harald Hökmark

Clay Technology AB

January 2008

Svensk Kärnbränslehantering AB
Swedish Nuclear Fuel
and Waste Management Co

Box 250, SE-101 24 Stockholm
Phone +46 8 459 84 00

Report no.
IPR-08-16
No.
F12K
Author
Reza Goudarzi
Mattias Åkesson
Harald Hökmark
Date
January 2008
Checked by
Bertrand Vignal
Date
2008-08-11
Approved
Anders Sjöland
Date
2008-08-27

Äspö Hard Rock Laboratory

Temperature Buffer Test

Sensors data report (Period 030326-080101) Report No:11

Reza Goudarzi
Mattias Åkesson
Harald Hökmark

Clay Technology AB

January 2008

Keywords: Field test, Data, Repository, Bentonite, Rock, Canister, Measurements, Water pressure, Total pressure, Relative humidity, Temperature, Displacements

Résumé

TBT (Test de Barrière ouvragée en Température) est un projet mené par SKB et l'ANDRA, soutenu par ENRESA (en modélisation) et DBE (en instrumentation) qui vise à comprendre et modéliser le comportement thermo-hydro-mécanique de barrières ouvragées à base d'argile gonflante soumises à des températures élevées (> 100°C) pendant leur hydratation.

L'essai est conduit dans le HRL d'Äspö dans une alvéole verticale de 8 m de profondeur et 1,75 m de diamètre. Deux sondes chauffantes (chacune de 3 m de long et 0,6 m de diamètre) sont entourées d'argile gonflante, une bentonite MX 80 qui est confinée par un bouchon ancré dans la roche par 9 câbles. L'essai fonctionne depuis le printemps 2003. Les sondes ont été chauffées chacune à la puissance de 1500 W du 15ème au 1171ème jour et à 1600 W ensuite. Autour du 1700ème jour, les puissances ont été portées par paliers à 2000 W pour la sonde inférieure et à 1000 W pour la sonde supérieure.

Ce rapport présente les données de TBT enregistrées depuis son début le 26 mars 2003 jusqu'au premier janvier 2008.

Dans la bentonite la pression totale est mesurée en 29 points, la pression de pore en 8 points et l'humidité relative en 35 points. La température est mesurée en 92 points et aussi à l'emplacement de chaque capteur dont la mesure nécessite d'être compensée en température.

Des mesures additionnelles sont faites : température en 40 points dans la roche alentour, en 11 points à la surface et 6 à l'intérieur des sondes. La force de confinement est mesurée sur trois des neuf câbles. Le déplacement vertical du bouchon est mesuré en trois points. Le débit et la pression d'eau fournie au système sont également mesurés.

Des mesures de température et de pression dans les zones chaudes du test obtenues par des capteurs à fibres optiques installés par DBE sont rapportées dans l'Appendix B.

Globalement, le système de mesure et de transmission des données fonctionne bien et les capteurs fournissent des valeurs fiables. Une exception concerne la mesure d'humidité relative au droit de la sonde inférieure où plusieurs capteurs ne fonctionnent plus.

La densité des dispositifs de mesure de température par thermocouples à mi-hauteur de chaque sonde chauffante s'est révélée utile pour observer de façon qualitative les cycles saturation - désaturation. Dans la section du bas des indications claires de désaturation sont apparues très tôt dans l'expérience sur une zone annulaire de 0.15 m autour de la sonde chauffante. Cette partie se resature très lentement à l'heure actuelle.

La baisse de pression totale et la hausse de la succion observées entre le 225ème et le 370ème jour autour de la sonde supérieure ont été provoquées par un déficit en eau inattendu du haut du filtre de sable. Lorsque ce filtre a été de nouveau rempli, la pression totale dans la bentonite s'est rétablie et la succion s'est remise à décroître.

Dans la bentonite, la plupart des mesures d’humidité ne sont plus significatives, car le matériau est désormais trop proche de la saturation. Cependant dans la section supérieure (au Ring 9), le fait que les pressions de pore s’équilibrent avec la pression d’eau du filtre de sable indique une saturation de l’argile.

Ce filtre de sable disposé entre la roche et la colonne de bentonite permet une alimentation artificielle du système en eau. Plus de la totalité de l'eau théoriquement nécessaire au remplissage du filtre et à la saturation de la bentonite a été injectée, ce qui montre que le système n’est pas hydrauliquement clos mais fuit dans l’environnement rocheux (EDZ). La pression croissante nécessaire pour maintenir le débit d'injection prouvait la fragilité du système d’injection (colmatage des embouts des injecteurs). De ce fait, une action de décolmatage a été entreprise en 2007 avec injection d’eau déminéralisée à la place de l’eau du site utilisée depuis le début du test. L’action a porté ses fruits et rendu possible le contrôle de la pression hyraulique dans le filtre de sable.

Abstract

TBT (Temperature Buffer Test) is a joint project between SKB/ANDRA and supported by ENRESA (modeling) and DBE (instrumentation), which aims at understanding and modeling the thermo-hydro-mechanical behavior of buffers made of swelling clay submitted to high temperatures (over 100°C) during the water saturation process.

The test is carried out in Äspö HRL in a 8 meters deep and 1.75 m diameter deposition hole, with two canisters (3 m long, 0.6 m diameter), surrounded by a MX 80 bentonite buffer and a confining plug on top anchored with 9 rods. It was installed during spring 2003. The canisters were heated with 1500 W power from day 15 to day 1171, when the power was raised to 1600 W. Around day 1700, the power was by steps raised in the lower heater to 2000 W and reduced in the upper heater to 1000 W.

This report presents data from the measurements in the Temperature Buffer Test from 030326 to 080101 (26 March 2003 to 01 January 2008).

The following measurements are made in the bentonite: Temperature is measured in 92 points, total pressure in 29 points, pore water pressure in 8 points and relative humidity in 35 points. Temperature is also measured by all gauges as an auxiliary measurement used for compensation.

The following additional measurements are done: Temperature is measured in 40 points in the rock, in 11 points on the surface of each canister and in 6 points inside each canister. The force on the confining plug is measured in 3 of the 9 rods and its vertical displacement is measured in three points. The water inflow and water pressure in the outer sand filter is also measured.

Temperature and total pressure measurements obtained in the hot parts of the system with fiber optic sensors installed by DBE are reported in Appendix B.

A general conclusion is that the measuring systems and transducers work well and almost all sensors deliver reliable values. An exception is the Relative Humidity sensors in the high temperature area around the lower canister, where sensors have failed.

The dense arrays of thermocouples at the mid-height of the two heaters appear to be useful for examining the dehydration/hydration process qualitatively. In the lower section there are clear signs of early dehydration in a 0.15 m annular zone around the heater. Resaturation of this part is now slowly in progress.

In the bentonite buffer, most humidity sensors measurements are now insignificant, the material being too close to saturation. However in the upper section (Ring 9), the fact that pore pressure start equilibrating with the water pressure in the sand slot indicates a quasi saturation of the clay material.

This sand slot set between the bentonite column and the surrounding rock is used for artificial wetting. More than the water theoretically needed to fill up the sand slot and to saturate the bentonite has already been injected, which proves that the system is not hydraulically closed but leaks towards the rock (EDZ). The high sand slot injection pressure required to maintain the inflow shows the weakness of the injection system

(clogging of the filter tips). Since the last report, an unclogging action has been taken by injecting demineralised water instead of ground water, as it was done since the beginning of the experiment. This action proved successful, and it is now possible to maintain the hydraulic pressure in the filter around 4 bar absolute.

The decrease in total pressure and increase in suction that was recorded around the upper canister from day 225 to day 370 has been caused by an unexpected lack of water supply in the upper part of the sand slot. When this slot got filled again with water, the total pressure resumed and increased and the suction decreased again.

Sammanfattning

TBT (Temperature Buffer Test) är ett gemensamt SKB/ANDRA projekt med deltagande av ENRESA (modellering) och DBE (instrumentering). Syftet är att öka förståelsen för de termiska, hydrauliska och mekaniska processerna i en buffert gjord av svällande lera som utsätts för höga temperaturer (över 100 ˚C) under vattenmättnadsfasen och att kunna modellera dessa processer.

Försöket görs på 420-metersnivån i Äspö HRL i ett 8 m djupt deponeringshål med diametern 1,75 m, där två kapslar, omgivande bentonitbuffert och en ovanliggande plugg, som förankrats med 9 stag, installerades våren 2003. Kapslarna värmdes med en effekt på 1500 W från dag 15 till dag 1171. Effekten på kapslarna ökades till 1600 W dag 1171. Från dag 1700 effekten har stegvis ökad i nedre kapsel till 2000W och samtidig stegvis minskad i övre kapsel till 1000 W.

I denna rapport presenteras data från mätningar i TBT under perioden 030326-080101.

Följande mätningar görs i bentoniten: Temperaturen mäts i 92 punkter, totaltryck i 29 punkter, porvattentryck i 8 punkter och relativa fuktigheten i 35 punkter. Temperaturen mäts även i alla relativa fuktighetsmätare, för att kompensera för temperaturens inverkan på mätresultaten.

Följande övriga mätningar görs: Temperaturen mäts i 40 punkter i berget, i 11 punkter på ytan av varje kapsel och i 6 punkter inne varje kapsel. Kraften på den ovanliggande pluggen mäts i 3 av de 9 stagen och vertikala förskjutningen av pluggen mäts i tre punkter. Vatteninflödet och vattentrycket i den yttre sandfyllda spalten mäts också.

Temperaturer och totaltryck registrerade med fiberoptiska sensorer, installerade av DBE, rapporteras i Appendix B.

En generell slutsats är att mätsystemen och givarna fungera bra och i stort sett alla givare leverar pålitliga mätvärden. Ett undantag är mätningarna av relativa fuktigheten i högtemperaturområdet runt den nedre kapseln, där ett flertal givare inte fungerar.

De täta linjerna av termoelement vid de två värmarnas höjdcentrum visar sig vara användbara för att undersöka torkning/mättnadsprocessen kvalitativt. I den undre sektionen finns det tydliga tecken på uttorkning inom ett avstånd av 0,15 m från värmarytan. En långsam återmättnad av denna zon pågår

Resultaten från de flesta relativ fuktighetsmätarna är nu mindre signifikanta, eftersom bentonitbufferten är för nära mättnad. Portrycksgivarna i Ring 9 börjar emellertid komma i jämvikt med vattentrycket i sandfiltret, vilket indikerar att full mättnad har uppnåtts i denna del.

Sandfiltret mellan bentonitblocken och omgivande berg används för artificiell bevätning. Mer vatten än den teoretiska mängden som behövs för att mätta hela systemet har nu tillförts. Detta visar att systemet inte är hydrauliskt stängt, utan att det finns ett läckage (sannolikt ut i berget). Det injekteringstryck i sandspalten som fordras för att upprätthålla inflödet visar på en svaghet hos injekteringssystemet. Detta beror sannolikt på en igensättning av filterspetsarna.

Den sänkning av totaltrycket och höjning av buffertens *suction* som noterats runt den översta kapseln mellan dag 225 och dag 370 orsakades av en brist på vattentillgång i övre delen av sandfiltret. När sandfiltret vattenfylldes och trycksattes höjdes totaltrycket åter medan buffertens *suction* minskade.

Contents

1 Introduction

The installation of the Temperature Buffer Test was made during spring 2003 in Äspö Hard Rock Laboratory, Sweden.

The Temperature Buffer Test, TBT, is a full-scale experiment that ANDRA and SKB carry out at the SKB Äspö Hard Rock Laboratory. In addition ENRESA supports TBT with THM modelling and DBE has installed a number of optic pressure sensors.

The test aims at understanding and modelling the thermo-hydro-mechanical behaviour of buffers made of swelling clay submitted to high temperatures (over 100°C) during the water saturation process. No other full scales tests have been carried out with buffer temperatures exceeding 100°C so far.

The test consists of a full-scale KBS3 deposition hole, 2 steel canisters equipped with electrical heaters simulating the power of radioactive decay and a mechanical plug at the top. Figure 1-1 shows the layout and denomination of blocks and canisters. The canisters are embedded in dense clay buffer consisting of blocks (cylindrical and ring shaped) of compacted bentonite powder.

An artificial water pressure is applied in the outer slot between the buffer and the rock, which is filled with compacted sand and functions as a filter.

The upper canister is surrounded by sand in order to reduce the temperature in the bentonite.

The buffer material is instrumented with pressure cells (total and water pressure), thermocouples and moisture gauges. Thermocouples are also installed in the rock.

A retaining plug is built in order to confine the buffer swelling.

Measured results and general comments concerning the collected data are given in chapter 2. A test overview with the positions of the measuring points and a brief description of the instruments are presented in chapters 3 and 4. Finally analyses and discussions of the results are given in chapter 5.

In general the data in this report are presented in diagrams covering the time period 030326 to 080101[1]. The time axis in the diagrams represents days from 030326. The diagrams are attached in Appendix A.

Results regarding the fibre optic sensing system are attached in Appendix B.

The results in Appendix B correlate as a trend with the other type of the sensor but the values seem to be not reliable.

[1] YYMMDD (Swedish way of expressing dates implying that the first two numbers are the year, the next two numbers are the month abd the final two numbers are the date)

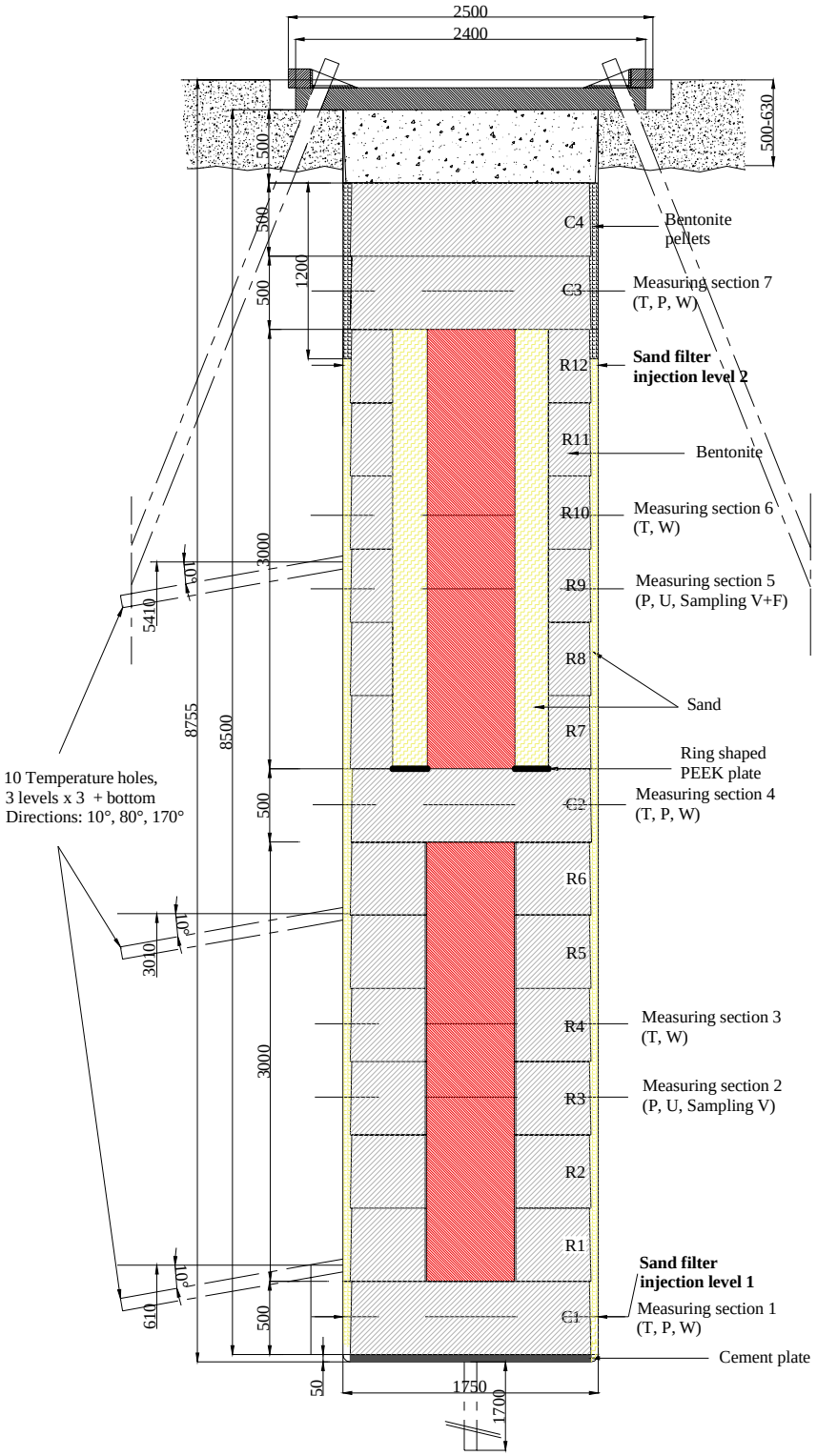

Figure 1-1*. Schematic view showing the layout of the experiment and the numbering of bentonite blocks. The lower heater is denominated No. 1 and the upper heater is No. 2.*

2 Comments

2.1 General

In this chapter short comments on general trends in the measurements are given. Sensors that are not delivering reliable data or no data at all are noted and comments on the data in general are given but no evaluation or comparison with predictions will be given here.

The heating of both canisters started with an initially applied constant power of 900 W on 030326. This date is also marked as start date. The power was raised to 1200 W on 030403. The power was further raised to 1500 W on 030410. Several power failures have occurred. The power was raised to 1600 W at 20060609 (day 1171).

The power in heater 1 was raised to 2000 W during three weeks (100 W/week) from 20071115 to 20071206 (day 1695-1716).

The power in heater 2 was decreased to 1000 W during five weeks (100 W/week) from 20071115 to 20071220 (day 1695-1730).

Important events and dates are shown in Table 2-1.

Table 2-1. Key dates for TBT.

Activity	Date (time)	Day No.
900 W power applied	030326	0
Start water filling of filter	030327	1
1200 W power applied	030403	8
1500 W power applied	030410	15
Finished water filling	~030604	~70
Power failure heater 1	030423 (~20.00)-030424 (~10.00)	27-28
Power failure heater 1	030527 (~01.00)-030527 (~12.00)	62
Power failure heater 1	030603 (~12.00)-030603 (~14.00)	69
Power failure heater 1	030606 (~19.00)-030609 (~10.00)	72-75
Power failure heater 1	030612 (~12.00)-030612 (~14.00)	78
Power failure heaters 1 and 2	030923 (~12.00[1)])-030923 (~18.00[1)])	181
Power failure heaters 1 and 2	031028 (~18.00[1)])-031029 (~11.00[1)])	216
Injection pump replaced by gas tube	031104	223
Power failure heater 1	040120 (~16.00)-040120 (~19.00)	300
Power failure heater 2	040120 (~18.00)-040120 (~20.00)	300
Filling and pressurisation of the sand filter also through the upper tubes	040406	377

Flushing and pressurisation of filters through both upper and lower tubes (160 kPa)	040615-040616	448-449
Pressurisation of filters through both upper and lower tubes	041011-041014	565-568
Filling and pressurisation of the sand filter through AS205 and AS207	041014	568
Filling and pressurisation of the sand filter through AS201, AS202, AS204, AS205, AS206 and AS208	041110	595
Power failure heater 2 50 w more power	050629-050706	826- 833
Filling and pressurisation of the sand filter through AS201, AS203, AS204, AS205, AS207 and AS208	050728	856
Water filling of filter mats. Airvents AS212-AS215 closed. AS209 connected to artificial saturation. AS210 connected to artificial saturation.	051209 051212	989 992
Back flushing of filters through both upper and lower tubes. Only AS203 is still closed.	060517-060614	1148- 1176
1600 W power applied	060609-	1171-
Power failure heater 1	060903-060904	1257-1258
Change in water quality for injection	070417	1483
1700 W power applied heater 1	071115-071122	1695-1702
1500 W power applied heater 2	071115-071122	1695-1702
1800 W power applied heater 1	071122-071129	1702-1709
1400 W power applied heater 2	071122-071129	1702-1709
1900 W power applied heater 1	071129-071206	1709-1716
1300 W power applied heater 2	071129-071206	1709-1716
2000 W power applied heater 1	071206-	1716-
1200 W power applied heater 2	071206-071213	1716-1723
1100 W power applied heater 2	071213-071220	1723-1730
1000 W power applied heater 2	071220-	1730-

1) The duration of the power loss is not known since no data was recorded between the times noted.

The water filling was done through four tubes leading to the bottom of the sand filter. The filling was slow due to flow resistance in the sand and the rate was increased by pressurizing the water (see chapter 2.6). The filling was completed after 60-80 days. The water pressure in the bottom of the sand filter has been kept with periodical interruptions (see chapter 2.6) but the valves to the 4 upper tubes leading out water from the top of the sand filter have been open at all times until 040615.

On day 377 (040406) water was supplied to the sand filter also through the tubes leading to the top of the sand filter and a small pressure applied. On days 448-449 the filters were flushed and a water pressure of 160 kPa was applied on the sand filter through both the top tubes and the bottom tubes.

This report is the elevenths one and covers the results up to 080101.

2.2 Total pressure, Geokon (App. A, pages 53-61)

The measured pressure ranges from 5.8 to 9.3 MPa. The start of the pressure increase takes place shortly after the water filling has reached the level of the different transducer.

Notable is that all transducers in ring 9 around heater 2 except the one at the rock are recording decreasing total pressure in a period between day ~230 and day ~370. The reason for this and other observations are discussed in chapter 5.

The pressure increase by sensor placed in Cyl.3 at 20051209 (day 989) due to water filling of the filter mats between Cyl.3 and Cyl.4.

Eleven transducers are out of order.

2.3 Suction, Wescore Psychrometers (App. A, pages 62-66)

Wescor psychrometers are only working at suction below ~7000 kPa, which correspond to high relative humidity (higher than 95%).

Ten of twelve transducers have yielded interpretable values, which means that they are close to water saturation. Notable is that two transducers around heater 2 are yielding increasing suction (drying) during a period of about 80 days, which is consistent with the measured decrease in total pressure. On the other hand the suction of those transducers is again dropping in suction during the last 2 months, which is also in consistence with the total pressure observations.

WB233 placed in Cyl.3 begun to react during the previous measuring period due to water injection to the mat between Cyl.3 and Cyl.4.

2.4 Relative humidity, Vaisala and Rotronic (App. A, pages 67-72)

Relative humidity and temperature measured with Vaisala and Rotronic transducers are shown on pages 68-73. For most transducers RH starts to increase just after the filling of water has reached the sensor level. Only one sensor in the buffer shows an obvious reduction in RH, namely WB206, which is located in the high temperature zone close to the lower heater. Sensors WB221 and WB222 are located in the sand in contact with the bentonite rings 9 and 10. The high initial RH measured by WB221 may be caused by the free water in the sand that had the water content of about 1% from start.

All operational RH sensors now indicate 100%.

8 of 23 sensors are presently out of order for other reasons than high degree of saturation. Four of them are placed in ring 4.

2.5 Pore water pressure, Geokon (App. A, pages 73-74)

All sensor placed in Ring 9 show a decreasing of pore water pressure during this measuring period due to reduction of power in heater 2 from 1600 W to 1000 W. Pore pressure in Ring 9 is about 0.0 MPa to 0.4 MPa at the end of this measuring period.

All sensor placed in Ring 3 show a increasing of pore water pressure during this measuring period due to raising of power in heater 1 from 1600 W to 2000 W. Pore pressure in Ring 3 is about 0.1 MPa to 0.2 MPa at the end of this measuring period.

2.6 Water flow and water pressure in the sand (App. A, pages 75-77)

Water filling and measurement of water inflow into the sand started on 030327. The total inflow to the sand has since that date been 3811 litres. The total volume of voids in the sand filter was initially about 790 litres. The inflow rate has been in average about 2.3 l/day since day 110. The inflow rate has been in average about 1.52 l/day in the last sex month.

There was also an outflow that started after completed filling since the valves from the top of the sand filter was kept open. The outflow stopped rather early and the total outflow of water has been 44 litres.

The water injection pressure upstream the filter tips is shown on page 78. The water pressure was increased to 800 – 900 kPa during the first 50 days and then kept “constant” until day ~370. However, problems with the water pump have lead to many interruptions in the applied pressure. At day 377 the water pressure was reduced in connection with the start of water supply also from the tubes leading to the top of the filter.

It should be noted that the actual water pressure in the sand filter is only measured at those injection points that are closed to the atmosphere and not pressurized, at present (2008-01-01) points AS203 and AS207.

Water inflow to sand shield has started on 20070509.The cumulative inflow into the sand was 250 liter on 080101.

2.7 Forces on the plug (App. A, page 78)

The forces on the plug have been measured since 030404.The total force is about 14100 kN at 080101. The influence of the additional water supply from the upper tubes after ~370 days is clearly seen.

During the first about 15 days the plug was only fixed with 3 rods. When the total force exceeded 1100 kN the rest of the 9 rods were fixed in a prescribed manner. This procedure took place 10-11 April 2003 that is 15-16 days after test start. From that time only every third anchor is measured and the results should thus be multiplied with 3. The diagram shows both the actual measurements and after multiplication with 3.

One of the force transducers displayed some irregular trends during last and this measuring period.

2.8 Displacement of the plug (App. A, page 79)

The three displacement gauges were placed and started to measure displacements from 030409 (day 14) (except for zero reading that was done day 0). One of them (DP201) did not work well and was replaced on 030923 with a new transducer.

Transducer DP203 is out of order.

The measured displacements are in good agreement with the measured forces.

2.9 Canister power (App A, page 80-81)

The heating of both canisters started with an initially applied constant power of 900 W on 030326 and was raised to 1500 W according to Table 2-1. Only one out of three heaters in each canister is presently used (RAH1 and RAH2).

The failure in one of heater (RCH2) in canister 2 caused increasing of power with 50 W on 2005-06-29 to 2005-07-05.

The power has increased to 1600 W in both canisters on 2006-06-09 (day1171).

The power in heater 1 was raised in stages to 2000 W (100 W / week) from 20071115 to 20071206 (day 1695-1716).

The power in heater 2 was decreased in stages to 1000 W (100 W / week) from 20071115 to 20071220 (day 1695-1730).

2.10 Temperature in the buffer (App. A, pages 82-87)

Temperature is measured in a large number of points. The plotting of results is done so that the effect of wetting and cracking can be traced, since sensors placed close to each other are collected in the same diagrams.

The highest measured temperature in the bentonite is 156 °C by sensor TB215 located in the midplane of canister 1 at the distance 15 mm from the canister surface. The corresponding temperature on the canister surface is 159 °C, which shows that the temperature drop at the slot between the canister and the bentonite ring is very small.

Temperature is also measured (TB254, TB255 and TB256) in the sand around canister 2 (page 86), where the temperature drop is rather large (~2.5 °C/cm).

The increase in temperature with about one degree °C seen in the upper part of the buffer in the beginning of June (day ~435) is judged to be caused by the increase in tunnel air temperature that takes place in the summer (page 88).

On day ~335 three additional transducers (TB290, TB291 and TB292) placed in Ring 12 were connected to the data scanner and are reported on page 87. One of them was out of order from start.

The increase in temperature in the beginning of June 2006 (day ~1171) depends to increasing of power with 100 W.

The increase in temperature around canister 1 during this measuring period from the middle of November 2007 (day ~1695) depends to increasing of power with 400 W.

The decrease in temperature around canister 2 during this measuring period from the middle of November 2007 (day ~1695) depends to decreasing of power with 600 W.

10 of 92 transducers are out of order.

2.11 Temperature in the rock (App. A, pages 88-91)

The maximum temperature measured in the rock (75 degrees) is measured in the central section on the surface of the deposition hole. The deviation from axial symmetry of the temperature measured in the rock is caused by the influence from the heating of the neighbouring Canister Retrieval Test.

On October 11 (day 930) the power in Canister Retrieval Test was switched off.

The large changing of temperature in the rock during this measuring period (from day 1695) depends to changing of power from day 1695.

2.12 Temperature on the canister surface (App. A, pages 92-93)

The maximum temperature measured on the surface of canister 1 is about 159 °C and on the surface of canister 2 about 93 °C on 080101. There are strong temperature differences in the canisters, both radial and axial. The highest measured difference on the surface is 23 °C on canister 1 and 25 °C on canister 2.

The steady increase in temperature of heater 1 has turned into a slow decrease. The temperature of heater 2 has decreased since day 50.

The decreasing temperatures on the surface of canister 2 on day 1505 were a result of 30 litres of water injection into the sand shield.

One sensor (TH1 SE0) has stopped to work since day1234.

2.13 Temperature inside the canister (App. A, pages 94-95)

The maximum temperature measured inside canister 1 is about 184 °C and about 114 °C in canister 2 on 080101.

The very high value from sensor TH2 SI3 0° is not reliable before day 1080.

3 Coordinate system

Measurements are done in 7 measuring sections placed on different levels (see Figure 1-1). On each level, sensors are placed in eight main directions A, AB, B, BC, C, CD, D and DA according to Figure 3-1. Direction A and C are placed in the tunnels axial direction with A headed against the end of the tunnel i.e. almost to the South (see Figure 1-1, 3-1 and 4-1). The angle α is counted anti-clockwise from direction A. The z-coordinate is counted from the bottom of the deposition hole (the cement base).

The bentonite blocks are called cylinders and rings. The cylinders are numbered C1-C4 and the rings R1-R12 respectively (see Figure 1-1).

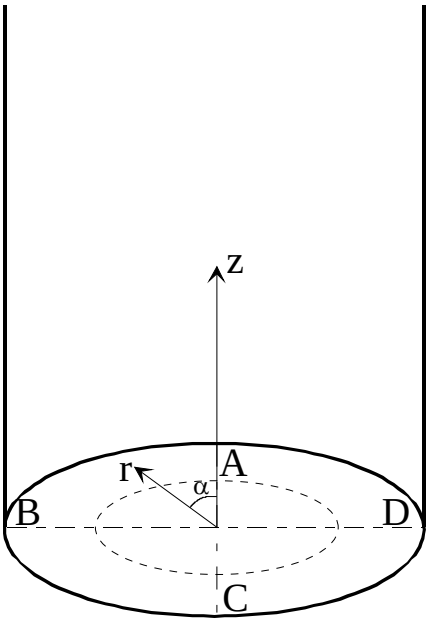

Figure 3-1. *Figure describing the coordinate system used when determining the instrument positions.*

4 Location of instruments

4.1 Brief description of the instruments

The different instruments that are used in the experiment are briefly described in this chapter. For additional information, see /4-1/.

Measurements of temperature

Buffer

Thermocouples from Pentronic have been installed for measuring temperature in the buffer. Measurements are done in 92 points in the test hole. In addition, temperature gauges are built in into the capacitive relative humidity sensors (23 sensors) as well as in the pressure gauges of vibrating wire type (37 gauges). Temperature is also measured in the psychrometers.

Canister

Temperature is measured in 11 points on the surface of the each canister. Temperature is also measured in each canister insert in 6 points.

Rock

Temperature in the rock and on the rock surface of the hole is measured in 40 points with thermocouples from Pentronic.

Measurement of total pressure in the buffer

Total pressure is the sum of the swelling pressure and the pore water pressure. It is measured with Geokon total pressure cells with vibrating wire transducers. 29 cells of this type have been installed.

Measurement of pore water pressure in the buffer

Pore water pressure is measured with Geokon pore pressure cells with vibrating wire transducer. 8 cells of this type have been installed.

Measurement of the water saturation process

The water saturation process is recorded by measuring the relative humidity in the pore system, which can be converted into water ratio or total suction (negative water pressure). The following techniques and devices are used:

- Vaisala relative humidity sensor of capacitive type. 29 cells of this type have been installed. The measuring range is 0-100 % RH.
- Wescor psychrometers measure the dry and the wet temperature in the pore system. The measuring range is 95.5-99.6 % RH corresponding to the pore water pressure -0.5 to -6MPa. 12 cells of this type have been installed.

Measurements of forces on the plug

The force on the plug caused by the swelling pressure of the bentonite is measured in 3 of the 9 anchors. The force transducers are of the type GLÖTZL.

Measurements of plug displacement

Due to straining of the anchors the swelling pressure of the bentonite will cause not only a force on the plug but also displacement of the plug. The displacement is measured in three points with transducers of the type LVDT with the range 0 – 50 mm.

Measurement of water flow into the sand

An artificial water pressure is applied in the outer slot, which is filled with sand. Titanium tubes equipped with filter tips are placed in the sand on two levels, 250 mm and 6750 mm from bottom (four at each level).

4.2 Strategy for describing the position of each device

Every instrument is named with a unique name consisting of 1 letter describing the type of measurement, (T-Temperature, P-Total Pressure, U-Pore Pressure, W-Relative Humidity, C-Chemical sampling, D-Displacement and A-Artificial water), 1 letter describing where the measurement takes place (B-Buffer, H-Heater, S-Sand, R-Rock and P-plug), 1 figure denoting the deposition hole (1 is used for the CRT test and 2 is used for this experiment), and 2 figures specifying the position in the buffer according to a separate list (see Table 4-1 to 4-7). Every instrument position is described with three coordinates according to Figure 3-1. The r-coordinate is the horizontal distance from the centre of the hole and the z-coordinate is the height from the bottom of the hole (the block height is set to 500mm). The coordinate is the angle from the vertical direction A (almost South).

The position of each instrument is described in the legend in the diagrams according to the following strategy:

Buffer: Three positions according to Figure 3-1: ($z \setminus \alpha \setminus r$) meaning ($z$-coordinate in m. from the bottom \ the angle α \ the radius in m.)

The cells measuring total pressure have been installed in three different directions in order to measure the radial stress (R), the axial stress (A) and the tangential stress (T). The direction of the pressure measurement is added in Table 4-2 and in the legend for each cell.

Rock: Three positions with the following meaning: (distance in meters from the bottom \ α according to Fig 3-1 \ distance in meters from the rock surface)

The bentonite blocks are called cylinders and rings. The cylinders are numbered C1-C4 and the rings R1-R12 respectively (Figure 1-1).

Canister: The denomination of the instruments in the canister differs a little from the other instruments. At first there are two letters and one figure describing the type of measurement and the place (TH for temperature and heater) and which heater (1 for lower heater and 2 for upper). Then there are again two letters describing if it is an external or internal sensor (SE or SI) and one figure describing the position on the canister (0-4 according to Figure 4-2). Finally the angle clockwise from direction A is written.

4.3 Position of each instrument in the bentonite

Measurements are done in 7 measuring sections placed on different levels (see Figure 1-1). On each level, sensors are placed in eight main directions A, AB, B, BC, C, CD, D and DA according to Figure 4-1. The bentonite blocks are called cylinders and rings. The cylinders are numbered C1-C4 and the rings R1-R12 respectively (see Figure 1-1).

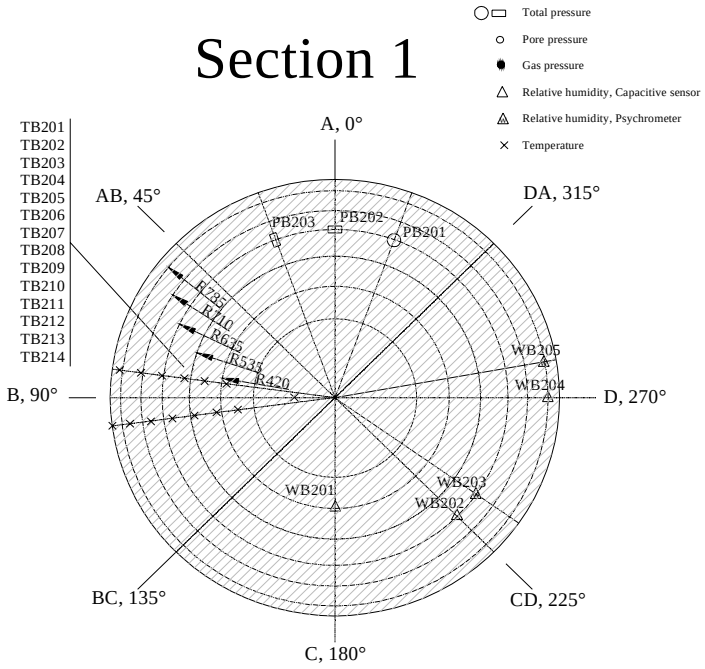

Figure 4-1. *Schematic view, showing the main directions of the instrument positioning. The drawing shows the instrumentation in measuring section 1.*

An overview of the positions of the instruments is shown in Fig 1-1 and 4-1. Exact positions are described in Tables 4-1 to 4-6. These tables have been updated since the last report and the measured exact position of the transducers have been inserted.

The instruments are located in three main levels in each instrumented block, the surface of the block (only total pressure cells measuring the horizontal pressure) and 50 mm and 250 mm from the upper block surface. The thermocouples and the total pressure cells are placed in the 50 mm level by practical reasons and the other sensors in the 250 mm level.

Table 4-1. Numbering and position of instruments for measuring temperature (T).

Type and number	Measuring section	Block	Instrument position in block				Instrument Fabricate
			Direction	α	r	z	
				degree	m	m	
TB201	1	Cyl. 1	B	90	0,150	0,452	Pentronic
TB202	1	Cyl. 1	B	95	0,360	0,452	Pentronic
TB203	1	Cyl. 1	B	85	0,400	0,452	Pentronic
TB204	1	Cyl. 1	B	95	0,440	0,452	Pentronic
TB205	1	Cyl. 1	B	85	0,480	0,452	Pentronic
TB206	1	Cyl. 1	B	95	0,520	0,452	Pentronic
TB207	1	Cyl. 1	B	85	0,560	0,452	Pentronic
TB208	1	Cyl. 1	B	95	0,600	0,452	Pentronic
TB209	1	Cyl. 1	B	85	0,640	0,452	Pentronic
TB210	1	Cyl. 1	B	95	0,680	0,452	Pentronic
TB211	1	Cyl. 1	B	85	0,720	0,452	Pentronic
TB212	1	Cyl. 1	B	95	0,760	0,452	Pentronic
TB213	1	Cyl. 1	B	85	0,800	0,452	Pentronic
TB214	1	Cyl. 1	B	95	0,840	0,452	Pentronic
TB215	3	Ring 4	B	97,5	0,320	2,469	Pentronic
TB216	3	Ring 4	B	82,5	0,360	2,469	Pentronic
TB217	3	Ring 4	B	97,5	0,390	2,469	Pentronic
TB218	3	Ring 4	B	92,5	0,420	2,469	Pentronic
TB219	3	Ring 4	B	87,5	0,435	2,469	Pentronic
TB220	3	Ring 4	B	82,5	0,450	2,469	Pentronic
TB221	3	Ring 4	B	97,5	0,465	2,469	Pentronic
TB222	3	Ring 4	B	92,5	0,480	2,469	Pentronic
TB223	3	Ring 4	B	87,5	0,495	2,469	Pentronic
TB224	3	Ring 4	B	82,5	0,510	2,469	Pentronic
TB225	3	Ring 4	B	97,5	0,525	2,469	Pentronic
TB226	3	Ring 4	B	92,5	0,540	2,469	Pentronic
TB227	3	Ring 4	B	87,5	0,555	2,469	Pentronic
TB228	3	Ring 4	B	82,5	0,570	2,469	Pentronic
TB229	3	Ring 4	B	97,5	0,585	2,469	Pentronic
TB230	3	Ring 4	B	92,5	0,600	2,469	Pentronic
TB231	3	Ring 4	B	87,5	0,615	2,469	Pentronic
TB232	3	Ring 4	B	82,5	0,630	2,469	Pentronic
TB233	3	Ring 4	B	97,5	0,645	2,469	Pentronic
TB234	3	Ring 4	B	92,5	0,660	2,469	Pentronic
TB235	3	Ring 4	B	87,5	0,690	2,469	Pentronic
TB236	3	Ring 4	B	92,5	0,720	2,469	Pentronic
TB237	3	Ring 4	B	87,5	0,750	2,469	Pentronic
TB238	3	Ring 4	B	92,5	0,780	2,469	Pentronic
TB239	3	Ring 4	B	87,5	0,810	2,469	Pentronic
TB240	4	Cyl. 2	B	90	0,150	3,983	Pentronic
TB241	4	Cyl. 2	B	95	0,360	3,983	Pentronic
TB242	4	Cyl. 2	B	85	0,400	3,983	Pentronic
TB243	4	Cyl. 2	B	95	0,440	3,983	Pentronic
TB244	4	Cyl. 2	B	85	0,480	3,983	Pentronic
TB245	4	Cyl. 2	B	95	0,520	3,983	Pentronic

Type and number	Measuring section	Block	Instrument position in block				Instrument Fabricate
			Direction	α	r	z	
				degree	m	m	
TB246	4	Cyl. 2	B	85	0,560	3,983	Pentronic
TB247	4	Cyl. 2	B	95	0,600	3,983	Pentronic
TB248	4	Cyl. 2	B	85	0,640	3,983	Pentronic
TB249	4	Cyl. 2	B	95	0,680	3,983	Pentronic
TB250	4	Cyl. 2	B	85	0,720	3,983	Pentronic
TB251	4	Cyl. 2	B	95	0,760	3,983	Pentronic
TB252	4	Cyl. 2	B	85	0,800	3,983	Pentronic
TB253	4	Cyl. 2	B	95	0,825	3,983	Pentronic
TB254	6	Ring 10	B	90	0,343	6,056	Pentronic
TB255	6	Ring 10	B	90	0,400	6,056	Pentronic
TB256	6	Ring 10	B	90	0,463	6,056	Pentronic
TB257	6	Ring 10	B	97,5	0,540	6,006	Pentronic
TB258	6	Ring 10	B	92,5	0,555	6,006	Pentronic
TB259	6	Ring 10	B	87,5	0,570	6,006	Pentronic
TB260	6	Ring 10	B	82,5	0,585	6,006	Pentronic
TB261	6	Ring 10	B	97,5	0,600	6,006	Pentronic
TB262	6	Ring 10	B	92,5	0,615	6,006	Pentronic
TB263	6	Ring 10	B	87,5	0,630	6,006	Pentronic
TB264	6	Ring 10	B	82,5	0,645	6,006	Pentronic
TB265	6	Ring 10	B	97,5	0,660	6,006	Pentronic
TB266	6	Ring 10	B	92,5	0,675	6,006	Pentronic
TB267	6	Ring 10	B	87,5	0,690	6,006	Pentronic
TB268	6	Ring 10	B	82,5	0,705	6,006	Pentronic
TB269	6	Ring 10	B	97,5	0,720	6,006	Pentronic
TB270	6	Ring 10	B	92,5	0,735	6,006	Pentronic
TB271	6	Ring 10	B	87,5	0,750	6,006	Pentronic
TB272	6	Ring 10	B	82,5	0,765	6,006	Pentronic
TB273	6	Ring 10	B	97,5	0,780	6,006	Pentronic
TB274	6	Ring 10	B	92,5	0,795	6,006	Pentronic
TB275	6	Ring 10	B	87,5	0,810	6,006	Pentronic
TB276	7	Cyl. 3	B	90	0,150	7,524	Pentronic
TB277	7	Cyl. 3	B	95	0,360	7,524	Pentronic
TB278	7	Cyl. 3	B	85	0,400	7,524	Pentronic
TB279	7	Cyl. 3	B	95	0,440	7,524	Pentronic
TB280	7	Cyl. 3	B	85	0,480	7,524	Pentronic
TB281	7	Cyl. 3	B	95	0,520	7,524	Pentronic
TB282	7	Cyl. 3	B	85	0,560	7,524	Pentronic
TB283	7	Cyl. 3	B	95	0,600	7,524	Pentronic
TB284	7	Cyl. 3	B	85	0,640	7,524	Pentronic
TB285	7	Cyl. 3	B	95	0,680	7,524	Pentronic
TB286	7	Cyl. 3	B	85	0,720	7,524	Pentronic
TB287	7	Cyl. 3	B	95	0,760	7,524	Pentronic
TB288	7	Cyl. 3	B	85	0,800	7,524	Pentronic
TB289	7	Cyl. 3	B	95	0,825	7,524	Pentronic
TB290		Ring 12	B	90	0,360	6,881	Pentronic
TB291		Ring 12	B	90	0,420	6,881	Pentronic
TB292		Ring 12	B	90	0,480	6,881	Pentronic

Table 4-2. Numbering and position of instruments measuring total pressure (P).

Type and number	Measuring section	Block	Instrument position in block				Instrument Fabricate	Direction of pressure measurement
			Direction	α	r	z		
				degree	m	m		
PB201	1	Cyl. 1	A	340	0,635	0,502	Geokon	Axial
PB202	1	Cyl. 1	A	0	0,635	0,452	Geokon	Radial
PB203	1	Cyl. 1	A	20	0,635	0,452	Geokon	Tangential
PB204	2	R3	D	250	0,420	1,968	Geokon	Radial
PB205	2	R3	D	290	0,420	2,018	Geokon	Axial
PB206	2	R3	A	8	0,535	1,968	Geokon	Radial
PB207	2	R3	A	20	0,535	1,968	Geokon	Tangential
PB208	2	R3	AB	45	0,585	2,018	Geokon	Axial
PB209	2	R3	B	100	0,635	1,968	Geokon	Tangential
PB210	2	R3	C	170	0,710	1,968	Geokon	Tangential
PB211	2	R3	C	180	0,710	1,968	Geokon	Radial
PB212	2	R3	D	260	0,748	2,018	Geokon	Axial
PB213	2	R3	D	270	0,875	1,950	Geokon	Radial on rock
PB214	4	Cyl. 2	A	340	0,635	4,033	Geokon	Axial
PB215	4	Cyl. 2	A	0	0,635	3,983	Geokon	Radial
PB216	4	Cyl. 2	A	20	0,635	3,983	Geokon	Tangential
PB217	5	Ring 9	D	270	0,535	5,319	Geokon	Radial,against sand
PB218	5	Ring 9	A	340	0,635	5,554	Geokon	Axial
PB219	5	Ring 9	A	0	0,635	5,504	Geokon	Radial
PB220	5	Ring 9	A	20	0,635	5,504	Geokon	Tangential
PB221	5	Ring 9	B	70	0,710	5,554	Geokon	Axial
PB222	5	Ring 9	B	110	0,710	5,504	Geokon	Radial
PB223	5	Ring 9	C	160	0,745	5,554	Geokon	Axial
PB224	5	Ring 9	C	180	0,770	5,504	Geokon	Radial
PB225	5	Ring 9	C	200	0,740	5,504	Geokon	Tangential
PB226	5	Ring 9	D	270	0,875	5,450	Geokon	Radial on rock
PB227	7	Cyl. 3	A	340	0,635	7,574	Geokon	Axial
PB228	7	Cyl. 3	A	0	0,635	7,524	Geokon	Radial
PB229	7	Cyl. 3	A	20	0,635	7,524	Geokon	Tangential
PB230	2	R3	C	180	0,315	1,968	DBE	Radial
PB231	5	R9	C	180	0,535	5,504	DBE	Radial

Table 4-3. Numbering and position of instruments measuring pore pressure (U).

Type and number	Measuring section	Block	Instrument position in block				Instrument Fabricate	Remark
			Direction	α	r	z		
				degree	m	m		
UB201	2	Ring 3	D	270	0,420	1,768	Geokon	
UB202	2	Ring 3	A	350	0,535	1,768	Geokon	
UB203	2	Ring 3	B	90	0,635	1,768	Geokon	
UB204	2	Ring 3	D	280	0,785	1,768	Geokon	
US205	5	Ring 9	D	270	0,510	5,304	Geokon	In sand
UB206	5	Ring 9	DA	315	0,635	5,304	Geokon	
UB207	5	Ring 9	B	90	0,710	5,304	Geokon	
UB208	5	Ring 9	CD	225	0,785	5,304	Geokon	
UB209	2	Ring 3	C	200	0,315	1,968	DBE	
UB210	5	Ring 9	C	150	0,510	5,304	DBE	

Table 4-4. Numbering and position of instruments measuring water content (W).

Type and number	Measuring section	Block	Instrument position in block				Instrument Fabricate	Remark
			Direction	α	r	z		
				degree	m	m		
WB201	1	Cyl.1	C	180	0,420	0,252	Rotronic	
WB202	1	Cyl.1	CD	225	0,635	0,252	Vaisala	
WB203	1	Cyl.1	CD	235	0,635	0,252	Wescor	
WB204	1	Cyl.1	D	270	0,785	0,252	Rotronic	
WB205	1	Cyl.1	D	280	0,785	0,252	Wescor	
WB206	3	Ring 4	BC	135	0,360	2,269	Vaisala	
WB207	3	Ring 4	C	180	0,420	2,269	Rotronic	
WB208	3	Ring 4	CD	225	0,485	2,269	Vaisala	
WB209	3	Ring 4	D	270	0,560	2,269	Rotronic	
WB210	3	Ring 4	DA	315	0,635	2,269	Vaisala	
WB211	3	Ring 4	DA	325	0,635	2,269	Wescor	
WB212	3	Ring 4	A	0	0,710	2,269	Rotronic	
WB213	3	Ring 4	A	10	0,710	2,269	Wescor	
WB214	3	Ring 4	AB	45	0,785	2,269	Vaisala	
WB215	3	Ring 4	AB	55	0,785	2,269	Wescor	
WB216	4	Cyl.2	C	180	0,420	3,783	Rotronic	
WB217	4	Cyl.2	CD	225	0,635	3,783	Vaisala	
WB218	4	Cyl.2	CD	235	0,635	3,783	Wescor	
WB219	4	Cyl.2	D	270	0,785	3,783	Rotronic	
WB220	4	Cyl.2	D	280	0,785	3,783	Wescor	
WS221	5	Ring 9	BC	135	0,525	5,304	Vaisala	In sand
WS222	6	Ring 10	BC	135	0,525	5,806	Vaisala	In sand
WB223	6	Ring 10	C	180	0,585	5,806	Rotronic	
WB224	6	Ring 10	CD	225	0,635	5,806	Vaisala	
WB225	6	Ring 10	D	270	0,685	5,806	Rotronic	
WB226	6	Ring 10	D	280	0,685	5,806	Wescor	
WB227	6	Ring 10	DA	315	0,735	5,806	Vaisala	
WB228	6	Ring 10	DA	325	0,735	5,806	Wescor	
WB229	6	Ring 10	A	0	0,785	5,806	Rotronic	
WB230	6	Ring 10	A	10	0,785	5,806	Wescor	
WB231	7	Cyl.3	C	180	0,420	7,374	Rotronic	
WB232	7	Cyl.3	CD	225	0,635	7,374	Vaisala	
WB233	7	Cyl.3	CD	235	0,635	7,374	Wescor	
WB234	7	Cyl.3	D	270	0,785	7,374	Rotronic	
WB235	7	Cyl.3	D	280	0,785	7,374	Wescor	

4.4 Instruments in the rock

Temperature measurements

40 thermocouples are located in ten boreholes in the rock (see Figure 1-1). The depth of each borehole is 1.5 m. In each borehole 4 thermocouples are placed at different distances from the rock surface. Observe that the coordinate system does not count the radius but the radial distance from the rock surface of the deposition hole. The position of each instrument is described in Table 4-5.

Table 4-5. Numbering and positions of thermocouples in the rock.

Mark	Level	Direction	Distance from rock surface	Instrument Fabricate
	m	degree	m	
TR201	0	Center	0,000	Pentronic
TR202	0	Center	0,375	Pentronic
TR203	0	Center	0,750	Pentronic
TR204	0	Center	1,500	Pentronic
TR205	0,61	10°	0,000	Pentronic
TR206	0,61	10°	0,375	Pentronic
TR207	0,61	10°	0,750	Pentronic
TR208	0,61	10°	1,500	Pentronic
TR209	0,61	80°	0,000	Pentronic
TR210	0,61	80°	0,375	Pentronic
TR211	0,61	80°	0,750	Pentronic
TR212	0,61	80°	1,500	Pentronic
TR213	0,61	170°	0,000	Pentronic
TR214	0,61	170°	0,375	Pentronic
TR215	0,61	170°	0,750	Pentronic
TR216	0,61	170°	1,500	Pentronic
TR217	3,01	10°	0,000	Pentronic
TR218	3,01	10°	0,375	Pentronic
TR219	3,01	10°	0,750	Pentronic
TR220	3,01	10°	1,500	Pentronic
TR221	3,01	80°	0,000	Pentronic
TR222	3,01	80°	0,375	Pentronic
TR223	3,01	80°	0,750	Pentronic
TR224	3,01	80°	1,500	Pentronic
TR225	3,01	170°	0,000	Pentronic
TR226	3,01	170°	0,375	Pentronic
TR227	3,01	170°	0,750	Pentronic
TR228	3,01	170°	1,500	Pentronic
TR229	5,41	10°	0,000	Pentronic
TR230	5,41	10°	0,375	Pentronic
TR231	5,41	10°	0,750	Pentronic
TR232	5,41	10°	1,500	Pentronic
TR233	5,41	80°	0,000	Pentronic
TR234	5,41	80°	0,375	Pentronic
TR235	5,41	80°	0,750	Pentronic
TR236	5,41	80°	1,500	Pentronic
TR237	5,41	170°	0,000	Pentronic
TR238	5,41	170°	0,375	Pentronic
TR239	5,41	170°	0,750	Pentronic
TR240	5,41	170°	1,500	Pentronic

4.5 Instruments in the canister

Temperature is measured both on the canister surface and inside the canister /4-2/. Eleven thermocouples are installed on each canisters surface. Three groups of three thermocouples are installed 100 mm from each heater end, and in the middle of the heater, with a distribution of 120°. Two additional thermocouples are installed in the centre of the bottom lid and the top cover. Temperature inside the canister insert is measured at 6 points with thermocouples.

Figure 4-2 shows how these thermocouples are placed (see also chapter 4.2). Table 4-6 and 4-7 show the positions.

Table 4-6. Numbering and position of instruments for measuring the temperature on the heaters surface (T).

Type and number	Heater	Instruments coordinates				Instrument Fabricate	Remark
		Position	α	r	z		
			degree	m	m		
TH1 SE0	1	Bottom	0	0,000	0,500		
TH1 SE1 0º	1	Lower sec.	0	0,305	0,600		
TH1 SE1 240º	1	Lower sec.	240	0,305	0,600		
TH1 SE1 120º	1	Lower sec.	120	0,305	0,600		
TH1 SE2 0º	1	Middle sec.	0	0,305	2,000		
TH1 SE2 240º	1	Middle sec.	240	0,305	2,000		
TH1 SE2 120º	1	Middle sec.	120	0,305	2,000		
TH1 SE3 0º	1	Upper sec.	0	0,305	3,400		
TH1 SE3 240º	1	Upper sec.	240	0,305	3,400		
TH1 SE3 120º	1	Upper sec.	120	0,305	3,400		
TH1 SE4	1	Top	0	0,000	3,500		
TH2 SE0	2	Bottom	0	0,000	4,000		
TH2 SE1 0º	2	Lower sec.	0	0,305	4,100		
TH2 SE1 240º	2	Lower sec.	240	0,305	4,100		
TH2 SE1 120º	2	Lower sec.	120	0,305	4,100		
TH2 SE2 0º	2	Middle sec.	0	0,305	5,500		
TH2 SE2 240º	2	Middle sec.	240	0,305	5,500		
TH2 SE2 120º	2	Middle sec.	120	0,305	5,500		
TH2 SE3 0º	2	Upper sec.	0	0,305	6,900		
TH2 SE3 240º	2	Upper sec.	240	0,305	6,900		
TH2 SE3 120º	2	Upper sec.	120	0,305	6,900		
TH2 SE4	2	Top	0	0,000	7,000		

Table 4-7. Numbering and position of instruments for measuring the temperature inside the heaters (T).

Type and number	Heater	Instruments coordinates			Instrument Fabricate	Remark
		Position	α	Z		
			degree	m		
TH1 SI1 0º	1	Lower sec.	0	0,60		
TH1 SI1 180º	1	Lower sec.	180	0,60		
TH1 SI2 0º	1	Middle sec.	0	2,00		
TH1 SI2 180º	1	Middle sec.	180	2,00		
TH1 SI3 0º	1	Upper sec.	0	3,40		
TH1 SI3 180º	1	Upper sec.	180	3,40		
TH2 SI1 0º	2	Lower sec.	0	0,60		
TH2 SI1 180º	2	Lower sec.	180	0,60		
TH2 SI2 0º	2	Middle sec.	0	2,00		
TH2 SI2 180º	2	Middle sec.	180	2,00		
TH2 SI3 0º	2	Upper sec.	0	3,40		
TH2 SI3 180º	2	Upper sec.	180	3,40		

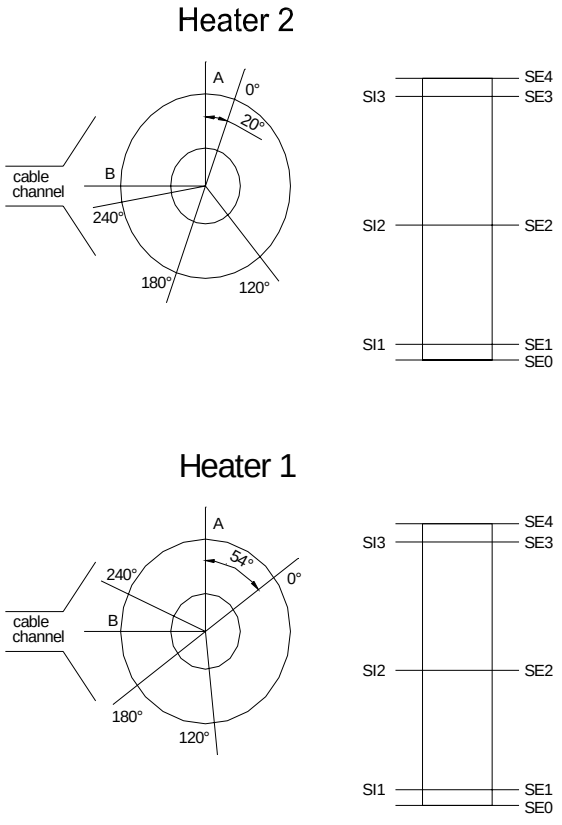

Figur 4-2. *Location of thermocouples inside (SI) and on (SE) the canisters.*

4.6 Instruments on the plug

Three force transducers and three displacement transducers have been placed on the plug to measure the force of the anchors and the displacement of the plug. The location of these transducers can be described in relation to Fig 4-3, which shows a schematic view of the plug with the slots, rods and cables.

The rods are numbered 1-9 anti-clockwise and number 1 is the northern rod 18 degrees from direction A. The force transducers are placed on rods 3, 6, and 9. The displacement transducers are placed between the rods on the steel ring in the periphery of the plug. They are fixed on the rock surface and measure thus the displacement relative to the rock.

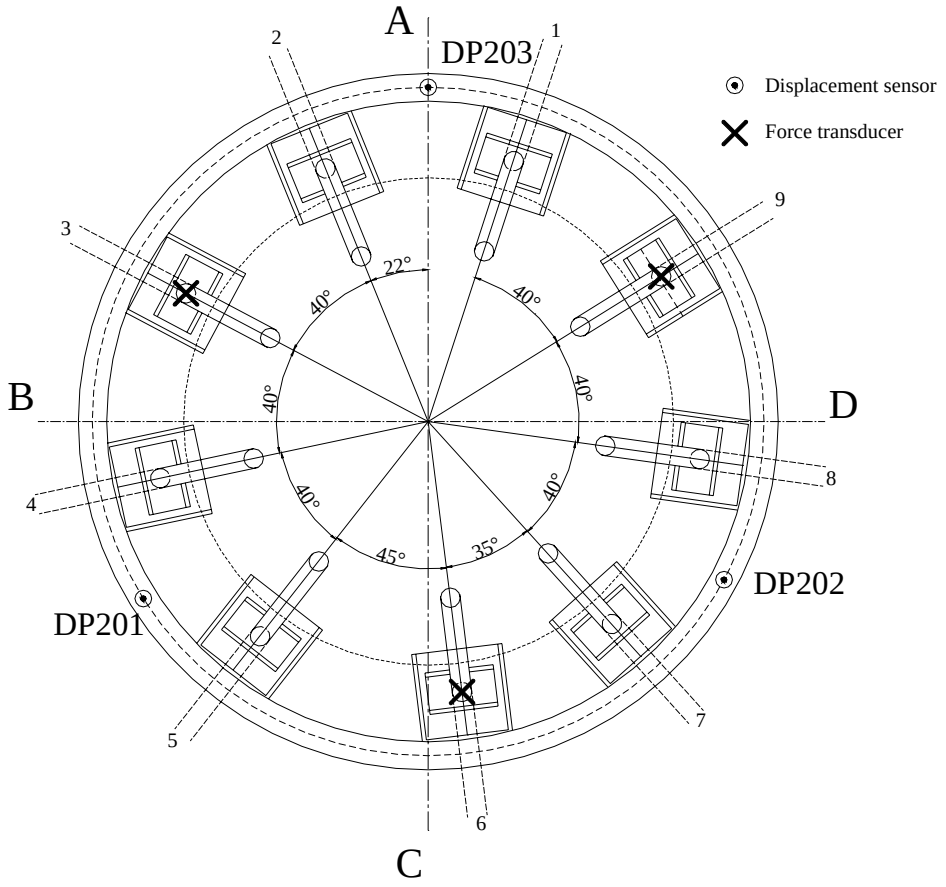

Figure 4-3. *Schematic view showing the positions of the rods and the displacement and force transducers on the retaining plug.*

5 Discussion of results

5.1 General

The aim of this chapter is two-parted: (i) to give an updated interpretation of the project as a whole; and (ii) to highlight the latest developments. More detailed discussions of earlier results can be found in previous data reports.

5.2 Total inflow of water

The total injected water volume into sand filter is shown in (App.A\page 75) and was slightly higher than 3.8 m^3 on January 1, 2008. Table 5-1 shows the pore space available at the beginning of the test. The calculated available pore volume has thereby been exceeded with 1.1 m^3. This discrepancy appears to be caused by a water leakage, possibly into the rock. This has previously been elaborated /5-1/.

The inflow has varied significantly during the test period. During the first 75 days the inflow was about 15 l/d, while it dropped to about 1.3 l/d during the subsequent 250 days. On average during the period from January 1, 2007 to January 1, 2008, the inflow was 0.9 l/d.

Two major events can be noticed in the applied scheme for pressurization (Table 5-2):

- During the first 377 days, the sand filter was only pressurized through the lower injection points, while the upper were open to the atmosphere. After this day, upper injection points have also been pressurized while none of the injection points has been open to the atmosphere.

- The second event was the installation of equipment for measuring pressure at each injection point on October 8, 2004 (day 562) (see Figure 5-1). Since then, at least one out of eight injection points have been closed and used for monitoring of the actual pressure in the sand filter.

- The third event was the change of water quality on April 17, 2007. The background for this was that the injection points in the sand filter have exhibited a high flow resistance during the operation phase of the test. In order to reduce this resistance, the formation water used earlier was replaced by de-ionized water.

The effect of the third modification, with increasing inflow, was noticed almost immediately. Two ports used earlier for injection were closed in order to avoid frequent refilling of the rather small pressure tank in use at that time (see Table 5-2). Later on (on August 13) the small tank was replaced by a larger tank which enabled a higher inflow without the need of frequent refilling. This change enabled the control of the filter pressure of 3-4 bar with an injection pressure of 5 bar (see Figure 5-2).

Table 5-1. TBT Pore space.

	Available at test start [m^3]	
Sand filter	0.77	
Pellets filling	0.24	1.38
Bentonite	1.08	
Heater/bentonite clearance	0.06	
Sand shield	0.55	
Total	2.70	

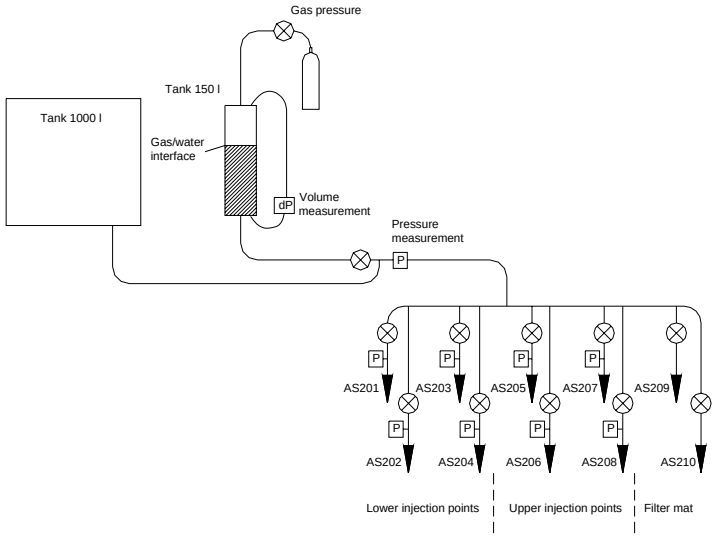

Figure 5-1. *Schematic view of injection system.*

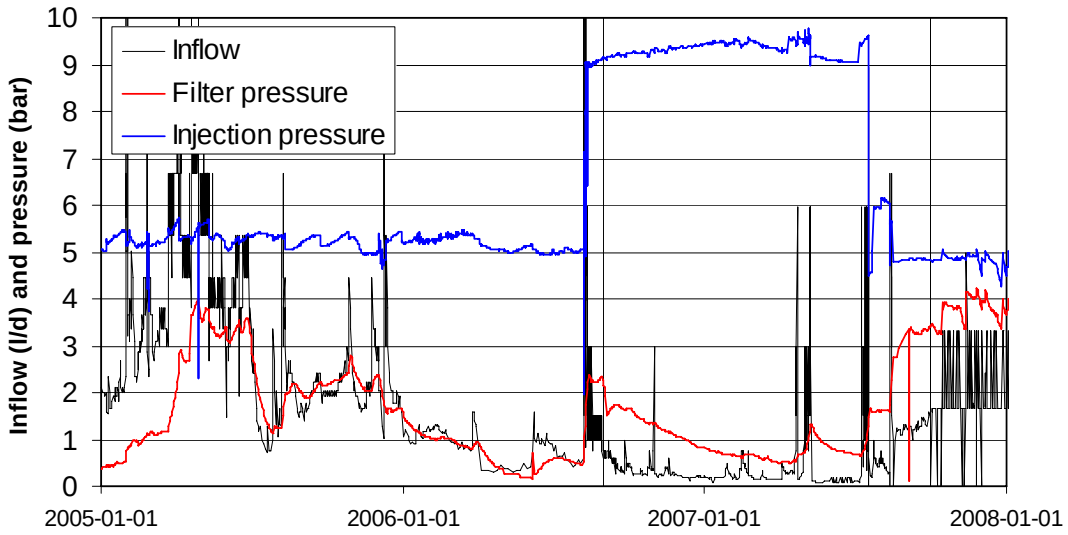

Figure 5-2. *Development of relative pressures (injection and in sand filter) and inflow since the second hydraulic test.*

Table 5-2. Injection point pressurization scheme (values are relative pressures). The actual water pressure in the sand filter is only measured at those points that are closed.

Intervals	Lower injection points				Upper injection points				Filter mat		p (bar)
	201	202	203	204	205	206	207	208	209	210	
030326 – 040406 *Day 0 – 377*	O	O	O	O	⊕	⊕	⊕	⊕	⊗	⊗	7
040406 – 040615 *Day 377 – 447*	O	O	O	O	O	O	O	O	⊗	⊗	0
040615 – 040616 *Day 447 – 448*	Hydraulic test I										
040616 – 041008 *Day 448 – 562*	O	O	O	O	O	O	O	O	⊗	⊗	1.5
041008 – 041014 *Day 562 – 568*	Hydraulic test II										
041014 – 041110 *Day 568 – 595*	⊗	⊗	⊗	⊗	O	⊗	O	⊗	⊗	⊗	5
041110 – 050728 *Day 595 – 856*	O	O	⊗	O	O	O	⊗	O	⊗	⊗	5
050728 – 051209 *Day 856 – 989*	O	⊗	O	O	O	⊗	O	O	⊗	⊗	5
051209 – 051212 *Day 989 – 992*	O	⊗	O	O	O	⊗	O	O	O	⊗	5
051212 – 060517 *Day 992 – 1148*	O	⊗	O	O	O	⊗	O	O	O	O	5
060517 – 060614 *Day 1148 – 1176*	Back flushing of injection points										
060614 – 060807 *Day 1176 – 1230*	O	O	⊗	O	O	O	O	O	O	O	5
060807 – 060811 *Day 1230 – 1234*	Increase of injection pressure										
060811 – 070417 *Day 1234 – 1483*	O	O	⊗	O	O	O	O	O	O	O	9
070417 *Day 1483*	Change in water quality										
070417 – 070423 *Day 1483 – 1489*	O	O	⊗	O	O	O	O	O	O	O	9
070423 – 070509 *Day 1489 – 1505*	O	O	⊗	O	O	O	⊗	O	O	O	9
070509 – 070716 *Day 1505 – 1573*	O	O	⊗	O	O	⊗	⊗	O	O	O	9
070717– 070723 *Day 1574 – 1580*	O	O	⊗	O	O	⊗	⊗	O	O	O	5
070724– 070812 *Day 1581 – 1600*	O	O	⊗	O	O	⊗	⊗	O	O	O	6
070813– 070815 *Day 1601 – 1603*	O	O	⊗	O	O	O	O	⊗	O	O	5.5
070816– 070905 *Day 1604 – 1624*	O	O	⊗	O	O	O	O	⊗	O	O	5
070906– *Day 1625 –*	O	O	⊗	O	O	O	⊗	O	O	O	5

O = Open and pressurized
⊕ = Open to atmosphere
⊗ = Closed

5.3 Hydration of sand shield

This section describes the activity of saturating the sand shield around the upper heater with water. The aim of this activity was to facilitate a number of hydraulic tests and gas injection tests through the upper buffer package. This activity spans over a time period that surpass the period devoted for the current sensors data report. Nevertheless, for facilitating an overview of this extensive activity, it is reported in full in this report.

This section is divided in five parts: The first part gives a description of the sand shield with related instrumentation and equipment. The second part describes the hydration and the pressurizations test performed within the activity “Dry gas venting of sand shield” (APTD F12.2-07-028). The third part describes the hydration through continuous pressurization which was performed within the activity “Sand shield hydration” (APTD F12.2-07-042), during which the shield was actually filled with water. The fourth part describes a preliminary hydraulic test performed within the same activity. This test gave clear indications that the upper buffer package is not tight. No gas injection test will therefore be performed. In the fifth part the observed behavior regarding high flow resistance and leakage are discussed.

System description

The pore volume of the sand shield was calculated to be approximately 580 l. This volume was regarded to be virtually dry before the hydration was initiated.

The sand shield is equipped with two injection points at mid-height: CS202 and CS203 (see Figure 5-3). Water was injected through both these port during the first hydration attempt. During the continuous pressurization, the following ports and instruments were used:

- Water was injected into the shield through port CS203.
- The CS203 port was connected to two pressurized tanks joined in parallel, in which the water volume was monitored with a differential pressure sensor, thereby enabling a quantification of the inflow.
- The CS203 port was also equipped with a pressure sensor which measured the injection pressure when the port was open. This sensor also gave reliable data on shield pressure when the port was closed.
- The second port in the shield (CS202) was closed and was used for monitoring of the shield pressure. Due to the high flow resistance, the reliability was minor.
- The pore pressure sensor (UB205) is located in the shield and was also used for monitoring of the shield pressure.
- The filter pressure was sustained and measured through the filter ports (AS201-208).

First hydration attempts

Water was injected through both ports (CS202 and 203) with a micro annular gear pump during the course of the dry gas venting activity. This took place on May 9 – 11 and May 25, 2007. Significant amounts of water could at first be injected with fairly low pressure levels. At the same time gas was extracted with vacuum. The amounts of injected and extracted water and gas are shown in Table 5-3. In total approximately 30 liters were injected during the first hydration attempts.

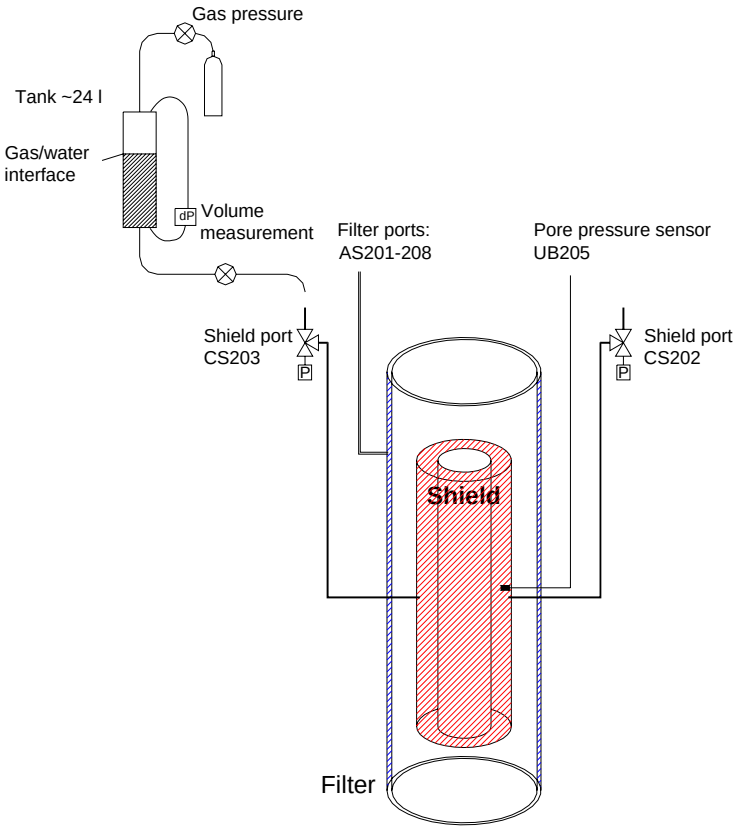

Figure 5-3. *Ports and instrumentation for shield hydration. One pressurized tank with level sensor is located in the gallery; two ports (CS202 and CS203) are located in the shield; one pore pressure sensor (UB205) is located in the shield; and eight ports (AS201-208) are located in the filter.*

It was soon noticed, however, that both injection points (or their surrounding) started to exhibit a high flow resistance. The ports were therefore pressurized with GDS in two attempts to purge the injection points (Table 5-4).

These tests showed that inflow through one of the ports (CS203) could be increased significantly if the pressure was raised to 40 bar. Still, the inflow was limited (150 ml/h) which implied that the filling of the shield had to be executed through continuous pressurization.

Table 5-3. Volumes injected into and extracted from the sand shield.

Date	Injected water volume (liters)	Extracted water volume (liters)	Extracted gas volume (liters)
2007-05-09	4.5	0.1	37
2007-05-10	6.1	0.5	21
2007-05-11	19.6	1.8	>> 2
2007-05-25	0.1	0.6	>> 5
Total	30.3	3.0	>> 65

Table 5-4. Pressurization tests with GDS.

Date	Port CS202 Maximum pressure & flow rate	Port CS203 Maximum pressure & flow rate
2007-06-08	20 bar & 0.6 ml/h	25 bar & 20 ml/h
2007-06-29	60 bar & 0.4 ml/h	40* bar & 150 ml/h

* The target value was 60 bar, but the maximum flow rate was reached at 40 bar.

Hydration through continuous pressurization

The continuous pressurization began on September 10. After minor modification of the system the pressure could be increased from 20 to 30 bar on September 19. A second parallel tank, which doubled the water volume, was installed on October 4 which facilitated an increase up to 40 bar on October 4.

With this system, the inflow was eventually found to increase significantly in the middle of November. This may have been a purely hydro-mechanical effect. However, it should not be excluded that the concurrent decrease in power output from the upper heater contributed to this reduction in the flow resistance. After this event, the pressure was regulated manually with lower pressures during weekends and holydays (see Figure 5-4).

In the middle of January 2008, a leakage was detected with water coming up through two slots under the lid. At this time, it was not known from where the leakage originated. Three possible sources were identified: the injection pressure for the *sand filter* was reduced from 5.5 to 4 bar on January 28 and subsequently to 2.5 bar on February 4; the pressurization of the *filter mat* was turned of on February 1; and pressurization of the shield was reduced to 25 bar on February 1. These measures reduced the leakage significantly, from approximately 5 l/d to less than 1 l/d. It was noted at the time that these amounts surpassed the inflow into the filter and that the shield therefore could be identified as the source of the leakage. Still, there was virtually no correlation between the injection pressure for the shield and the monitored filter pressure. No definitive conclusion about the origin of the leakage could therefore be made at that time. More over, on February 10 the CS202 sensor responded to the pressure increase in the shield and showed 4 bar. This gave a small indication that the shield was tight. Due to increased shield pressure, the injection pressure for the shield was reduced to 10 bar on February 11. This condition was sustained up to the preliminary hydraulic test on March 17.

The total amount of water injected during the first hydration attempt and the continuous pressurization was approx. 540 liters.

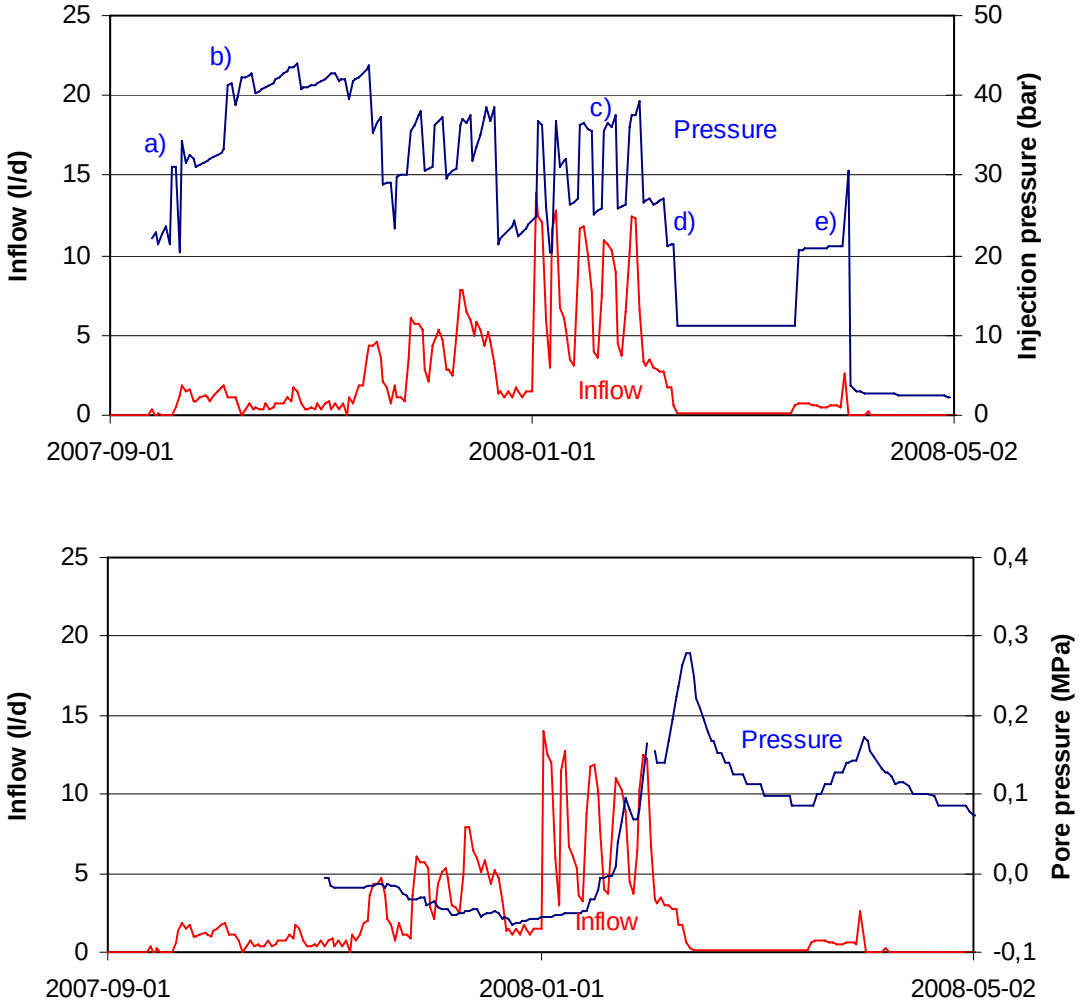

Figure 5-4. *Pressure and inflow during the continuous pressurization. Upper graphs shows the injection pressure and lower graph shows pore pressure as registered with the UB205 sensor. a) Significant inflow when the injection pressure was increased from 20 to 30 bar on September 19; b) injection pressure was increased from 30 to 40 bar on October 4; c) leakage was detected in the middle of January; d) pressurization was reduced to 10 bar with the peaking of pore pressure; and e) preliminary hydraulic test.*

Preliminary hydraulic test

The hydraulic test, which started on March 17, was at first planned to be a *pulse test*. The idea of such a test is to inject a known volume of water into one of the ports of the shield during a relatively short time period and to observe and evaluate the shield pressure response. The filter pressure is kept constant during the test and the goal is to quantify the hydraulic conductivity of the buffer.

An injection pressure of 20 bar was chosen, which yielded an inflow of approx. 0.6 l/d. This inflow was kept for 14 days. It was noticed that the pore pressure did not increase as expected, but rather tended to level out. Therefore the injection pressure was increased to 30 bar on March 31, which yielded an inflow of 2.6 l/d. The pore pressure responded more rapidly to this inflow, but after one day (on April 1) a leakage was again detected from one of the slots. The pressurization of port CS203 was therefore

terminated. In addition, the port was closed thereby enabling the monitoring of the pore pressure with the sensor connected to port CS203. In addition to the closing of port CS203, the port CS202 was pressurized and filter mats were opened on April 1. The reason for pressurizing port CS202 was to check the possibility that the leakage originated from the *tube* to port CS203.

The pressure response of the hydraulic test is illustrated in Figure 5-5 together with model results. The data from the UB205 sensor is here given an offset of 1.6 bar in order to match the CS203 data. The model results were fitted with a compressible gas volume of 20 liters and a hydraulic conductivity of $2 \cdot 10^{-11}$ m/s. This value exceeds the expected value with two orders of magnitude and reflects therefore the leakage from the shield.

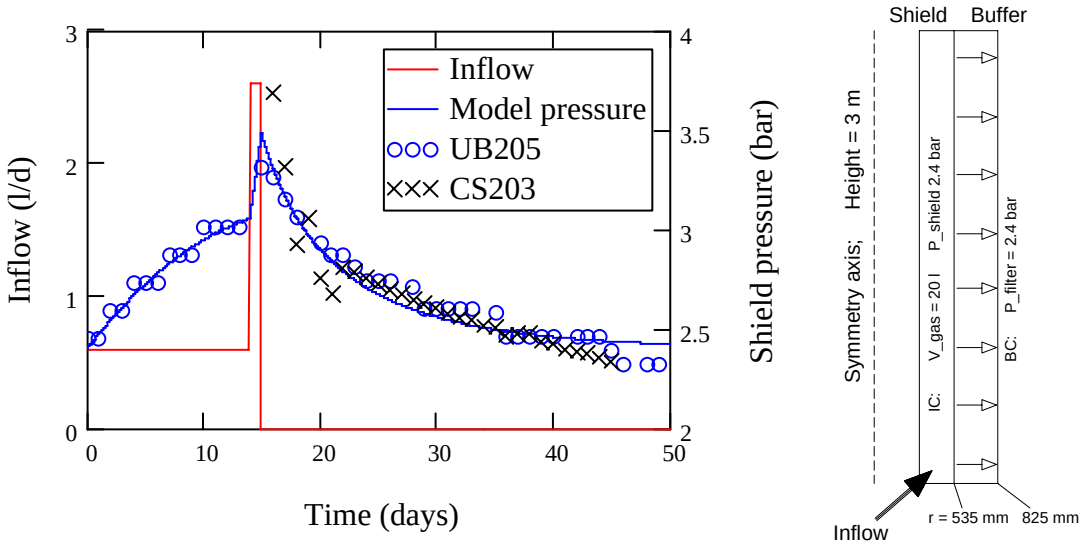

Figure 5-5. *Measured and modeled shield pressure during the preliminary hydraulic test (left). Schematic model description (right).*

Interpretation of high flow resistance and leakage

During the first hydration attempts, the flow resistance of the injection points showed a marked increase. This behavior could possibly be an effect of bentonite swelling past the filter tips. These were at installation located approx. 30 mm from the sand-bentonite interface (see Figure 5-6). The future dismantling of the experiment can possibly confirm or falsify this interpretation.

The leakage from the sand shield could possibly occur through the array of external thermo-couples or through the slots cut out for the heater cables (see Figure 5-7). A third alternative could possibly be that water would be flushed “backwards” along the tubes of the injection points. This is however not supported by the apparent lack of correlation between injection pressure and filter pressure. More over, the first leakage coincided with the buildup of pore pressure as recorded by the UB205 sensor and approx. 400 liters had been injected at that time. These facts support the notion that the leakage took place at the top of the shield. It can also be noted that the volume above the top section of Ring 12 is separated from the sand filter by 0.25 m bentonite pellets filling. This could possibly explain the independence of the shield pressure and the filter pressure.

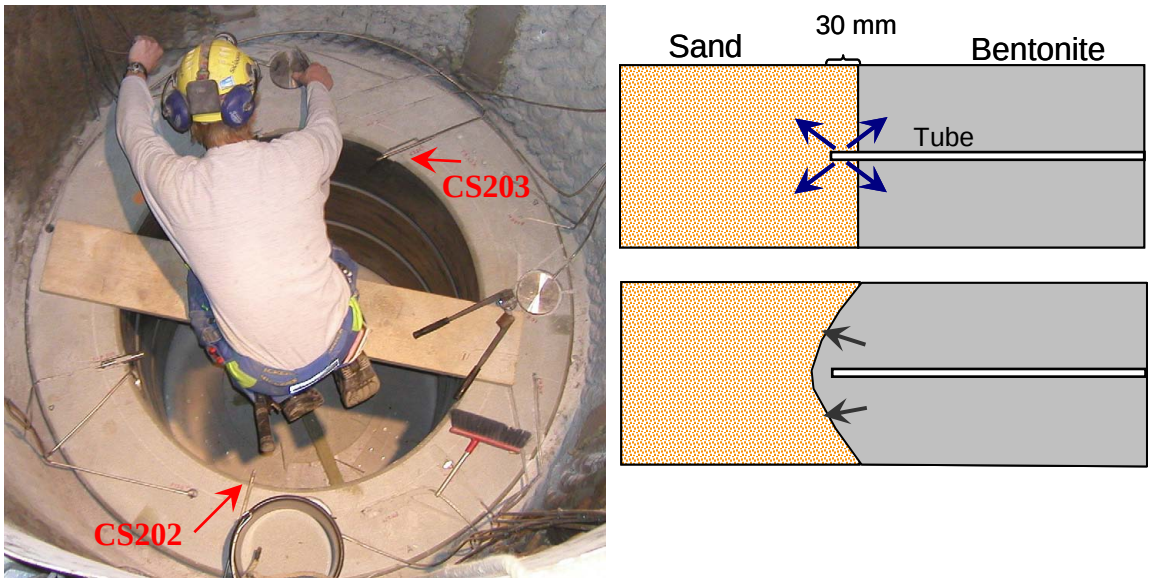

Figure 5-6. *Installation of injection points at top of Ring 9 (left) and schematic interpretation of increased flow resistance.*

Figure 5-7. *Possible pathways for leakage from sand shield. Left: Slots for heater power cables. These were subsequently sealed with bentonite powder. Right: External thermocouples from heater.*

5.4 Temperatures

Temperatures are monitored by use of thermocouples in three cylinders (C1, C2 and C3) and two rings (R4 and R10), cf. Figure 1-1. In addition, temperature readings are provided by the capacitance-type relative humidity (RH) sensors. In general, the temperature results exhibit consistent trends up to maximum values after about 200 days (App.A\pages 82-87). A few exceptions have occurred for inner parts in Cyl 2 and the inner sand shield at Ring 10, where the maximum temperatures were reached after only about 40 and 60 days, respectively (App.A\pages 84-85).

The TBT experiment is located 6 m from the CRT experiment. The latter was initiated approximately 880 days before the start of the TBT experiment and has therefore contributed with a certain heat flux. The CRT was terminated in October 2005. In order to compensate for this loss, the power output from the TBT heaters was increased from 1500 to 1600 W on June 9, 2006.

Change in power output

The power output from the heaters was changed during the last two months of 2007. The power from the lower heater was increased from 1600 to 2000 W, while the output from the upper heater was decreased from 1600 W to 1000 W. All changes were made in weekly steps of 100 W. This change has altered the thermal conditions in the experiment. At the end of the year the temperature on the mid-section of the lower heater was 158 ºC. The corresponding value for the upper heater was 89 ºC (Figure 5-8).

It can be noted that the hydration of the sand shield influenced the conditions around the upper heater and this is reflected by some of the temperature data. The temperatures on the upper heater (App.A\ page 93) tended to decrease whereas the temperatures in Ring 10 tended to increase (App.A\page 85). This change can be explained as an increased heat transport through the sand shield.

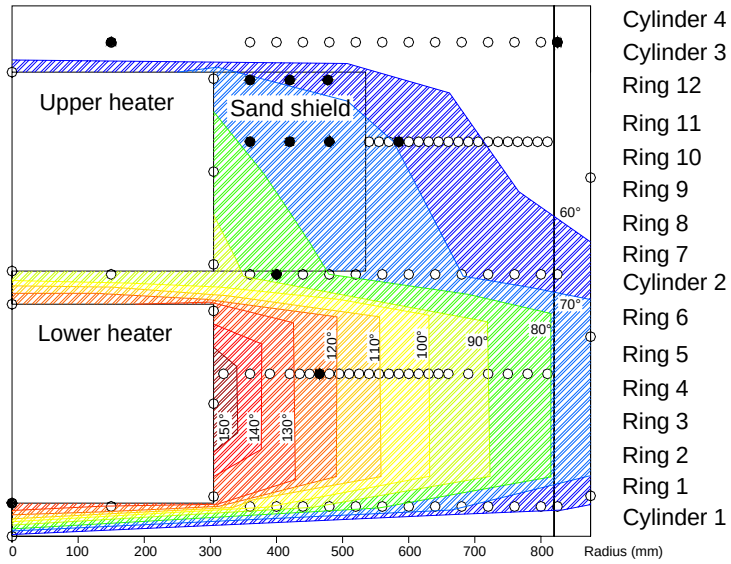

Figure 5-8. *Temperature distribution on January 1, 2008. Rings indicate sensor positions. Filled rings indicate sensors out of order.*

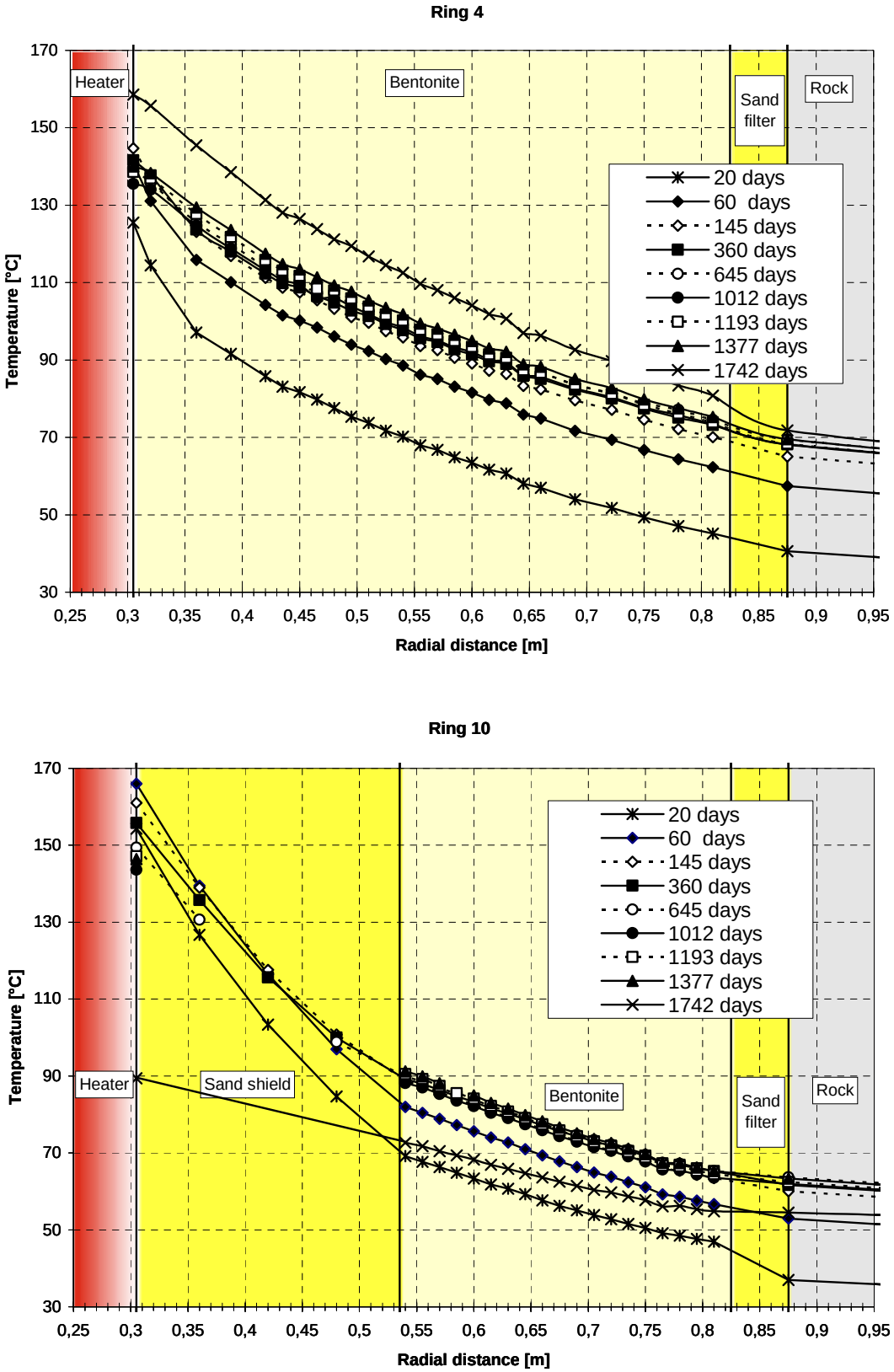

Figure 5-9. *Temperatures measured at mid-height of Heater 1 (Ring 4) and Heater 2 (Ring 10).*

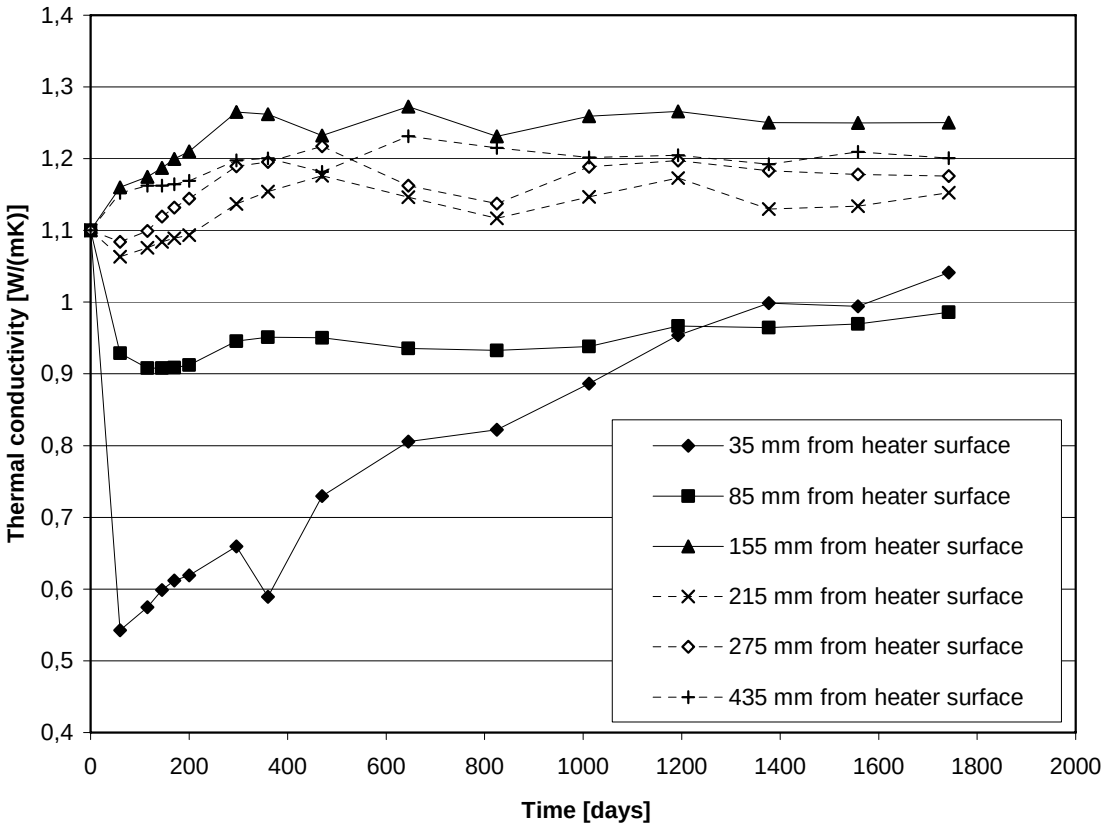

Figure 5-10. *Thermal conductivity development in Ring 4.*

Temperature profiles and thermal conductivities

Temperature profiles in Ring 4 and Ring 10 are shown for different points of time in Figure 5-9. The effect of the change in power output is very distinct, with a higher temperature level in Ring 4 and a lower level in Ring 10 (especially in the sand shield).

Figure 5-10 illustrates the evolution of the apparent thermal conductivity in Ring 4. These results are based on the slopes of temperature-distance curves derived from thermocouple readings in Ring 4, and on the assumption that the heat flux at mid-height can be approximated to be strictly radial. The thermal conditions after the change in power output were very different than the preceding conditions. The evaluated conductivity values for the latest point of time were therefore calibrated so that the conductivity at 155 mm from the heater surface was the same as previously. In general, these graphs should be interpreted with some caution: some of the changes may be due to variation of the mid-height heat flux, and some may be due to dislocation of individual sensors.

It can be noted that the innermost point, at 35 mm from the heater surface, dropped immediately after test start, but has thereafter increased steadily. In contrast, a point at 155 mm from the heater appears to have undergone a rapid increase in the beginning and has thereafter remained fairly constant.

5.5 Relative humidity/suction

Recorded RH values and suctions indicate that moisture contents generally increase: RH from 72 to maximum 100 % (App.A\pages 67-72); suction between 6 and 1 MPa (App.A\pages 62-66).

A significant exception was the suction *increase* in Ring 10 at radius 785 and 735 mm after day 225 (App.A\page 65). Although this increase correlated with a general decrease in stresses in parts of Ring 9, it was most likely caused by a shortage in water supply, resulting in a localized desiccation cycle to occur. The trend was also reversed when water injection through the upper tubes was introduced (see Section 5.2), which supports the water supply explanation for these observations.

The hydration of the buffer, as recorded by the RH-sensors, is illustrated in Figure 5-9. Occasions when capacitive sensor signals showing RH ≈ 100 % (Vaisala and Rotronic), and all *active* signals from psychrometers, corresponding to RH > 95 % (Wescor), are compiled. These occasions are taken as indications of *vapor* saturation rather than of *buffer* saturation. The reason for this is that the rapid evolution of the RH-sensors is contrasted by the slow response of the pore pressure sensors. The current understanding is that the process of reaching full saturation is slow.

The change in the power output is reflected by the most recent vapor saturation event in the lower part (see Figure 5-9). All operational capacitive RH sensors now indicate saturated vapor.

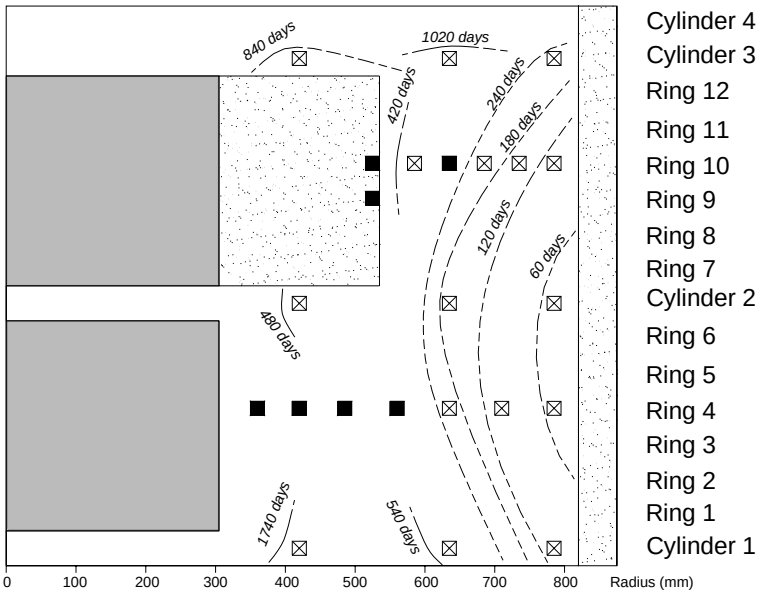

Figure 5-9. *Occurrences of vapour saturation up till January 1, 2008. Boxes are sensor positions. Ticked boxes indicate saturation. Filled boxes indicate sensors out of order. Percentage is current RH values.*

5.6 Pore pressure

Ideally, pore pressure sensors should give a zero signal as long as the condition isn't totally saturated. The first build-up of pore pressure at the outermost sensor in Ring 9 coincided with the filter pressure increase in the beginning of 2005, whereas the other sensors in Ring 9 responded within 200 days afterwards.

The data from the sensors that have responded appears to be correlated with the pressure in the sand filter. The absolute level of the sensors is however higher than the sand filter pressure, which can put the accuracy of the pore pressure sensors into question.

The change in power output and the shield hydration has both influenced the pore pressures. On January 1 2008, all the sensors in Ring 3, but only the outermost sensor in Ring 9 showed significant values (App.A\pages 73-74\). Short afterwards, however, all remaining sensors in Ring 9 had recovered. The influence of the change in power output and the shield hydration is described in the next section.

5.7 Total pressure

Results from pressure monitoring are shown in App.A\pages 53-61\. A compilation of recent total pressures is shown in Figure 5-10. The conditions in the lower and the mid-section cylinders are quite isostatic, while the sections around the heaters are characterized by deviatoric stresses, with relatively lower radial stresses. This appears to reflect that the largest displacements occur in radial direction around the heaters. In these sections, the sand filter and the sand shield, and perhaps also the dehydration of the inner parts around the lower heater, enable the radial swelling of the hydrating buffer. In general, all recorded total pressure is now quite stable.

The hydration of the sand shield resulted in a decrease in total pressure and pore pressure in Ring 9. This was especially apparent after May 9 during the first hydration attempts, but also at the end of the year (App.A\ pages 58-60 and page 74). This appears to be an effect of swelling of the buffer into the sand shield (see Figure 5-6). An alternative explanation for the pressure drop recorded in May could be the increasing temperature level in the bentonite. The opposite response, with increasing pressures, would however be expected if this would be the cause.

This type of effect was exhibited after the change in power output, which also influenced the total pressures and the pore pressures. Significant increase in pore pressure levels around the lower heater indicates the ongoing water saturation process. However, the pore pressure levels were still below the pressure in the sand filter (Figure 5-2). The total pressures around the lower heater (Ring 3) also displayed a minor increase, after which they decreased slightly more than the initial increase. The cause of the general pressure decrease in Ring 9 observed at the end of 2007 is difficult to identify, since the decrease in power output coincided with the shield hydration.

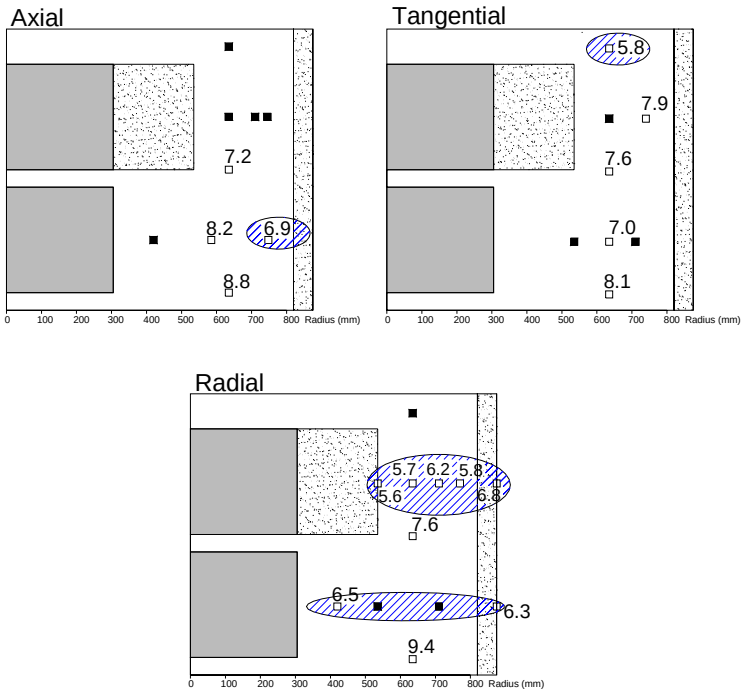

Figure 5-10. *Total pressure distribution on January 1, 2008. Values in MPa. Boxes are sensor positions. Filled boxes indicate sensors out of order. Levels below 7 MPa marked blue.*

6 References

/4-1/ Sandén T and Börgesson L. Report on instruments and their positions for THM measurements in buffer and rock and preparation of bentonite blocks for instruments and cables. Temperature Buffer Test, Report R5 , 2002. SKB ITD-02-05

/4-2/ Garcia-Sineriz, J.L and Fuentes- Cantillana. Feasibility study for the heating system at the TBT test carried out at the Äspö HRL in Sweden. Temperature Buffer Test , October 2002. SKB IPR-03-18

/5-1/ Goudarzi R., Åkesson M., Hökmark H. Äspö Hard Rock Laboratory. Temperature Buffer Test. Sensors data report (period 030326-060701) Report No:8, 2006, SKB IPR-06-27.

Appendix A

Measured data

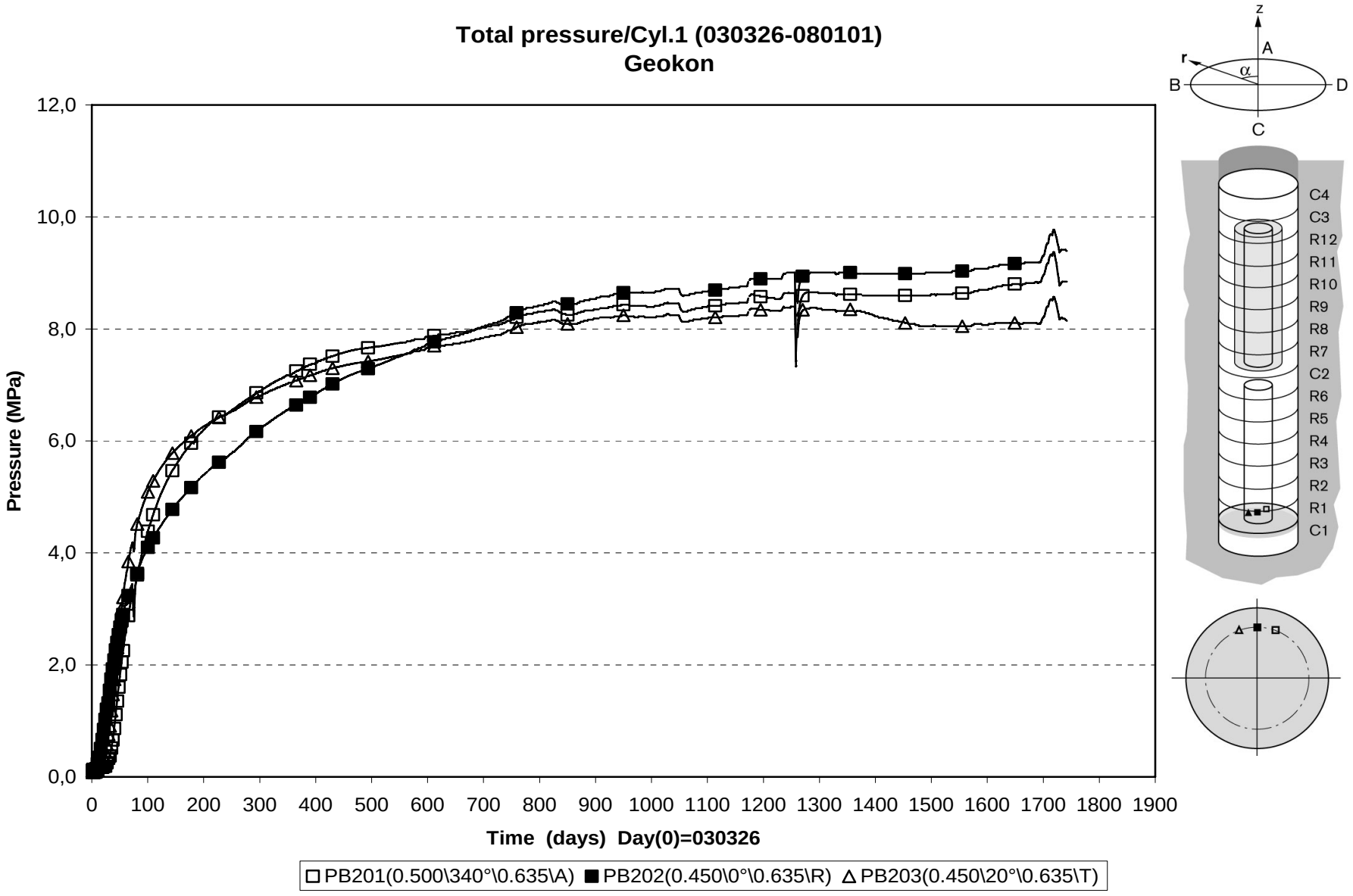
Total pressure/Cyl.1 (030326-080101)
Geokon
Pressure (MPa)
12,0
10,0
8,0
6,0
4,0
2,0
0,0
0
100
200
300
400
500
600
700
800
900
1000
1100
1200
1300
1400
1500
1600
1700
1800
1900
Time (days) Day(0)=030326
PB201(0.500\340°\0.635\A)
PB202(0.450\0°\0.635\R)
PB203(0.450\20°\0.635\T)
z
A
r
α
B
D
C
C4
C3
R12
R11
R10
R9
R8
R7
C2
R6
R5
R4
R3
R2
R1
C1

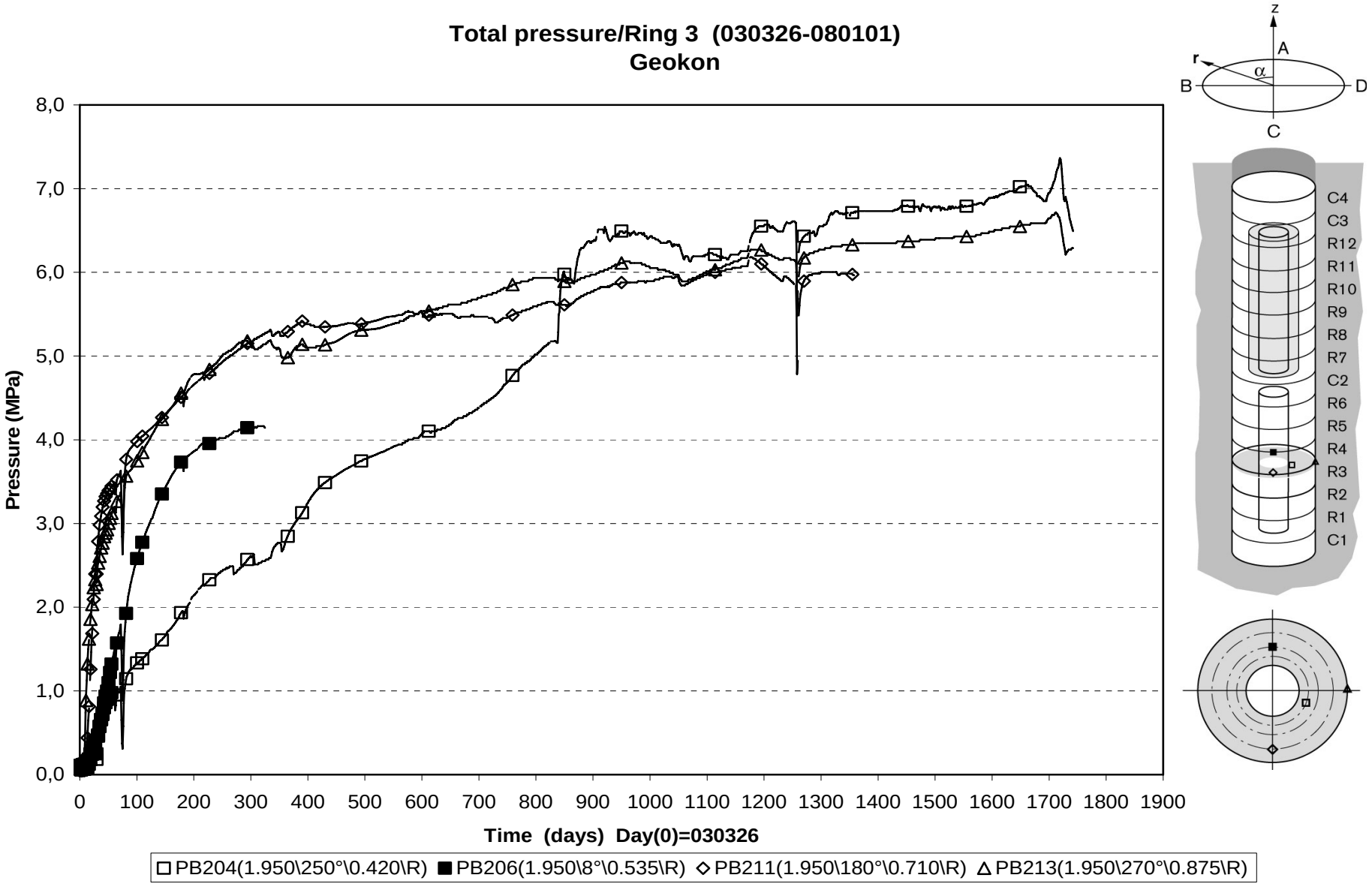
Total pressure/Ring 3 (030326-080101)
Geokon
Pressure (MPa)
8,0
7,0
6,0
5,0
4,0
3,0
2,0
1,0
0,0
0
100
200
300
400
500
600
700
800
900
1000
1100
1200
1300
1400
1500
1600
1700
1800
1900
Time (days) Day(0)=030326
PB204(1.950\250°\0.420\R)
PB206(1.950\8°\0.535\R)
PB211(1.950\180°\0.710\R)
PB213(1.950\270°\0.875\R)
z
A
r
α
B
D
C
C4
C3
R12
R11
R10
R9
R8
R7
C2
R6
R5
R4
R3
R2
R1
C1

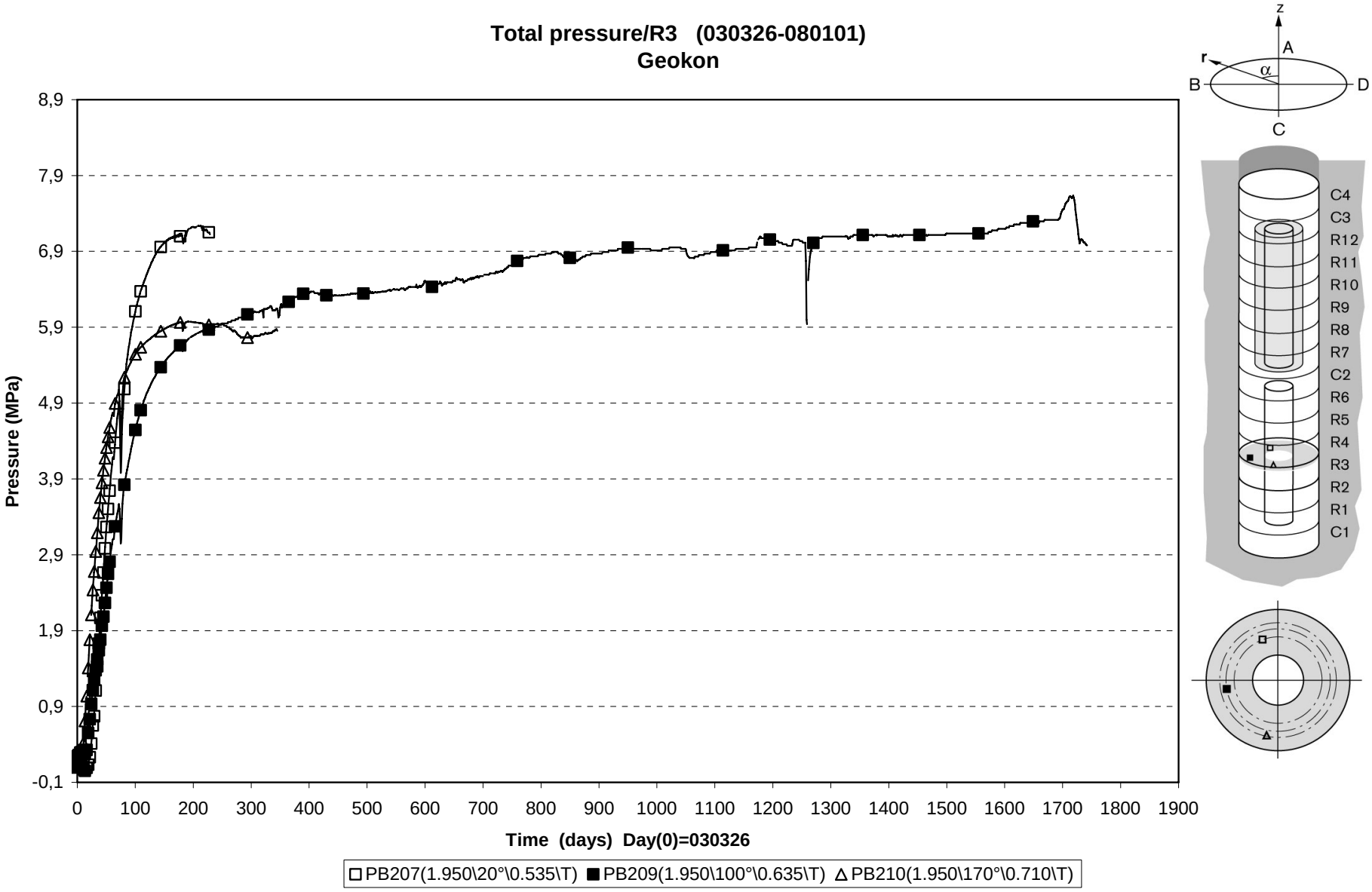
Total pressure/R3 (030326-080101)
Geokon
Pressure (MPa)
8,9
7,9
6,9
5,9
4,9
3,9
2,9
1,9
0,9
-0,1
0
100
200
300
400
500
600
700
800
900
1000
1100
1200
1300
1400
1500
1600
1700
1800
1900
Time (days) Day(0)=030326
PB207(1.950\20°\0.535\T)
PB209(1.950\100°\0.635\T)
PB210(1.950\170°\0.710\T)
z
A
r
α
B
D
C
C4
C3
R12
R11
R10
R9
R8
R7
C2
R6
R5
R4
R3
R2
R1
C1

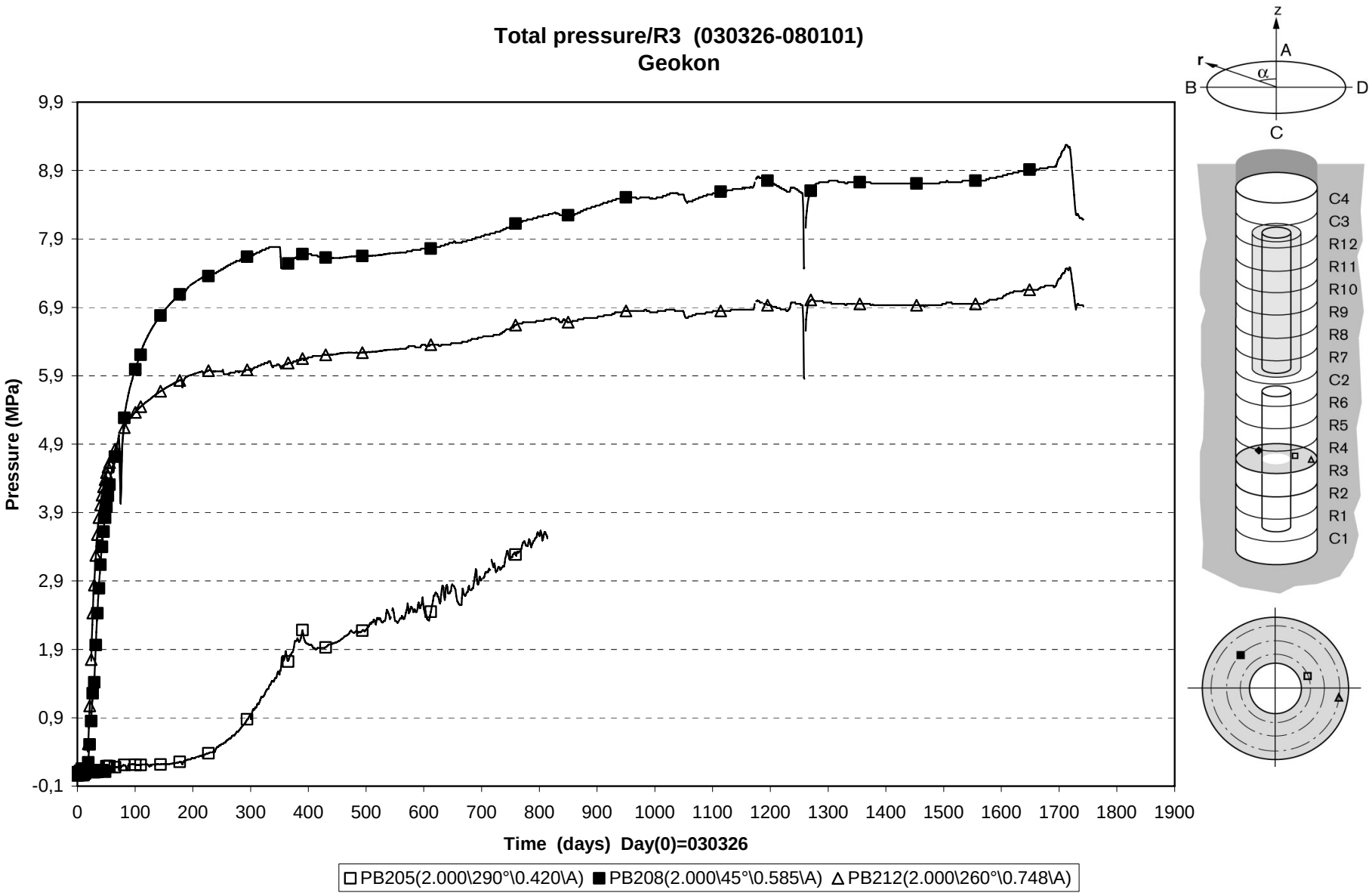
Total pressure/R3 (030326-080101)
Geokon
Pressure (MPa)
9,9
8,9
7,9
6,9
5,9
4,9
3,9
2,9
1,9
0,9
-0,1
0
100
200
300
400
500
600
700
800
900
1000
1100
1200
1300
1400
1500
1600
1700
1800
1900
Time (days) Day(0)=030326
PB205(2.000\290°\0.420\A)
PB208(2.000\45°\0.585\A)
PB212(2.000\260°\0.748\A)
z
A
r
α
B
D
C
C4
C3
R12
R11
R10
R9
R8
R7
C2
R6
R5
R4
R3
R2
R1
C1

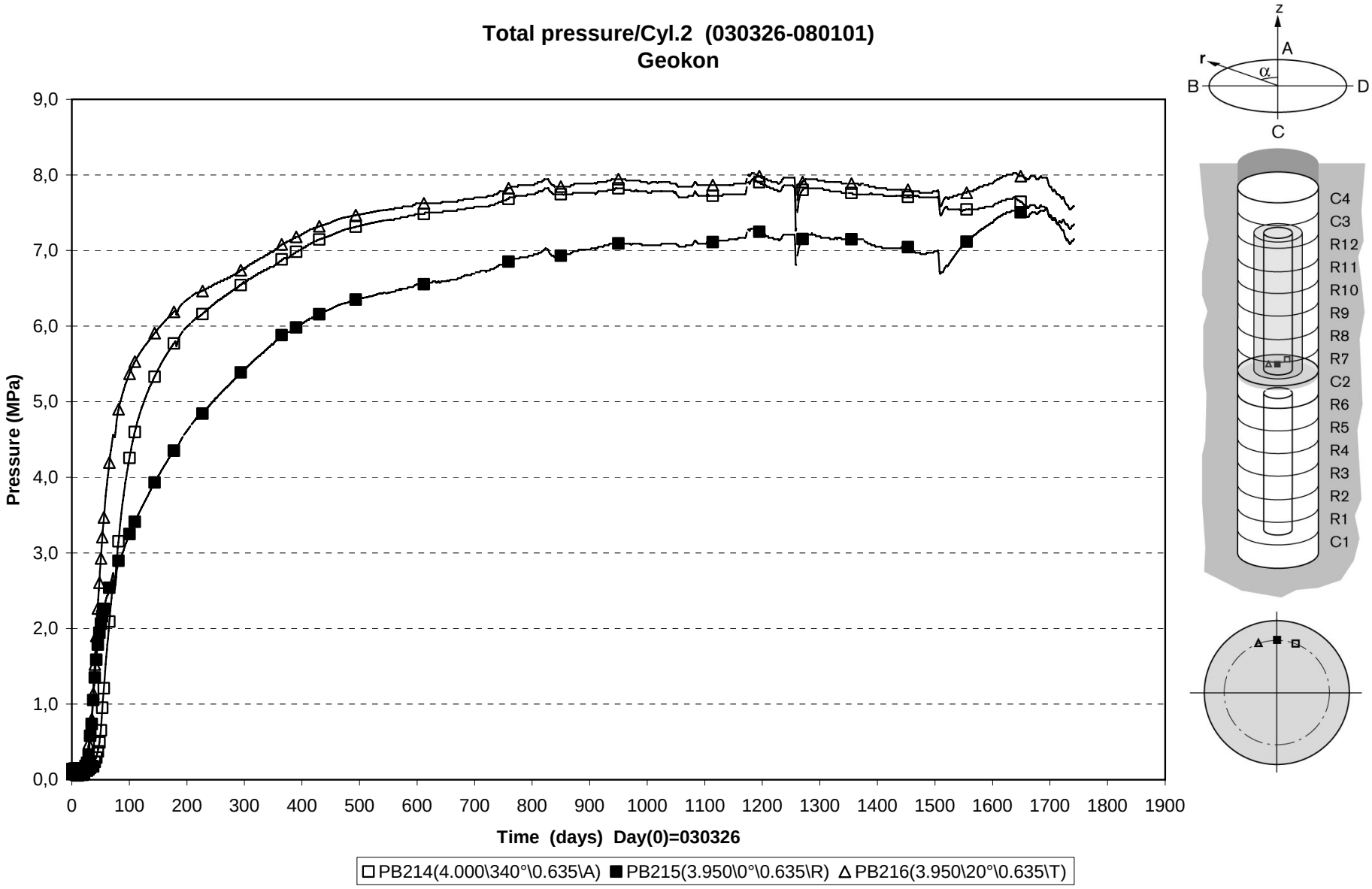
Total pressure/Cyl.2 (030326-080101)
Geokon
Pressure (MPa)
9,0
8,0
7,0
6,0
5,0
4,0
3,0
2,0
1,0
0,0
0
100
200
300
400
500
600
700
800
900
1000
1100
1200
1300
1400
1500
1600
1700
1800
1900
Time (days) Day(0)=030326
PB214(4.000\340°\0.635\A)
PB215(3.950\0°\0.635\R)
PB216(3.950\20°\0.635\T)
z
A
r
α
B
D
C
C4
C3
R12
R11
R10
R9
R8
R7
C2
R6
R5
R4
R3
R2
R1
C1

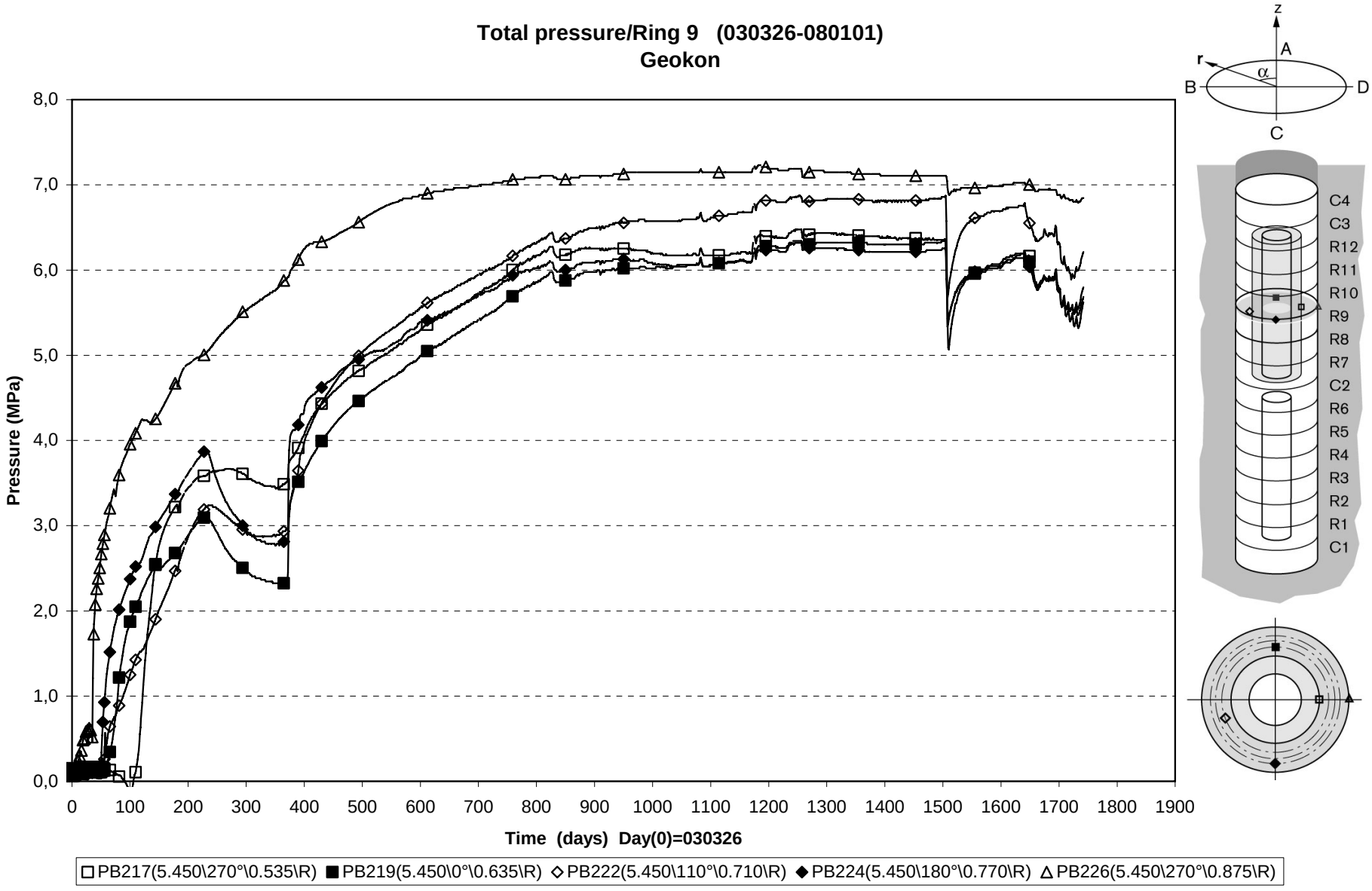
Total pressure/Ring 9 (030326-080101)
Geokon
Pressure (MPa)
8,0
7,0
6,0
5,0
4,0
3,0
2,0
1,0
0,0
0
100
200
300
400
500
600
700
800
900
1000
1100
1200
1300
1400
1500
1600
1700
1800
1900
Time (days) Day(0)=030326
z
A
r
α
B
D
C
C4
C3
R12
R11
R10
R9
R8
R7
C2
R6
R5
R4
R3
R2
R1
C1
PB217(5.450\270°\0.535\R)
PB219(5.450\0°\0.635\R)
PB222(5.450\110°\0.710\R)
PB224(5.450\180°\0.770\R)
PB226(5.450\270°\0.875\R)

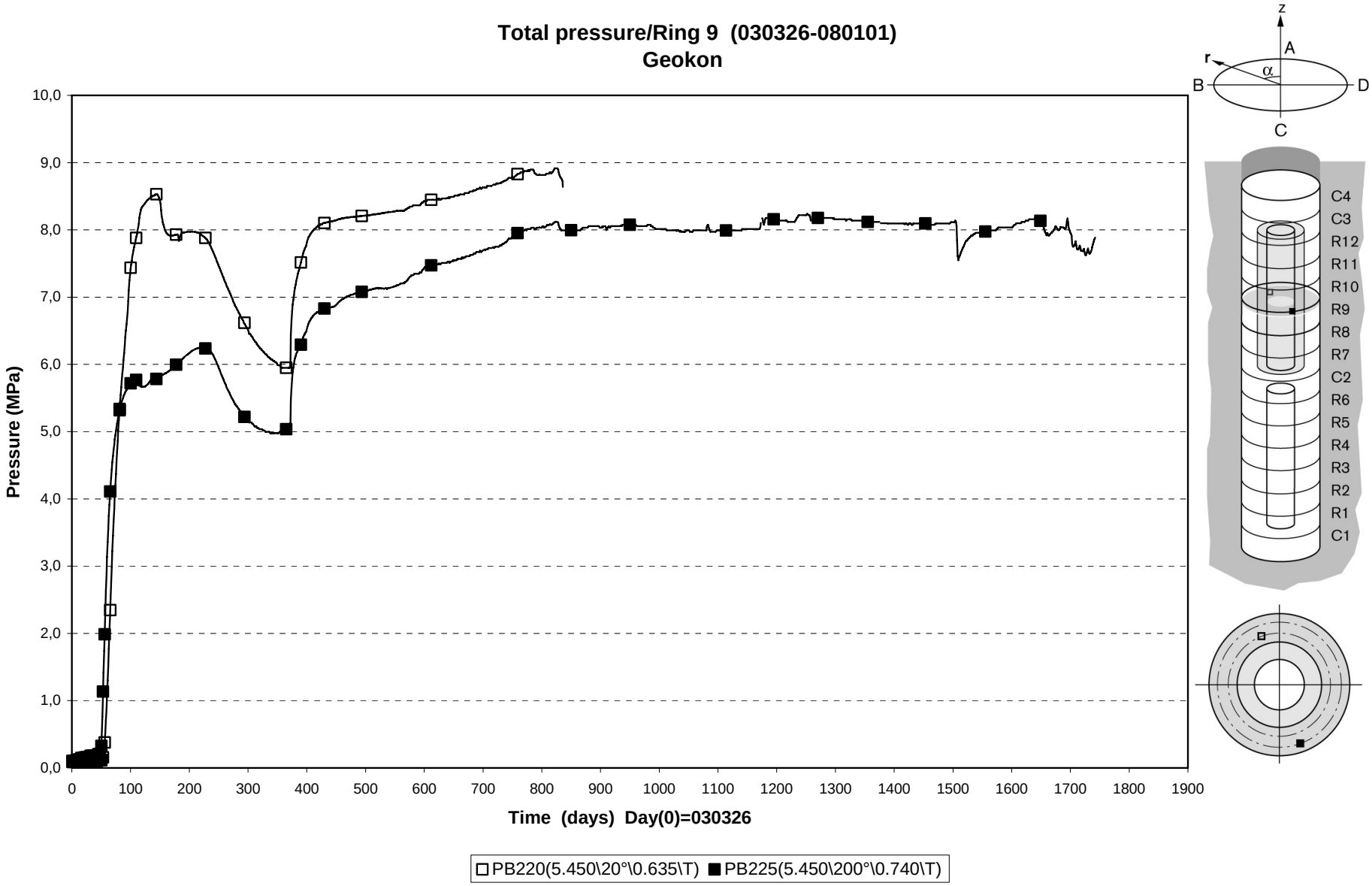
Total pressure/Ring 9 (030326-080101)
Geokon
Pressure (MPa)
Time (days) Day(0)=030326
PB220(5.450\20°\0.635\T)
PB225(5.450\200°\0.740\T)
z
A
r
α
B
D
C
C4
C3
R12
R11
R10
R9
R8
R7
C2
R6
R5
R4
R3
R2
R1
C1

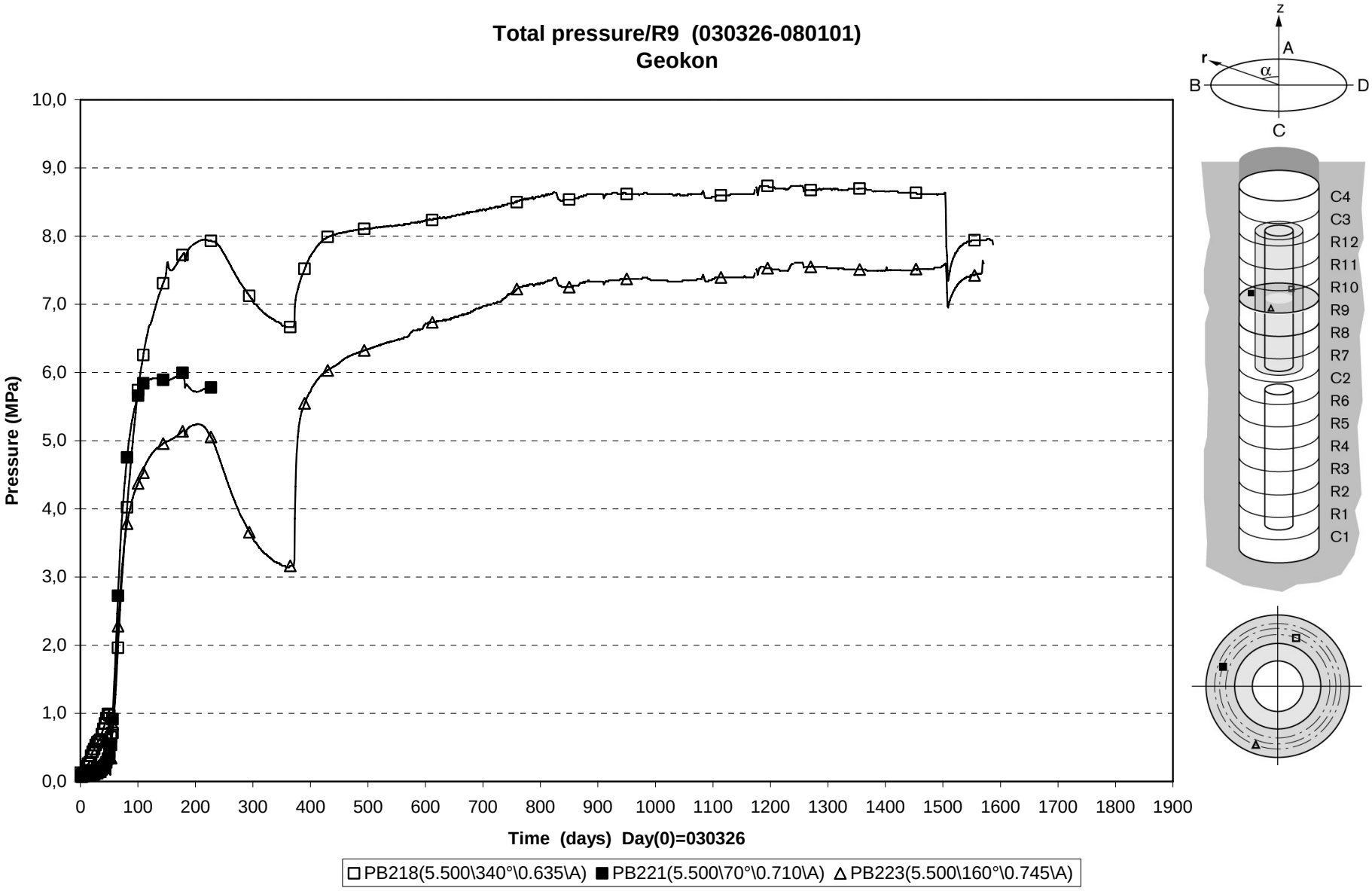
Total pressure/R9 (030326-080101)
Geokon
Pressure (MPa)
10,0
9,0
8,0
7,0
6,0
5,0
4,0
3,0
2,0
1,0
0,0
0
100
200
300
400
500
600
700
800
900
1000
1100
1200
1300
1400
1500
1600
1700
1800
1900
Time (days) Day(0)=030326
PB218(5.500\340°\0.635\A)
PB221(5.500\70°\0.710\A)
PB223(5.500\160°\0.745\A)
z
A
r
α
B
D
C
C4
C3
R12
R11
R10
R9
R8
R7
C2
R6
R5
R4
R3
R2
R1
C1

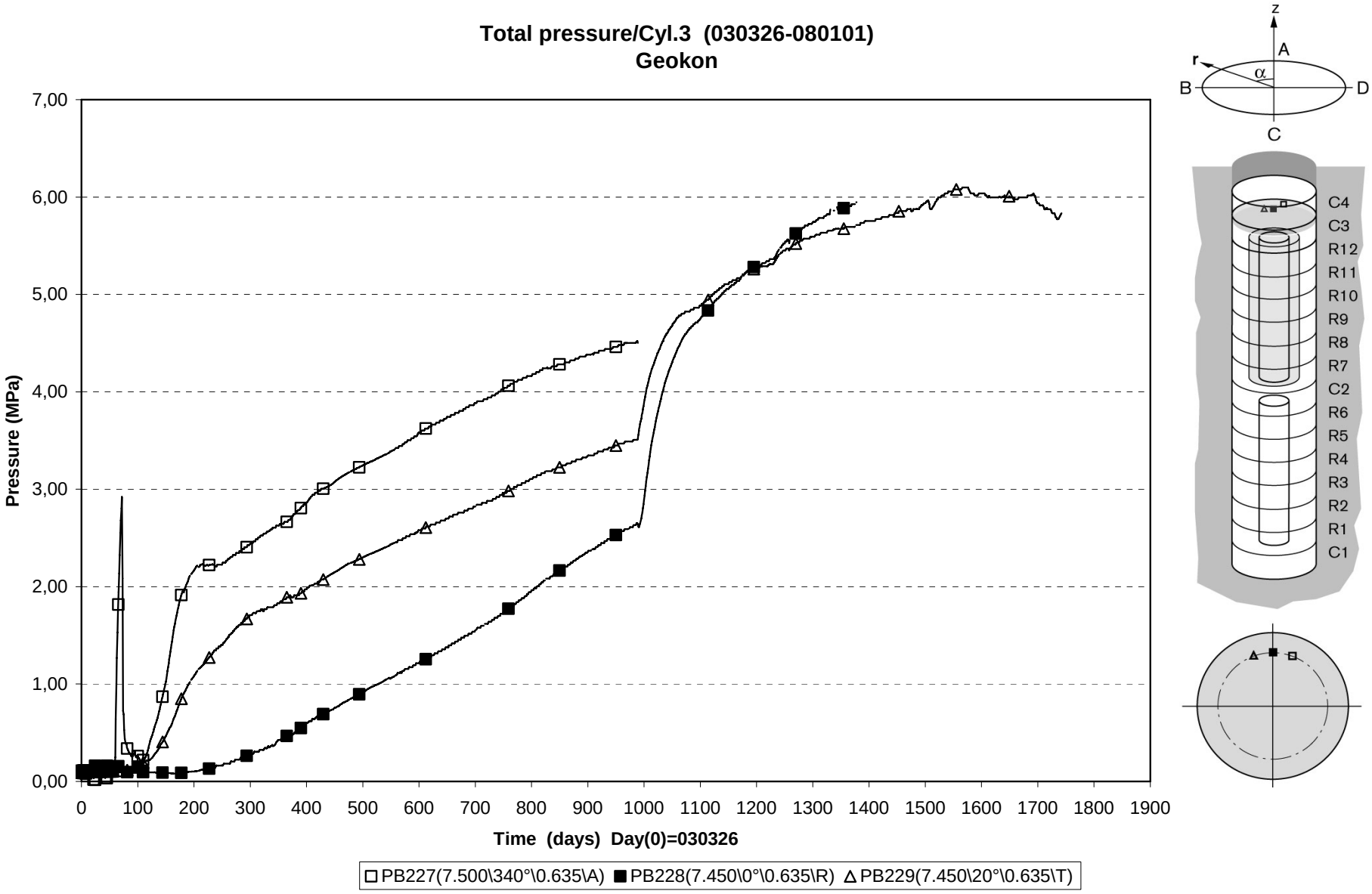
Total pressure/Cyl.3 (030326-080101)
Geokon
Pressure (MPa)
7,00
6,00
5,00
4,00
3,00
2,00
1,00
0,00
0
100
200
300
400
500
600
700
800
900
1000
1100
1200
1300
1400
1500
1600
1700
1800
1900
Time (days) Day(0)=030326
PB227(7.500\340°\0.635\A)
PB228(7.450\0°\0.635\R)
PB229(7.450\20°\0.635\T)
z
A
r
α
B
D
C
C4
C3
R12
R11
R10
R9
R8
R7
C2
R6
R5
R4
R3
R2
R1
C1

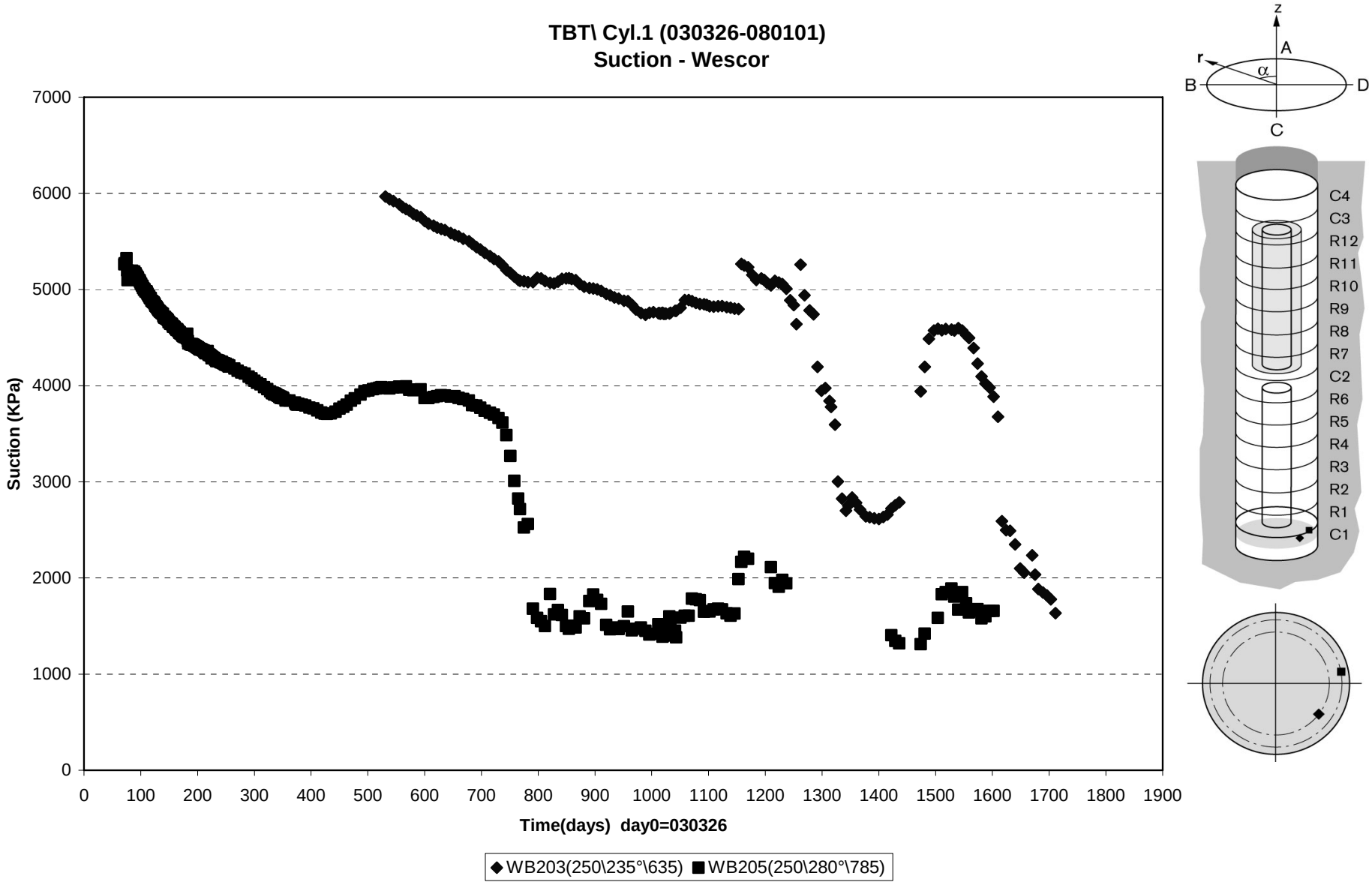
TBT\ Cyl.1 (030326-080101)
Suction - Wescor
Suction (KPa)
7000
6000
5000
4000
3000
2000
1000
0
0
100
200
300
400
500
600
700
800
900
1000
1100
1200
1300
1400
1500
1600
1700
1800
1900
Time(days) day0=030326
WB203(250\235°\635)
WB205(250\280°\785)
z
A
r
α
B
D
C
C4
C3
R12
R11
R10
R9
R8
R7
C2
R6
R5
R4
R3
R2
R1
C1

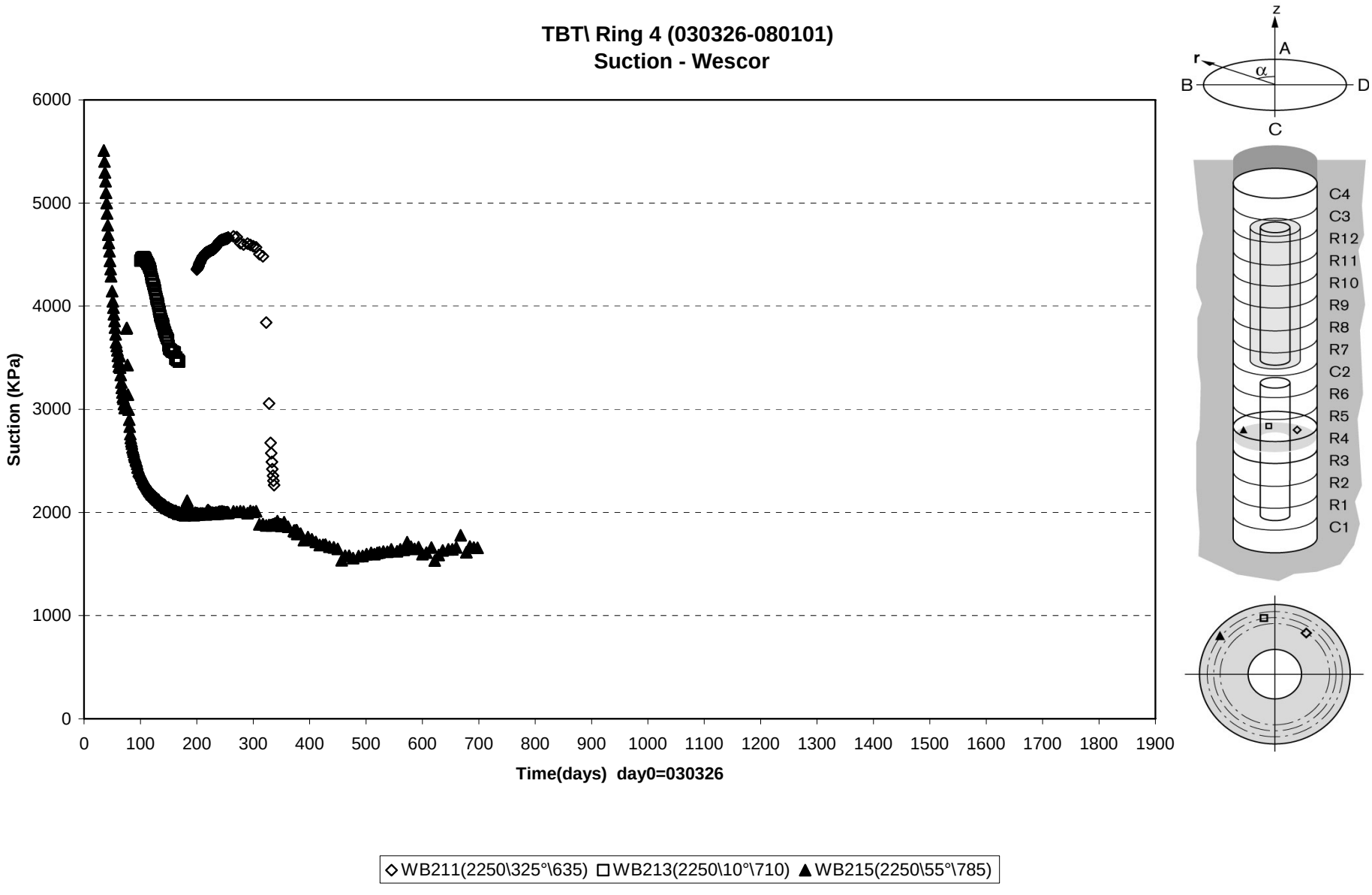
TBT\ Ring 4 (030326-080101)
Suction - Wescor
Suction (KPa)
Time(days) day0=030326
0
1000
2000
3000
4000
5000
6000
0
100
200
300
400
500
600
700
800
900
1000
1100
1200
1300
1400
1500
1600
1700
1800
1900
z
A
r
α
B
D
C
C4
C3
R12
R11
R10
R9
R8
R7
C2
R6
R5
R4
R3
R2
R1
C1
◇WB211(2250\325°\635) □WB213(2250\10°\710) ▲WB215(2250\55°\785)

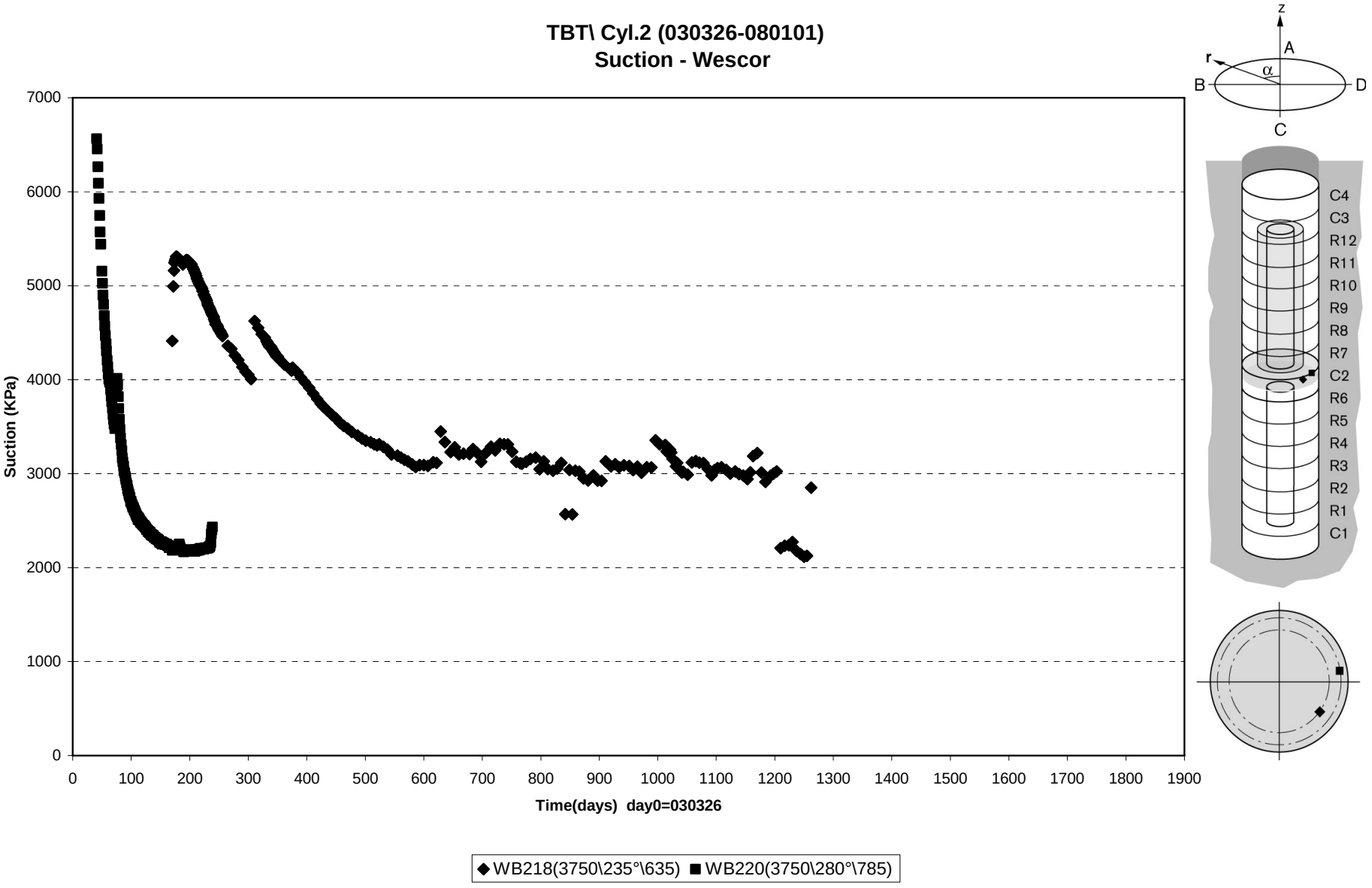
TBT\ Cyl.2 (030326-080101)
Suction - Wescor
Suction (KPa)
Time(days) day0=030326
WB218(3750\235°\635)
WB220(3750\280°\785)
z
A
r
α
B
D
C
C4
C3
R12
R11
R10
R9
R8
R7
C2
R6
R5
R4
R3
R2
R1
C1

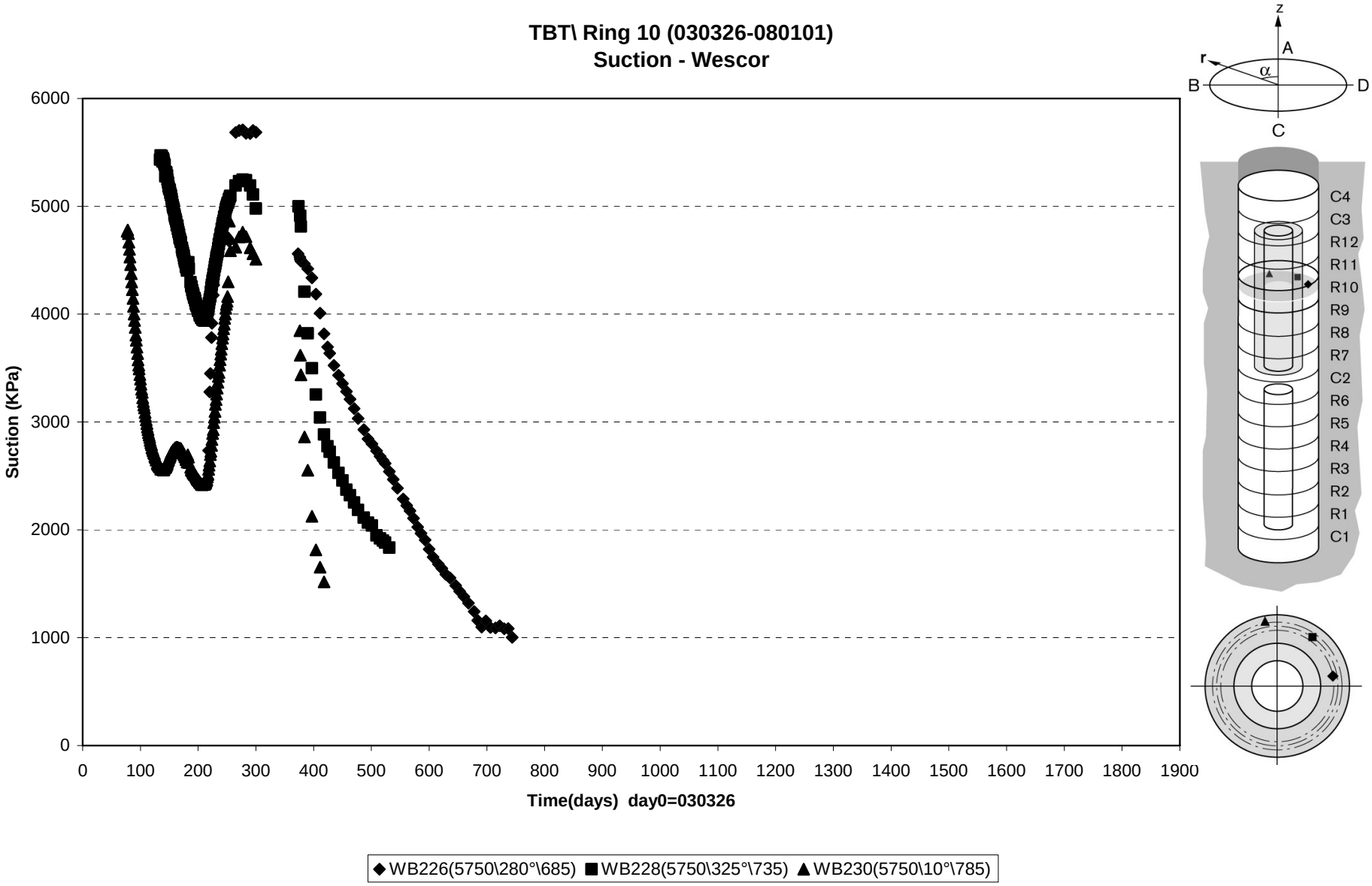
TBT\ Ring 10 (030326-080101)
Suction - Wescor
Suction (KPa)
Time(days) day0=030326
0
1000
2000
3000
4000
5000
6000
0
100
200
300
400
500
600
700
800
900
1000
1100
1200
1300
1400
1500
1600
1700
1800
1900
z
A
r
α
B
D
C
C4
C3
R12
R11
R10
R9
R8
R7
C2
R6
R5
R4
R3
R2
R1
C1
WB226(5750\280°\685)
WB228(5750\325°\735)
WB230(5750\10°\785)

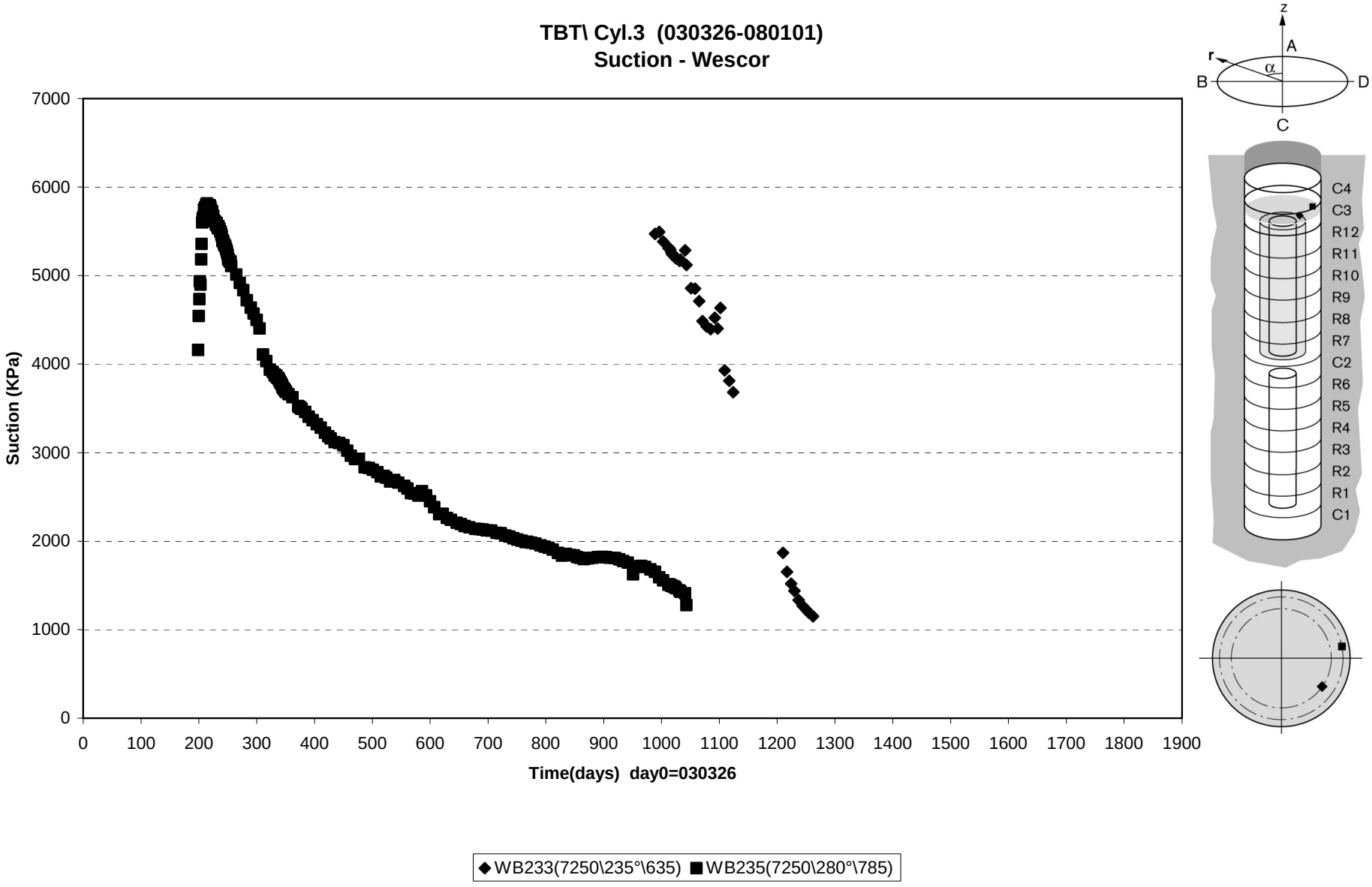
TBT\ Cyl.3 (030326-080101)
Suction - Wescor
Suction (KPa)
7000
6000
5000
4000
3000
2000
1000
0
0
100
200
300
400
500
600
700
800
900
1000
1100
1200
1300
1400
1500
1600
1700
1800
1900
Time(days) day0=030326
z
A
r
α
B
D
C
C4
C3
R12
R11
R10
R9
R8
R7
C2
R6
R5
R4
R3
R2
R1
C1
WB233(7250\235°\635)
WB235(7250\280°\785)

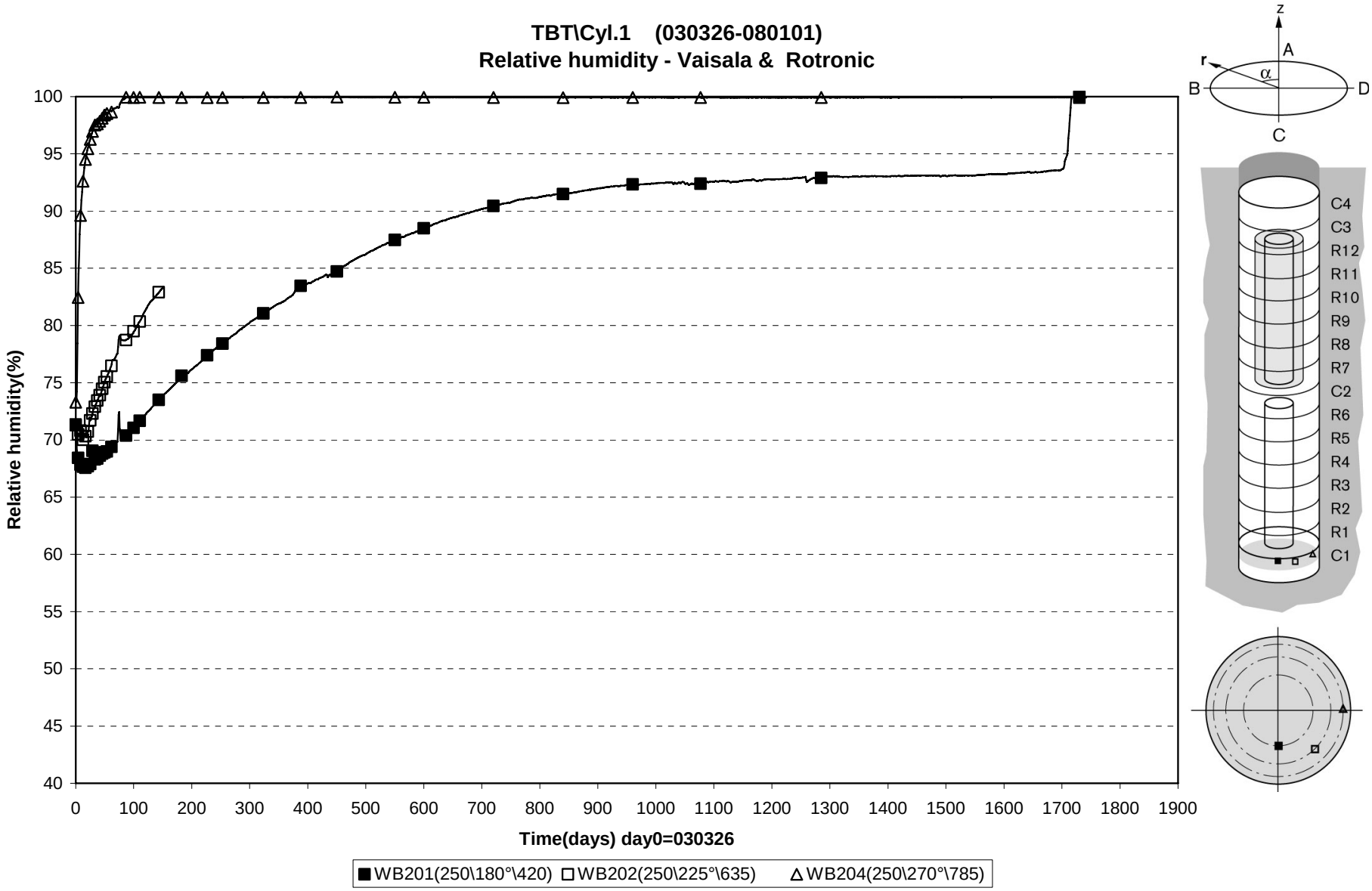
TBT\Cyl.1 (030326-080101)
Relative humidity - Vaisala & Rotronic
Relative humidity(%)
100
95
90
85
80
75
70
65
60
55
50
45
40
0
100
200
300
400
500
600
700
800
900
1000
1100
1200
1300
1400
1500
1600
1700
1800
1900
Time(days) day0=030326
WB201(250\180°\420)
WB202(250\225°\635)
WB204(250\270°\785)
z
A
r
α
B
D
C
C4
C3
R12
R11
R10
R9
R8
R7
C2
R6
R5
R4
R3
R2
R1
C1

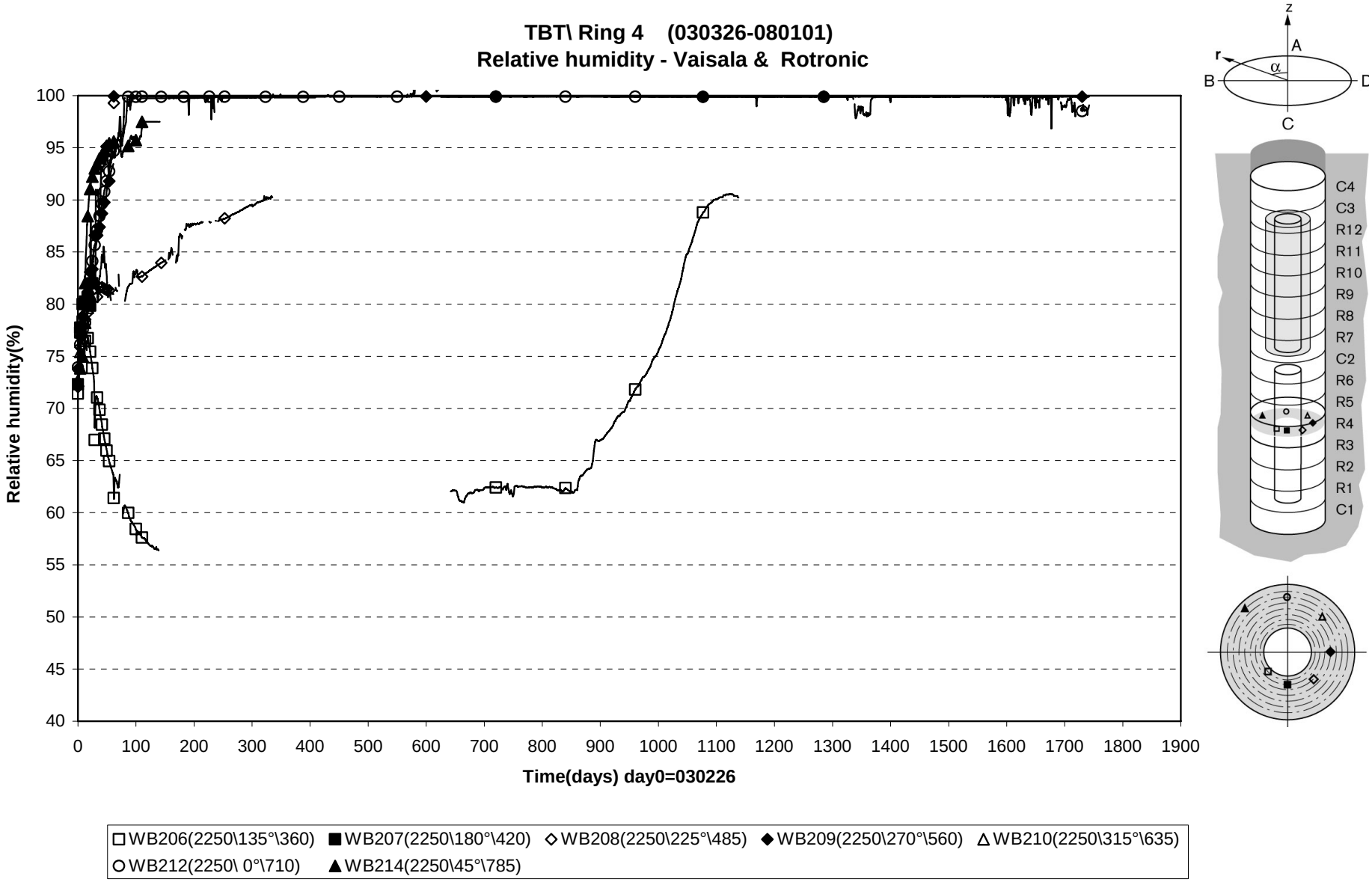
TBT\ Ring 4 (030326-080101)
Relative humidity - Vaisala & Rotronic
Relative humidity(%)
Time(days) day0=030226
100
95
90
85
80
75
70
65
60
55
50
45
40
0
100
200
300
400
500
600
700
800
900
1000
1100
1200
1300
1400
1500
1600
1700
1800
1900
z
A
r
α
B
D
C
C4
C3
R12
R11
R10
R9
R8
R7
C2
R6
R5
R4
R3
R2
R1
C1
WB206(2250\135°\360)
WB207(2250\180°\420)
WB208(2250\225°\485)
WB209(2250\270°\560)
WB210(2250\315°\635)
WB212(2250\ 0°\710)
WB214(2250\45°\785)

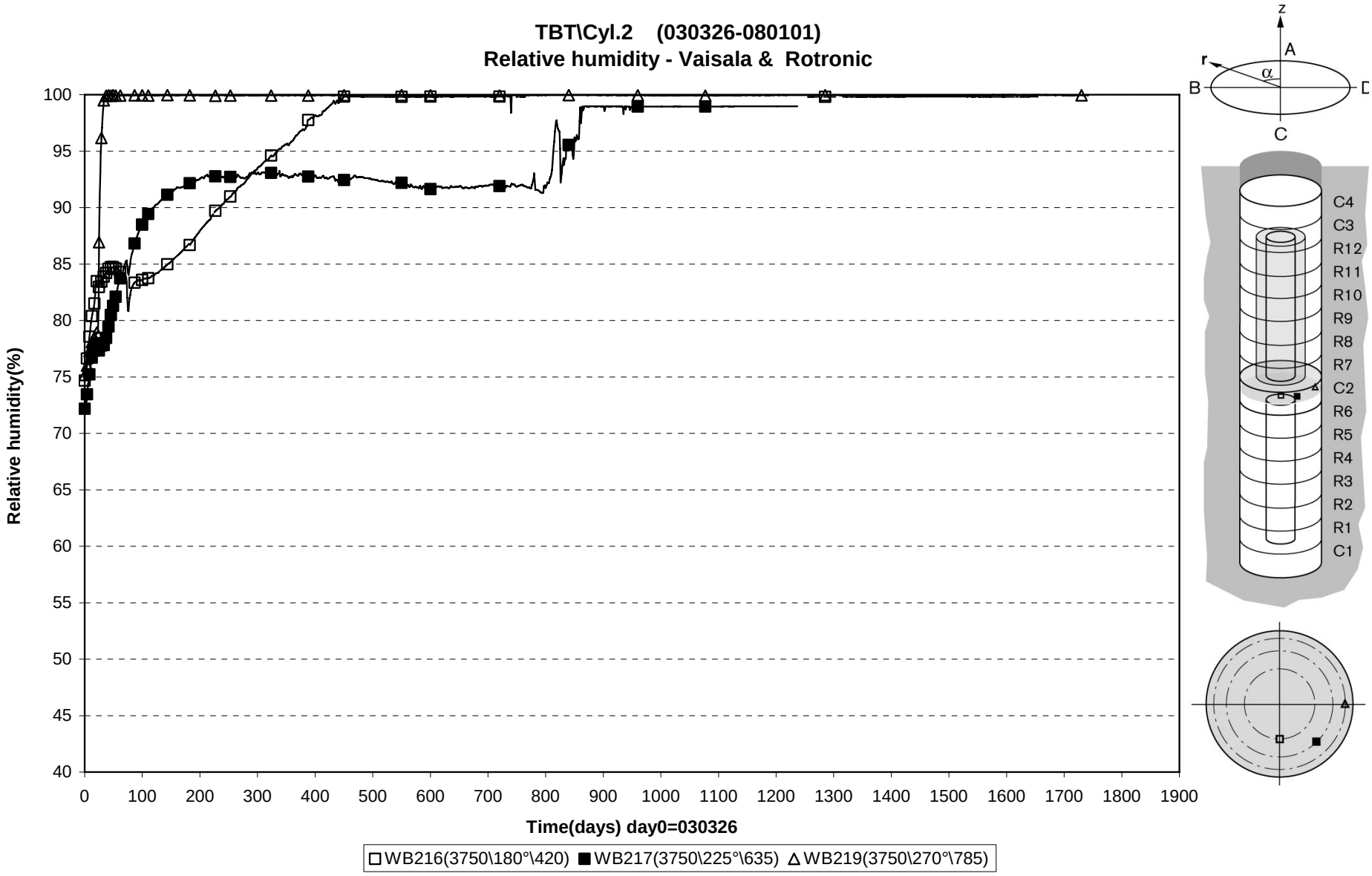
TBT\Cyl.2 (030326-080101)
Relative humidity - Vaisala & Rotronic
Relative humidity(%)
100
95
90
85
80
75
70
65
60
55
50
45
40
0
100
200
300
400
500
600
700
800
900
1000
1100
1200
1300
1400
1500
1600
1700
1800
1900
Time(days) day0=030326
WB216(3750\180°\420)
WB217(3750\225°\635)
WB219(3750\270°\785)
z
A
r
α
B
D
C
C4
C3
R12
R11
R10
R9
R8
R7
C2
R6
R5
R4
R3
R2
R1
C1

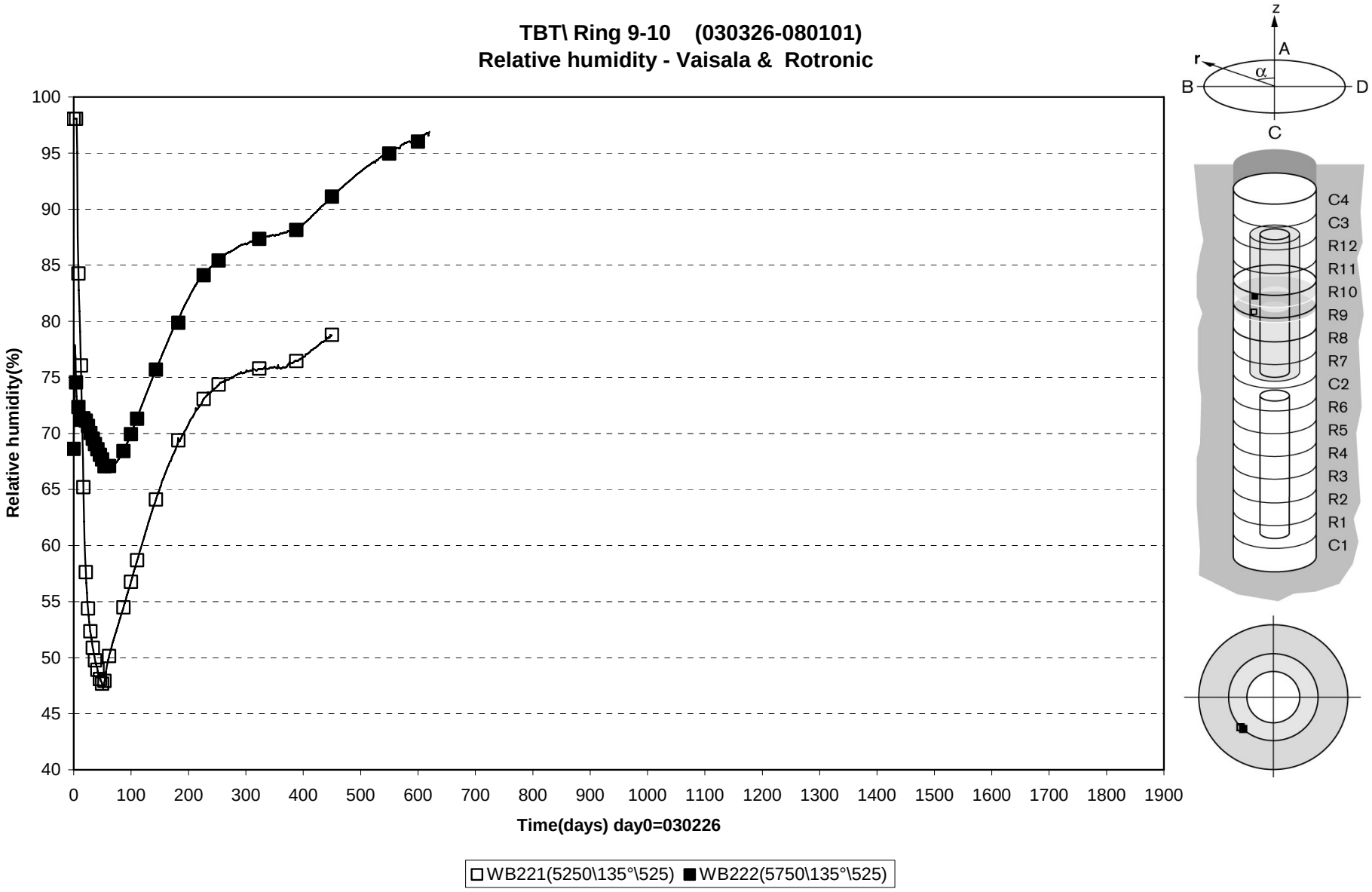
TBT\ Ring 9-10 (030326-080101)
Relative humidity - Vaisala & Rotronic
Relative humidity(%)
Time(days) day0=030226
WB221(5250\135°\525)
WB222(5750\135°\525)
z
A
r
α
B
D
C
C4
C3
R12
R11
R10
R9
R8
R7
C2
R6
R5
R4
R3
R2
R1
C1

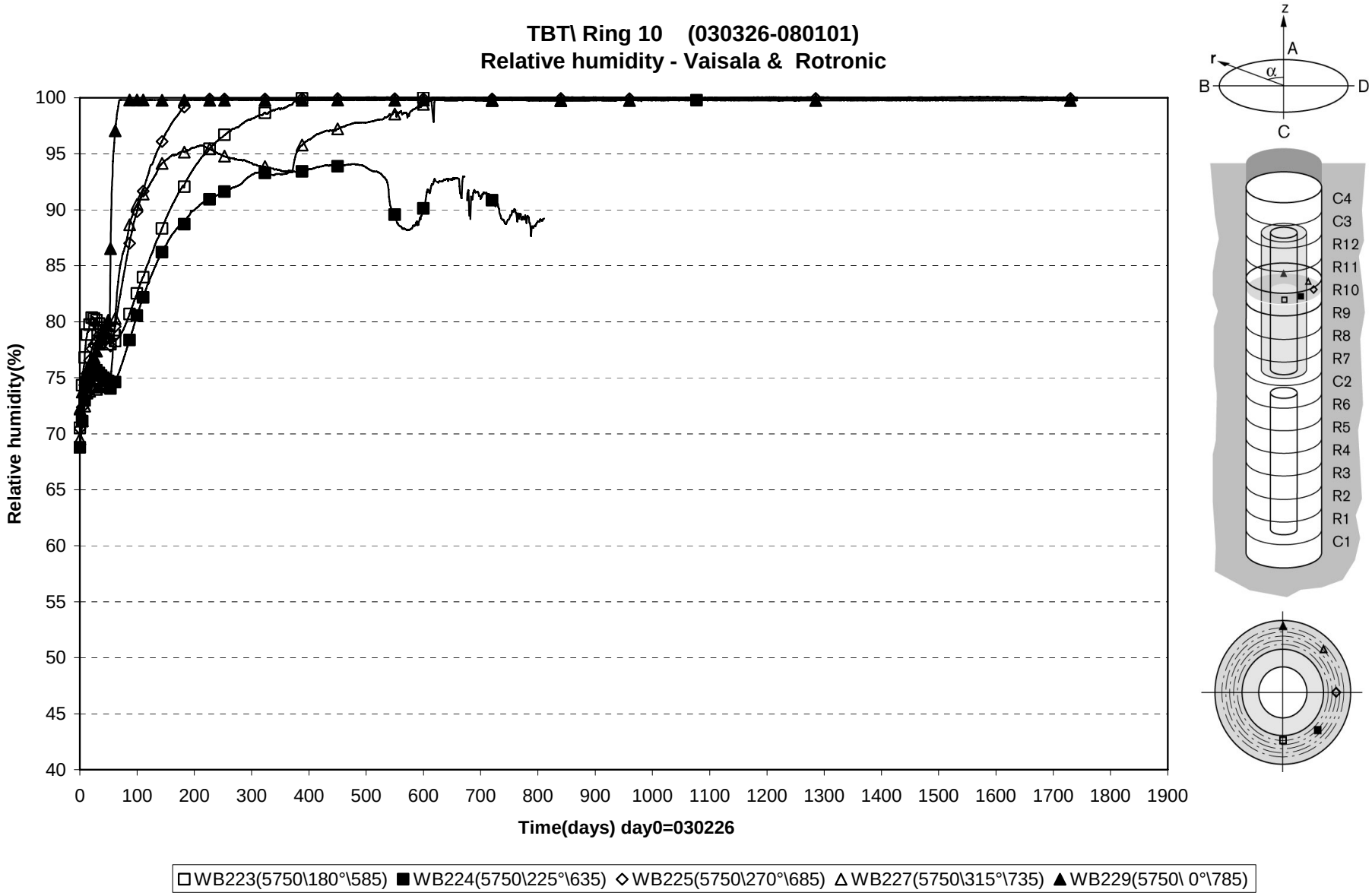
TBT\ Ring 10 (030326-080101)
Relative humidity - Vaisala & Rotronic
Relative humidity(%)
Time(days) day0=030226
WB223(5750\180°\585)
WB224(5750\225°\635)
WB225(5750\270°\685)
WB227(5750\315°\735)
WB229(5750\ 0°\785)
z
A
r
α
B
D
C
C4
C3
R12
R11
R10
R9
R8
R7
C2
R6
R5
R4
R3
R2
R1
C1

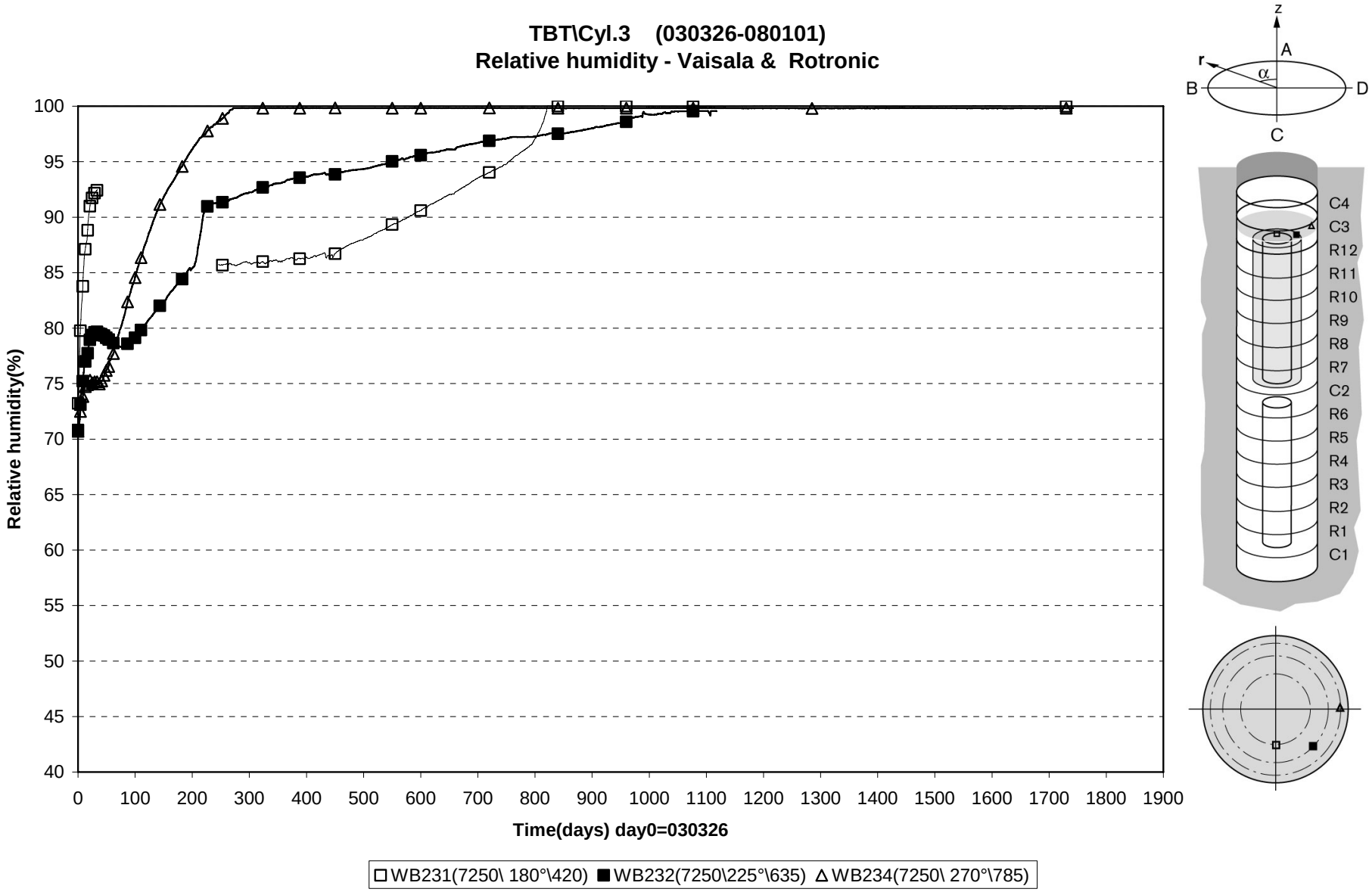
TBT\Cyl.3 (030326-080101)
Relative humidity - Vaisala & Rotronic
Relative humidity(%)
100
95
90
85
80
75
70
65
60
55
50
45
40
0
100
200
300
400
500
600
700
800
900
1000
1100
1200
1300
1400
1500
1600
1700
1800
1900
Time(days) day0=030326
WB231(7250\ 180°\420)
WB232(7250\225°\635)
WB234(7250\ 270°\785)
z
A
r
α
B
D
C
C4
C3
R12
R11
R10
R9
R8
R7
C2
R6
R5
R4
R3
R2
R1
C1

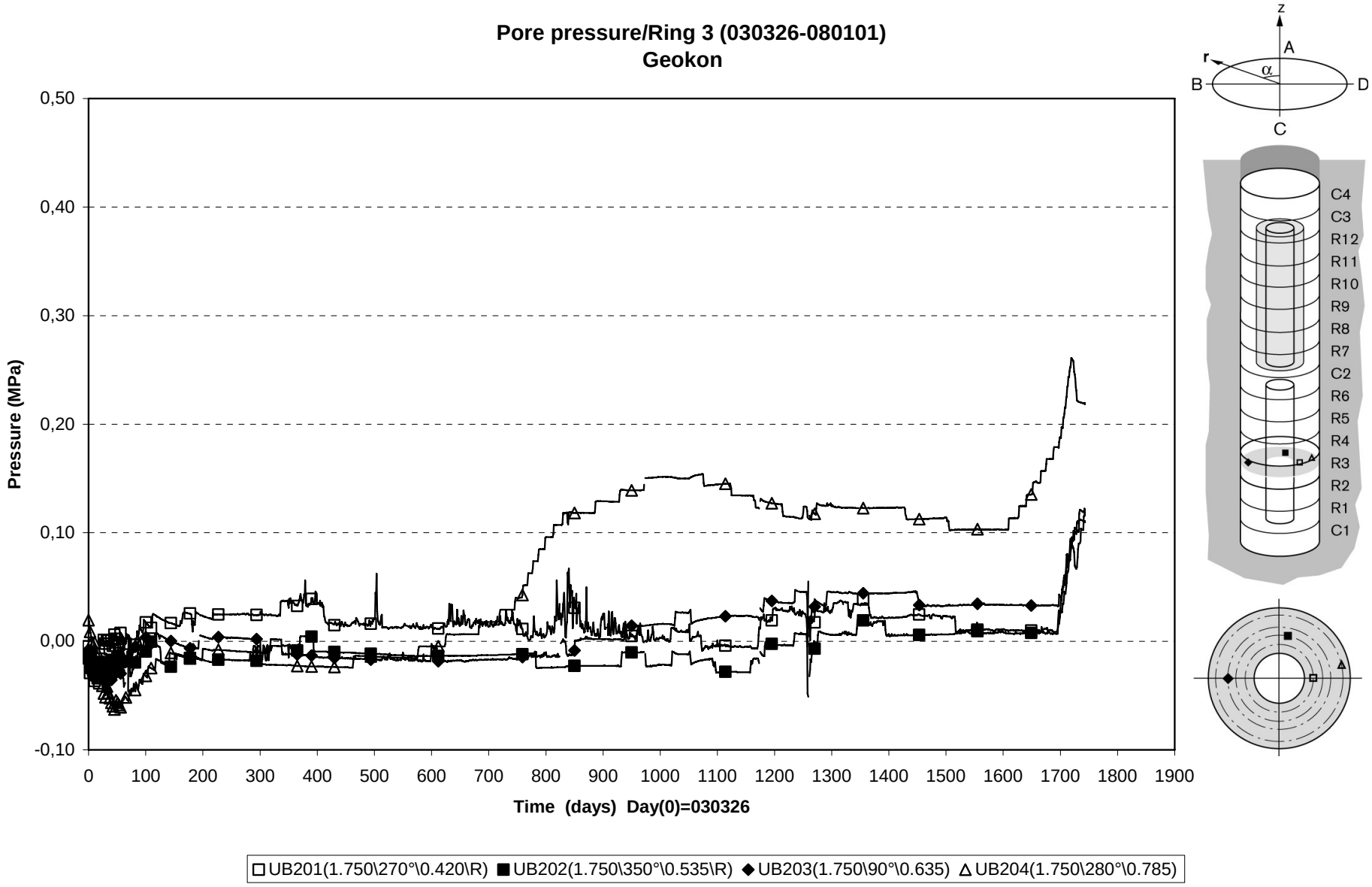
Pore pressure/Ring 3 (030326-080101)
Geokon
Pressure (MPa)
0,50
0,40
0,30
0,20
0,10
0,00
-0,10
0
100
200
300
400
500
600
700
800
900
1000
1100
1200
1300
1400
1500
1600
1700
1800
1900
Time (days) Day(0)=030326
z
A
r
α
B
D
C
C4
C3
R12
R11
R10
R9
R8
R7
C2
R6
R5
R4
R3
R2
R1
C1
UB201(1.750\270°\0.420\R)
UB202(1.750\350°\0.535\R)
UB203(1.750\90°\0.635)
UB204(1.750\280°\0.785)

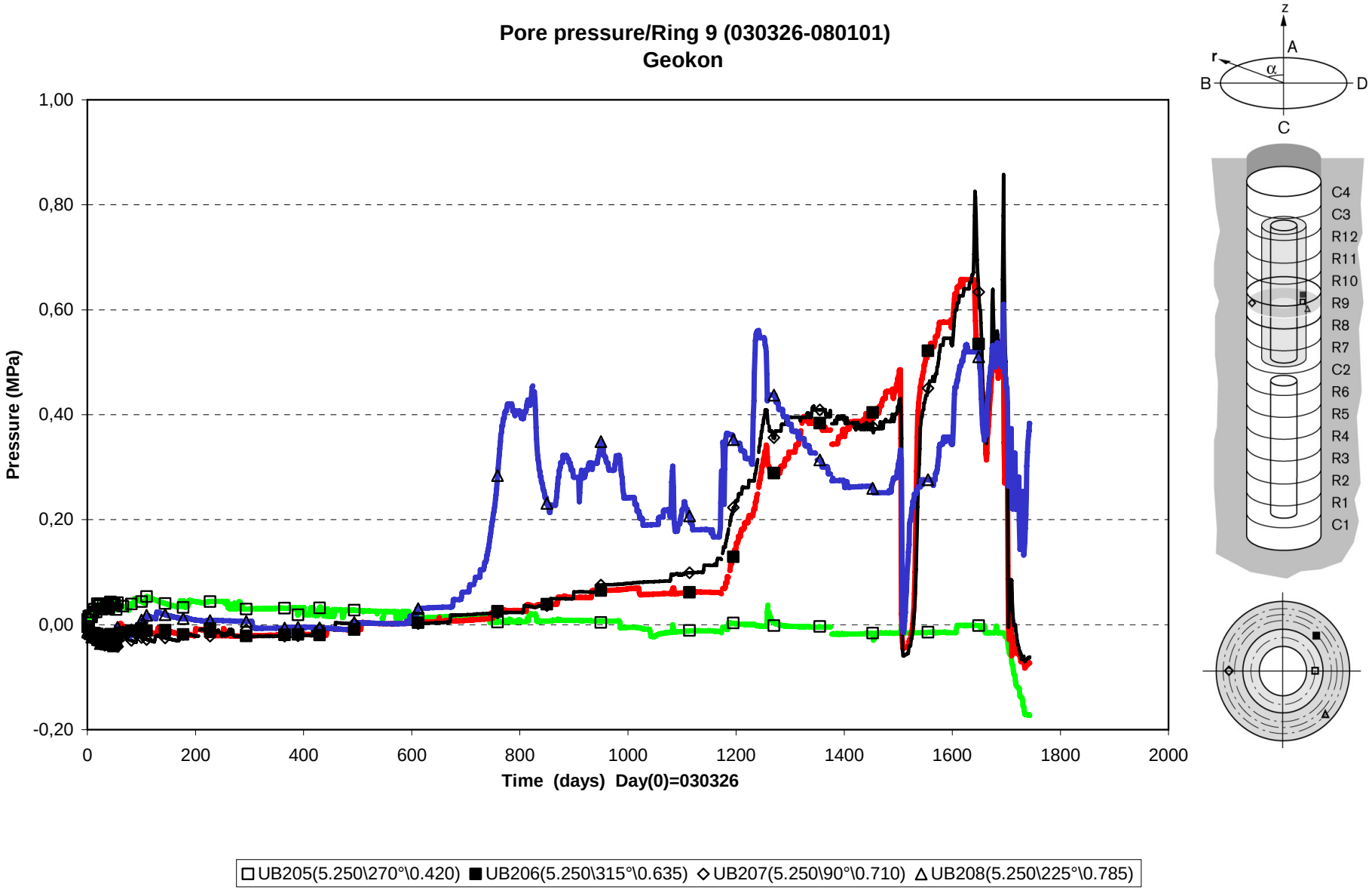
Pore pressure/Ring 9 (030326-080101)
Geokon
Pressure (MPa)
1,00
0,80
0,60
0,40
0,20
0,00
-0,20
0
200
400
600
800
1000
1200
1400
1600
1800
2000
Time (days) Day(0)=030326
z
A
r
α
B
D
C
C4
C3
R12
R11
R10
R9
R8
R7
C2
R6
R5
R4
R3
R2
R1
C1
UB205(5.250\270°\0.420)
UB206(5.250\315°\0.635)
UB207(5.250\90°\0.710)
UB208(5.250\225°\0.785)

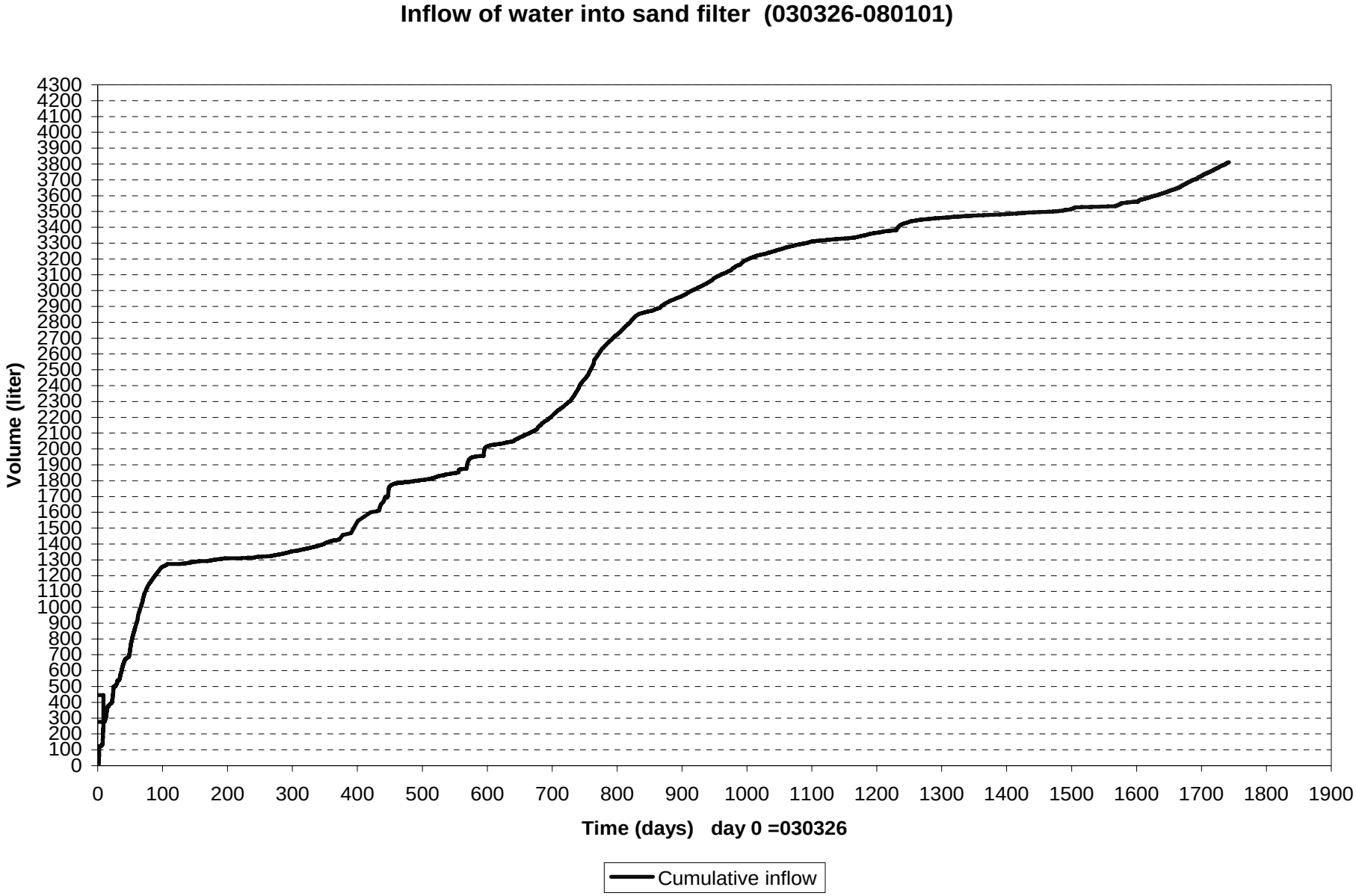
Inflow of water into sand filter (030326-080101)
Volume (liter)
4300
4200
4100
4000
3900
3800
3700
3600
3500
3400
3300
3200
3100
3000
2900
2800
2700
2600
2500
2400
2300
2200
2100
2000
1900
1800
1700
1600
1500
1400
1300
1200
1100
1000
900
800
700
600
500
400
300
200
100
0
0
100
200
300
400
500
600
700
800
900
1000
1100
1200
1300
1400
1500
1600
1700
1800
1900
Time (days) day 0 =030326
Cumulative inflow

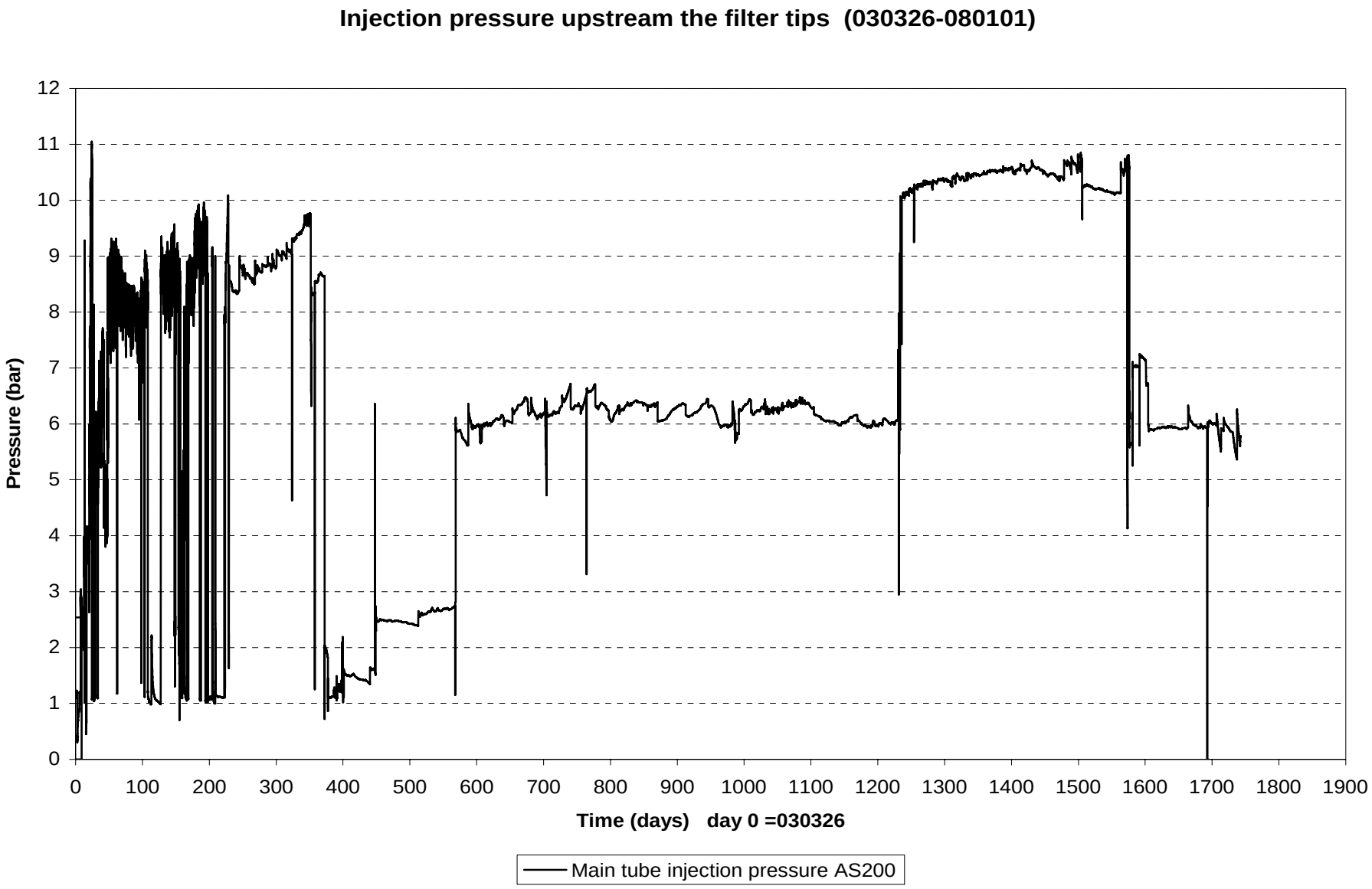
Injection pressure upstream the filter tips (030326-080101)
Pressure (bar)
0
1
2
3
4
5
6
7
8
9
10
11
12
0
100
200
300
400
500
600
700
800
900
1000
1100
1200
1300
1400
1500
1600
1700
1800
1900
Time (days) day 0 =030326
Main tube injection pressure AS200

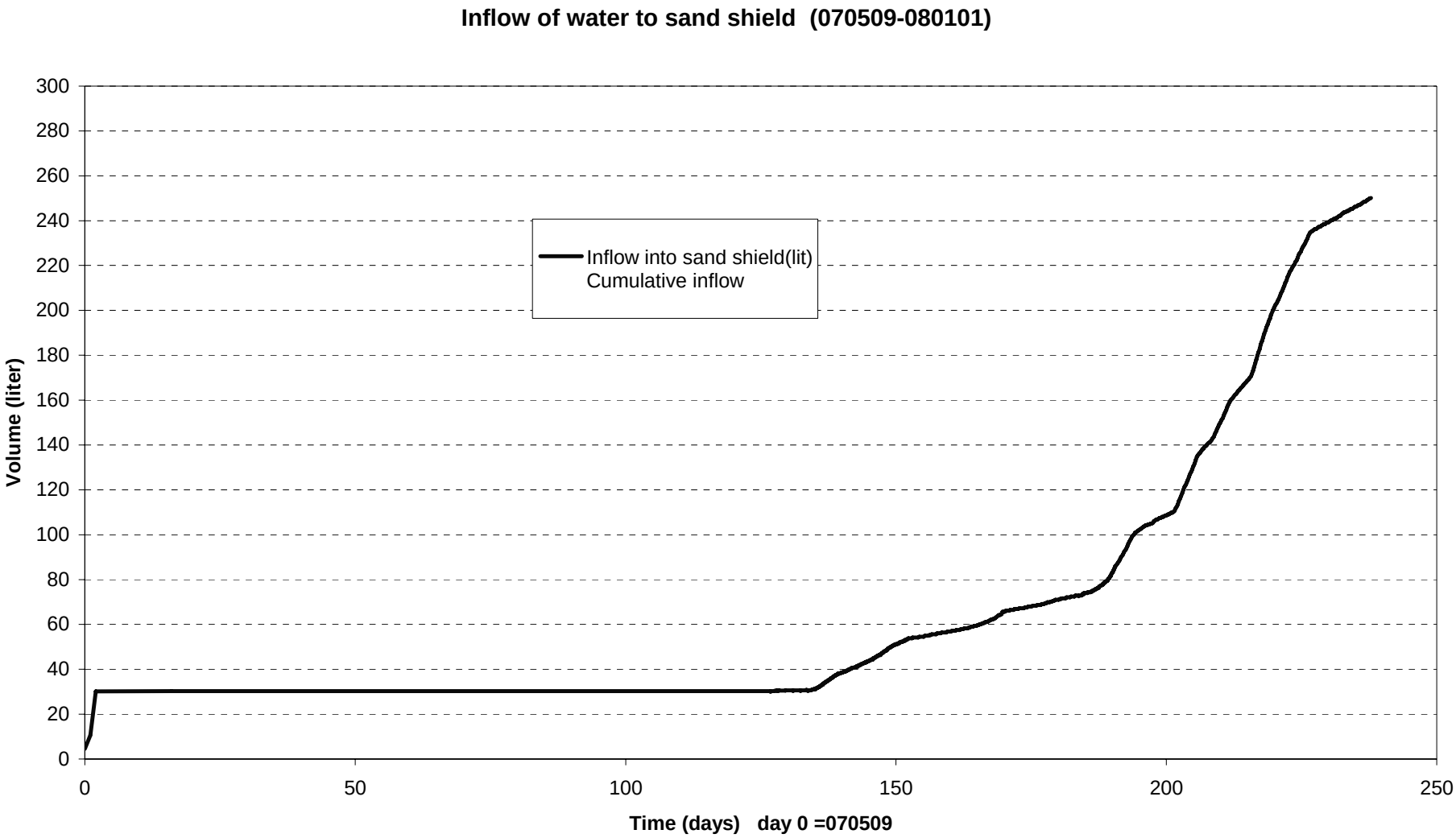
Inflow of water to sand shield (070509-080101)
Volume (liter)
300
280
260
240
220
200
180
160
140
120
100
80
60
40
20
0
0
50
100
150
200
250
Time (days) day 0 =070509
Inflow into sand shield(lit)
Cumulative inflow

Forces on plug (030326-080101)

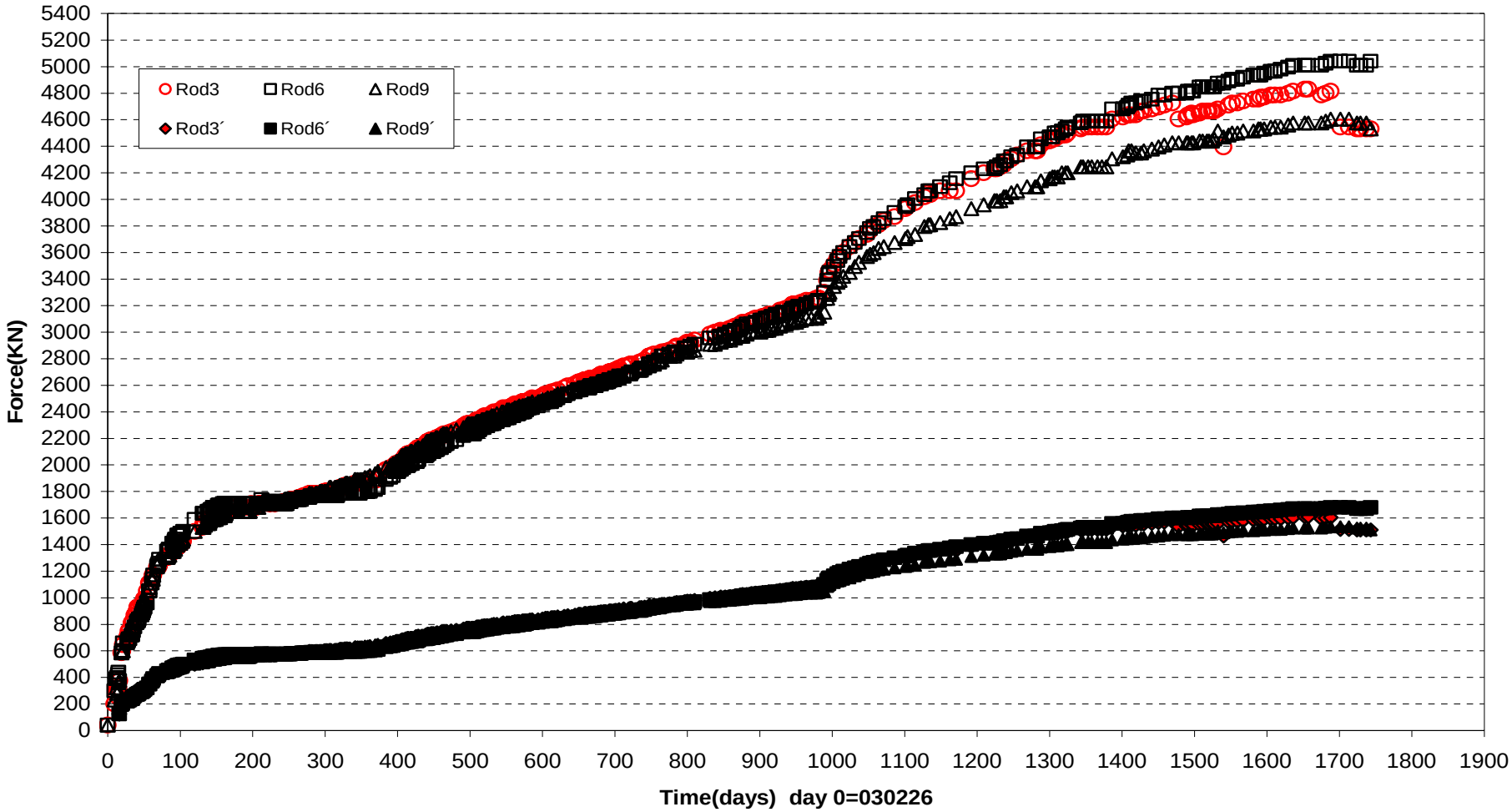

Displacement of plug (030326-080101)

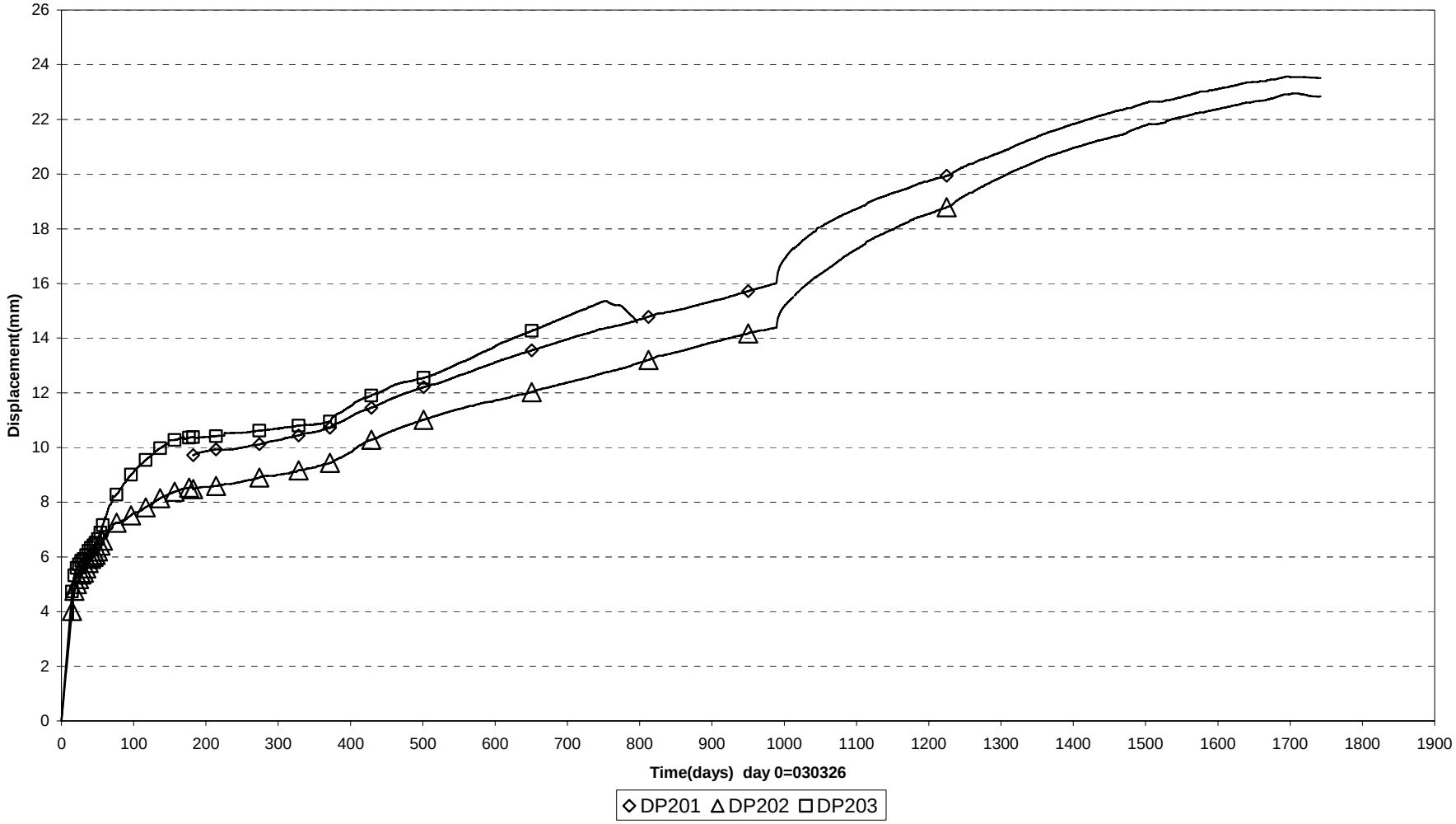

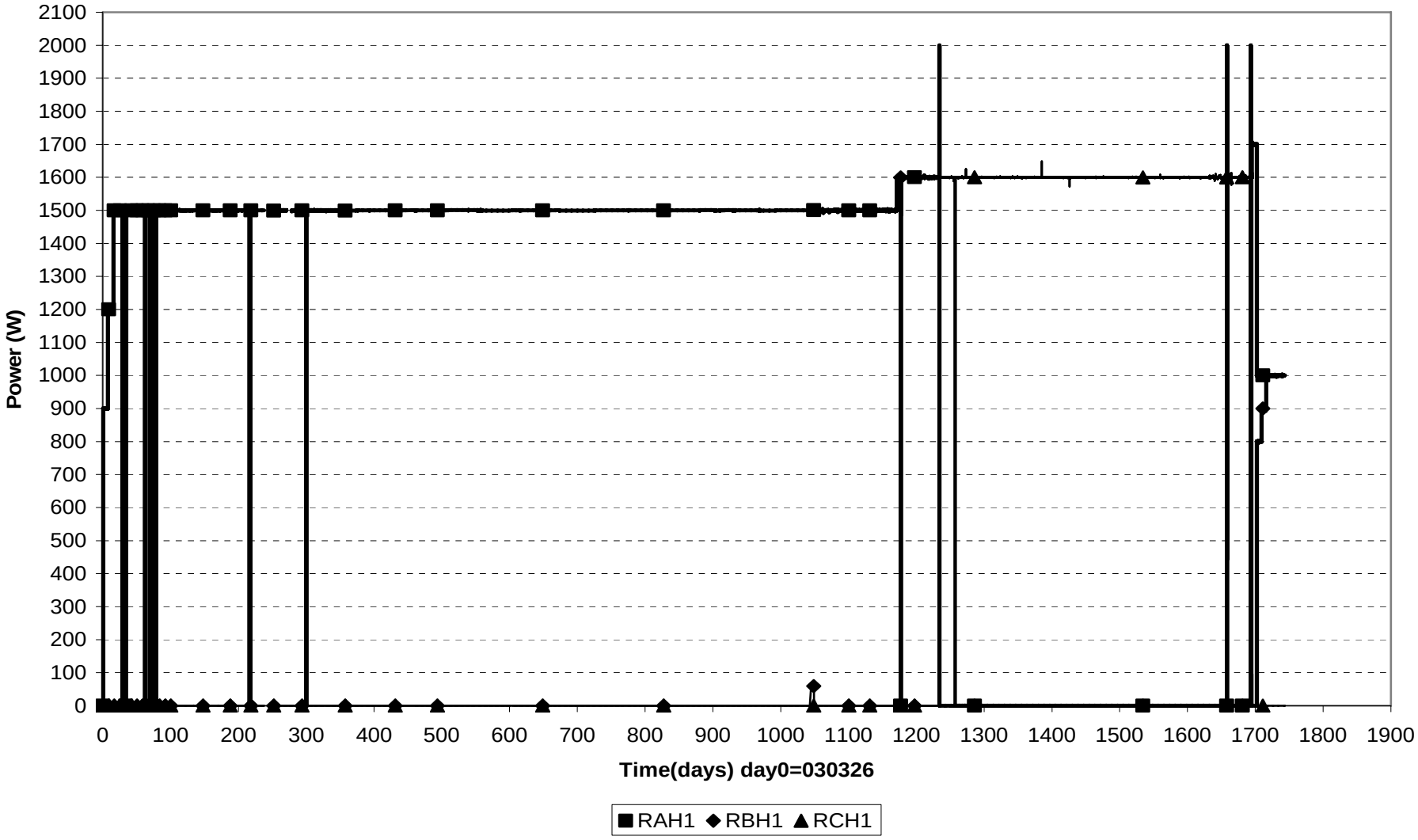
Power Heater 1 (030326-080101)
Power (W)
2100
2000
1900
1800
1700
1600
1500
1400
1300
1200
1100
1000
900
800
700
600
500
400
300
200
100
0
0
100
200
300
400
500
600
700
800
900
1000
1100
1200
1300
1400
1500
1600
1700
1800
1900
Time(days) day0=030326
RAH1
RBH1
RCH1

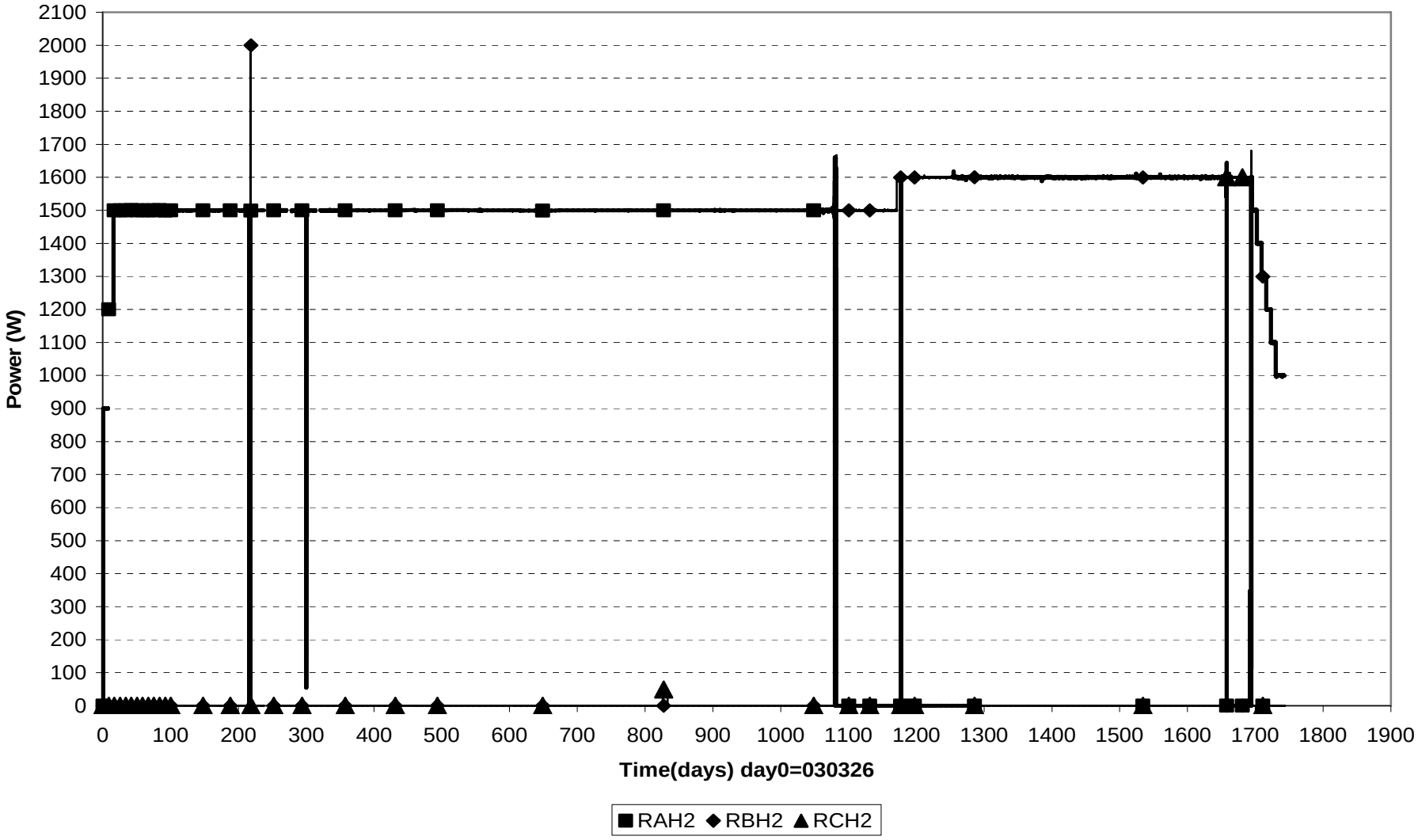
Power Heater 2 (030326-080101)
Power (W)
2100
2000
1900
1800
1700
1600
1500
1400
1300
1200
1100
1000
900
800
700
600
500
400
300
200
100
0
0
100
200
300
400
500
600
700
800
900
1000
1100
1200
1300
1400
1500
1600
1700
1800
1900
Time(days) day0=030326
RAH2
RBH2
RCH2

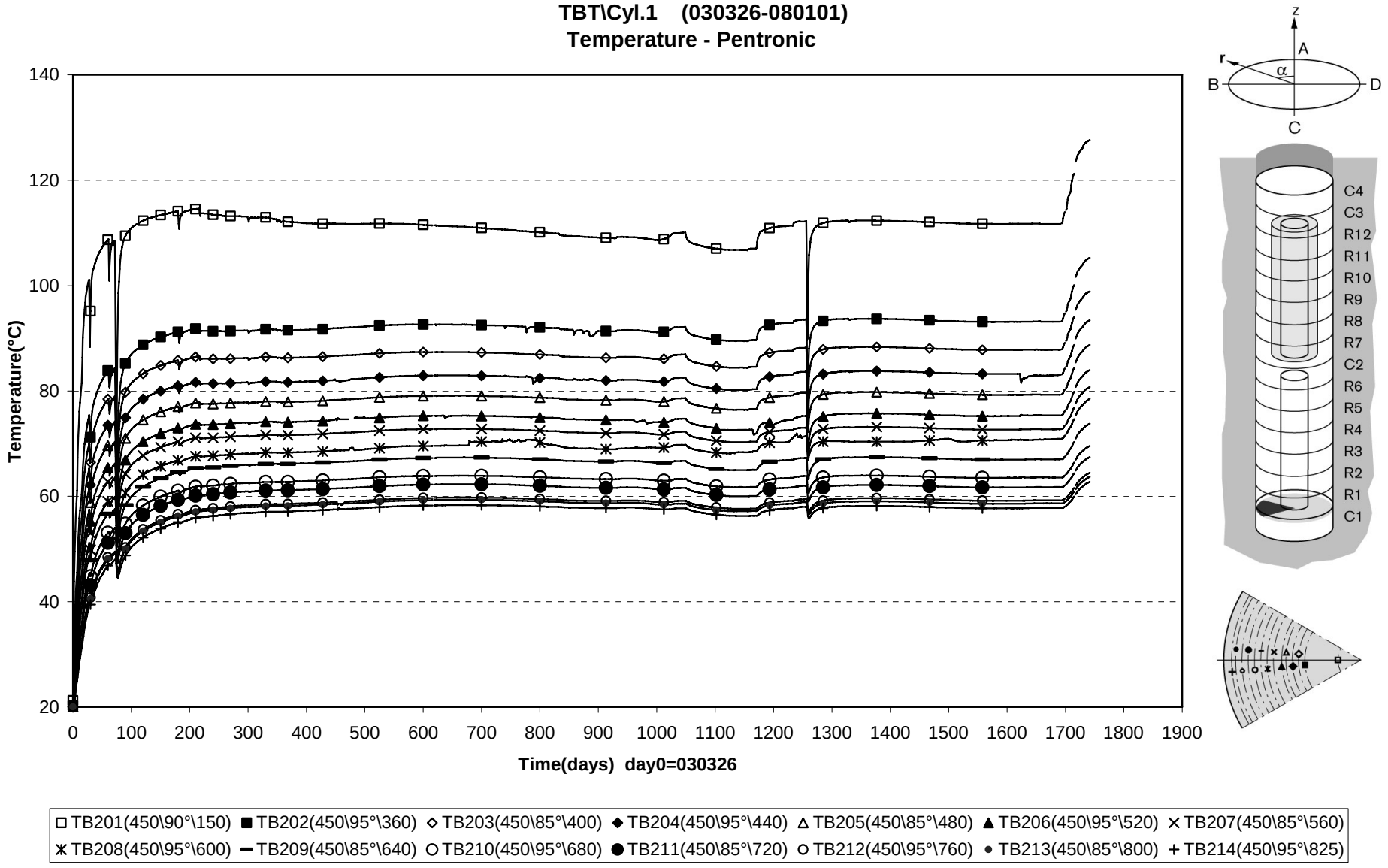
TBT\Cyl.1 (030326-080101)
Temperature - Pentronic
Temperature(°C)
Time(days) day0=030326
140
120
100
80
60
40
20
0
100
200
300
400
500
600
700
800
900
1000
1100
1200
1300
1400
1500
1600
1700
1800
1900
z
A
r
α
B
D
C
C4
C3
R12
R11
R10
R9
R8
R7
C2
R6
R5
R4
R3
R2
R1
C1
TB201(450\90°\150)
TB202(450\95°\360)
TB203(450\85°\400)
TB204(450\95°\440)
TB205(450\85°\480)
TB206(450\95°\520)
TB207(450\85°\560)
TB208(450\95°\600)
TB209(450\85°\640)
TB210(450\95°\680)
TB211(450\85°\720)
TB212(450\95°\760)
TB213(450\85°\800)
TB214(450\95°\825)

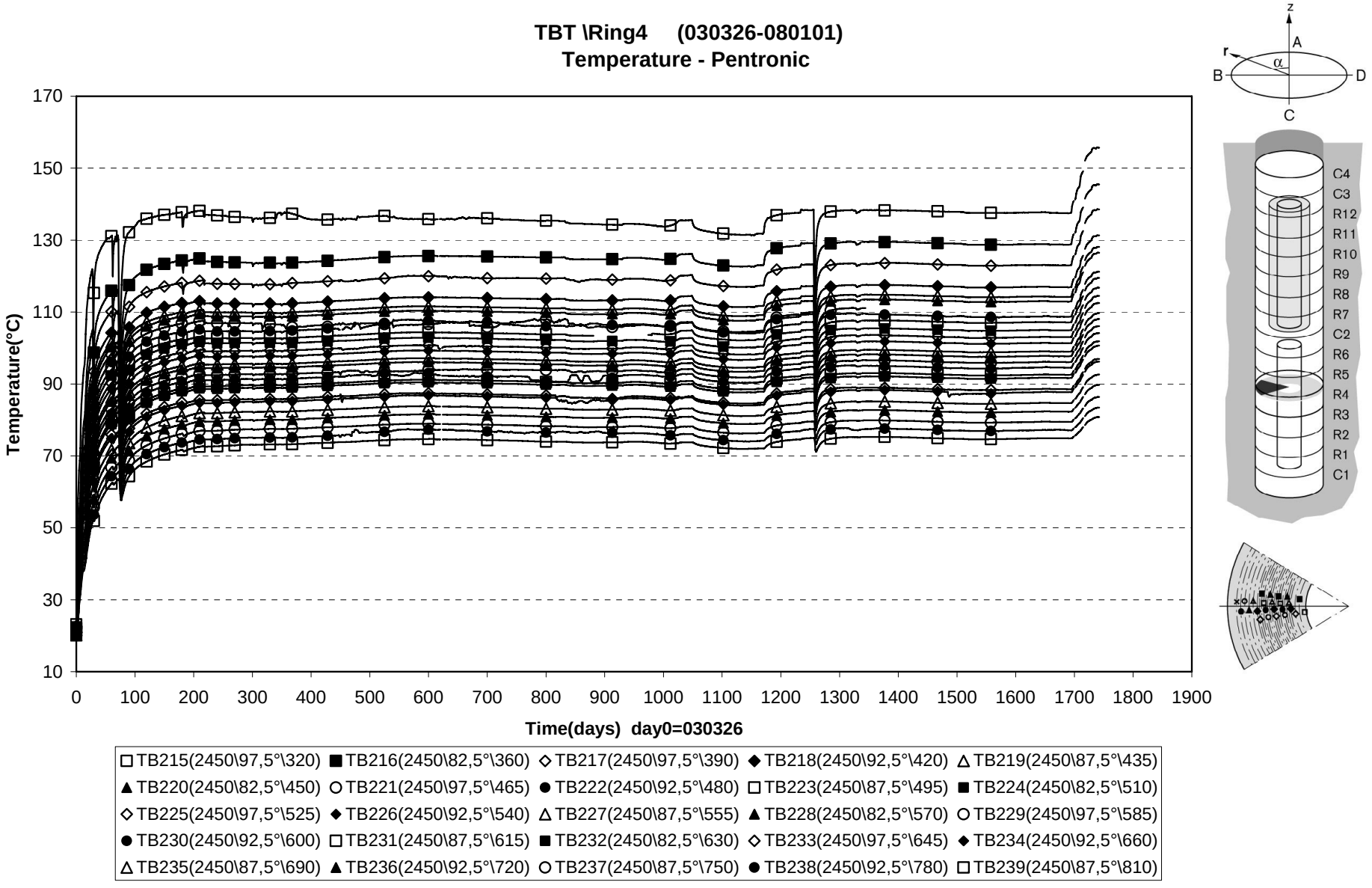
TBT \Ring4 (030326-080101)
Temperature - Pentronic
Temperature(°C)
Time(days) day0=030326
170
150
130
110
90
70
50
30
10
0
100
200
300
400
500
600
700
800
900
1000
1100
1200
1300
1400
1500
1600
1700
1800
1900
z
A
r
α
B
D
C
C4
C3
R12
R11
R10
R9
R8
R7
C2
R6
R5
R4
R3
R2
R1
C1
TB215(2450\97,5°\320) TB216(2450\82,5°\360) TB217(2450\97,5°\390) TB218(2450\92,5°\420) TB219(2450\87,5°\435)
TB220(2450\82,5°\450) TB221(2450\97,5°\465) TB222(2450\92,5°\480) TB223(2450\87,5°\495) TB224(2450\82,5°\510)
TB225(2450\97,5°\525) TB226(2450\92,5°\540) TB227(2450\87,5°\555) TB228(2450\82,5°\570) TB229(2450\97,5°\585)
TB230(2450\92,5°\600) TB231(2450\87,5°\615) TB232(2450\82,5°\630) TB233(2450\97,5°\645) TB234(2450\92,5°\660)
TB235(2450\87,5°\690) TB236(2450\92,5°\720) TB237(2450\87,5°\750) TB238(2450\92,5°\780) TB239(2450\87,5°\810)

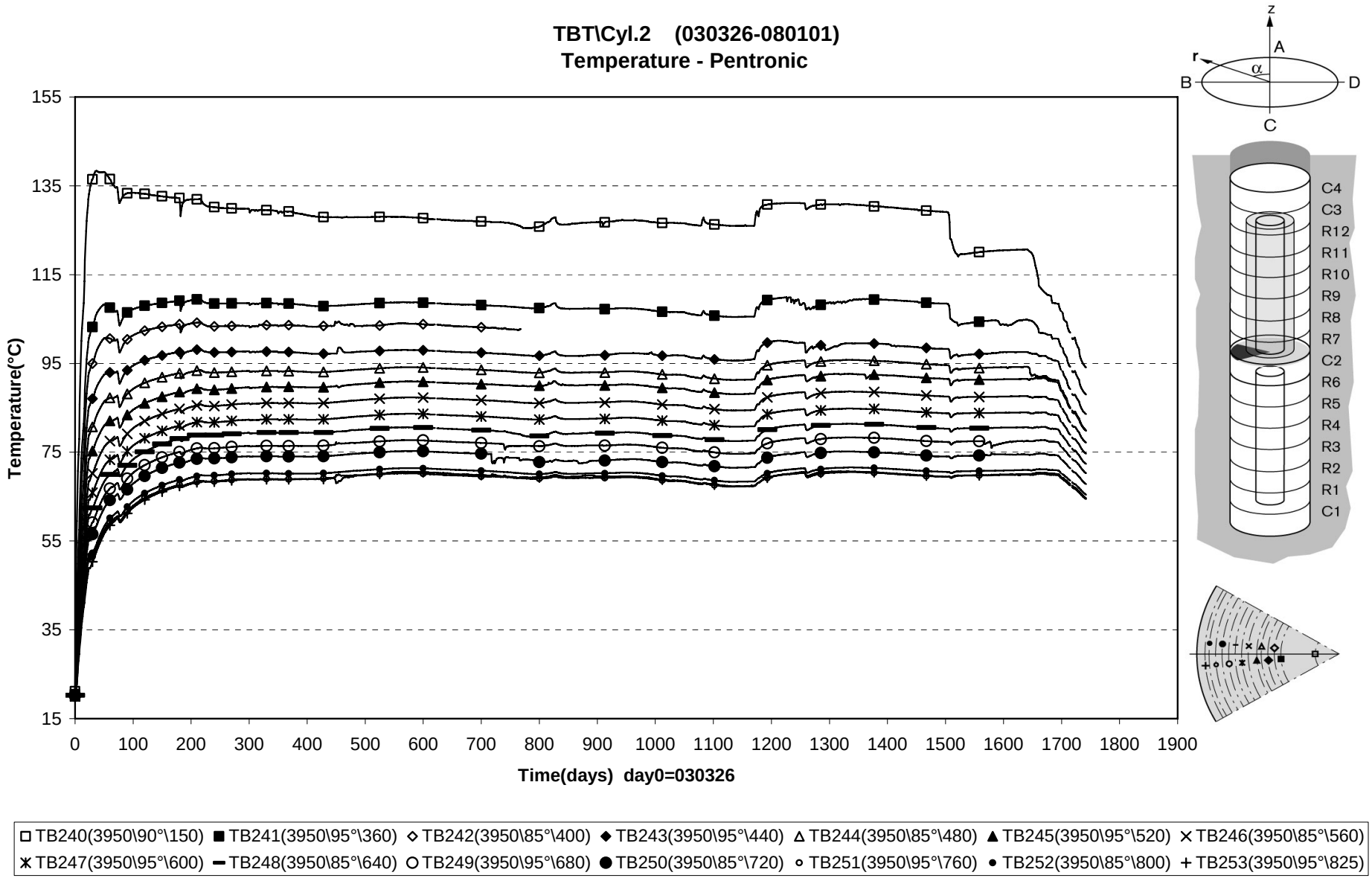
TBT\Cyl.2 (030326-080101)
Temperature - Pentronic
Temperature(°C)
155
135
115
95
75
55
35
15
0
100
200
300
400
500
600
700
800
900
1000
1100
1200
1300
1400
1500
1600
1700
1800
1900
Time(days) day0=030326
z
A
r
α
B
D
C
C4
C3
R12
R11
R10
R9
R8
R7
C2
R6
R5
R4
R3
R2
R1
C1
TB240(3950\90°\150)
TB241(3950\95°\360)
TB242(3950\85°\400)
TB243(3950\95°\440)
TB244(3950\85°\480)
TB245(3950\95°\520)
TB246(3950\85°\560)
TB247(3950\95°\600)
TB248(3950\85°\640)
TB249(3950\95°\680)
TB250(3950\85°\720)
TB251(3950\95°\760)
TB252(3950\85°\800)
TB253(3950\95°\825)

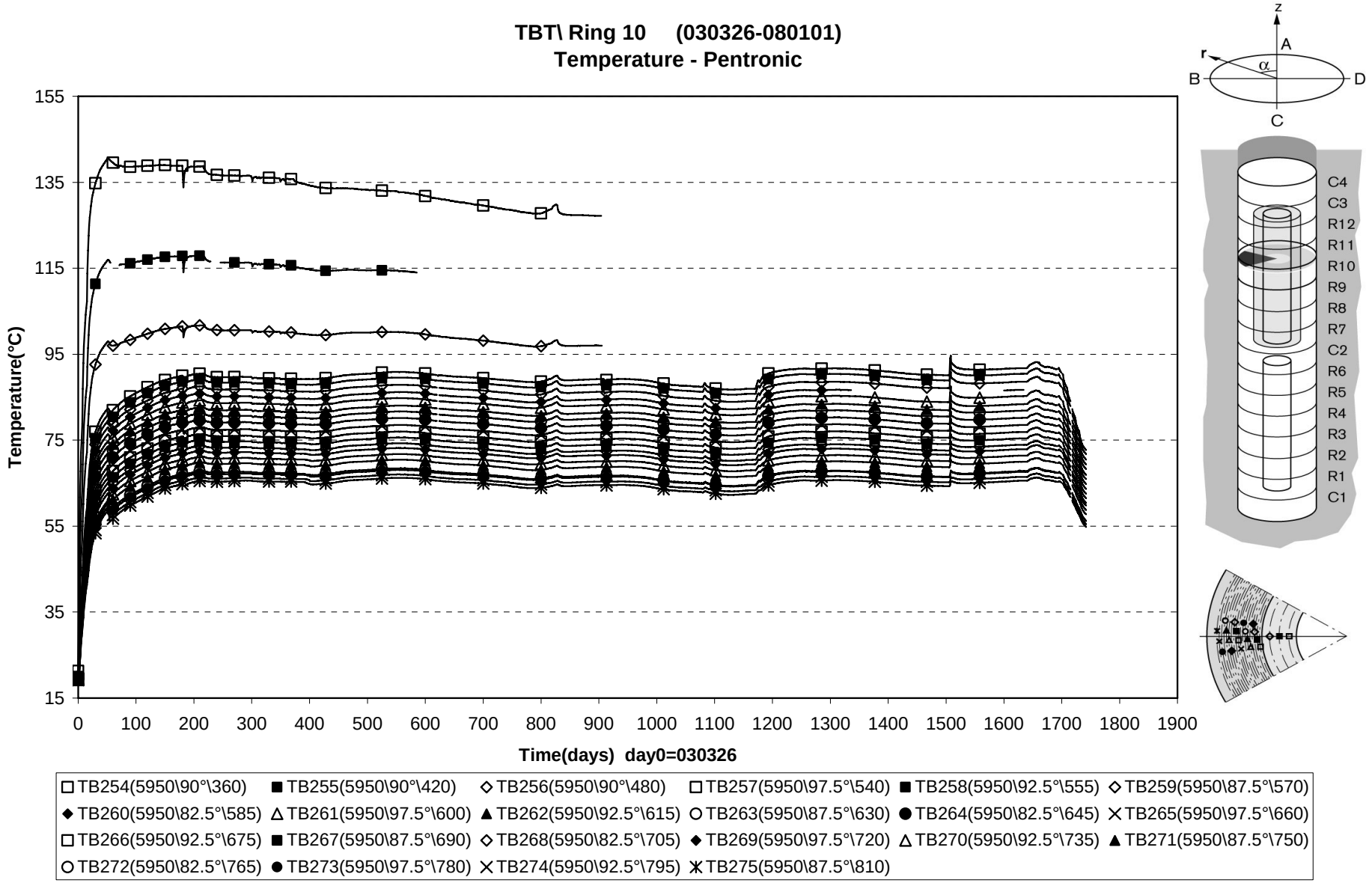
TBT\ Ring 10 (030326-080101)
Temperature - Pentronic
Temperature(°C)
155
135
115
95
75
55
35
15
0 100 200 300 400 500 600 700 800 900 1000 1100 1200 1300 1400 1500 1600 1700 1800 1900
Time(days) day0=030326
z
A
r
α
B
D
C
C4
C3
R12
R11
R10
R9
R8
R7
C2
R6
R5
R4
R3
R2
R1
C1
TB254(5950\90°\360) TB255(5950\90°\420) TB256(5950\90°\480) TB257(5950\97.5°\540) TB258(5950\92.5°\555) TB259(5950\87.5°\570)
TB260(5950\82.5°\585) TB261(5950\97.5°\600) TB262(5950\92.5°\615) TB263(5950\87.5°\630) TB264(5950\82.5°\645) TB265(5950\97.5°\660)
TB266(5950\92.5°\675) TB267(5950\87.5°\690) TB268(5950\82.5°\705) TB269(5950\97.5°\720) TB270(5950\92.5°\735) TB271(5950\87.5°\750)
TB272(5950\82.5°\765) TB273(5950\97.5°\780) TB274(5950\92.5°\795) TB275(5950\87.5°\810)

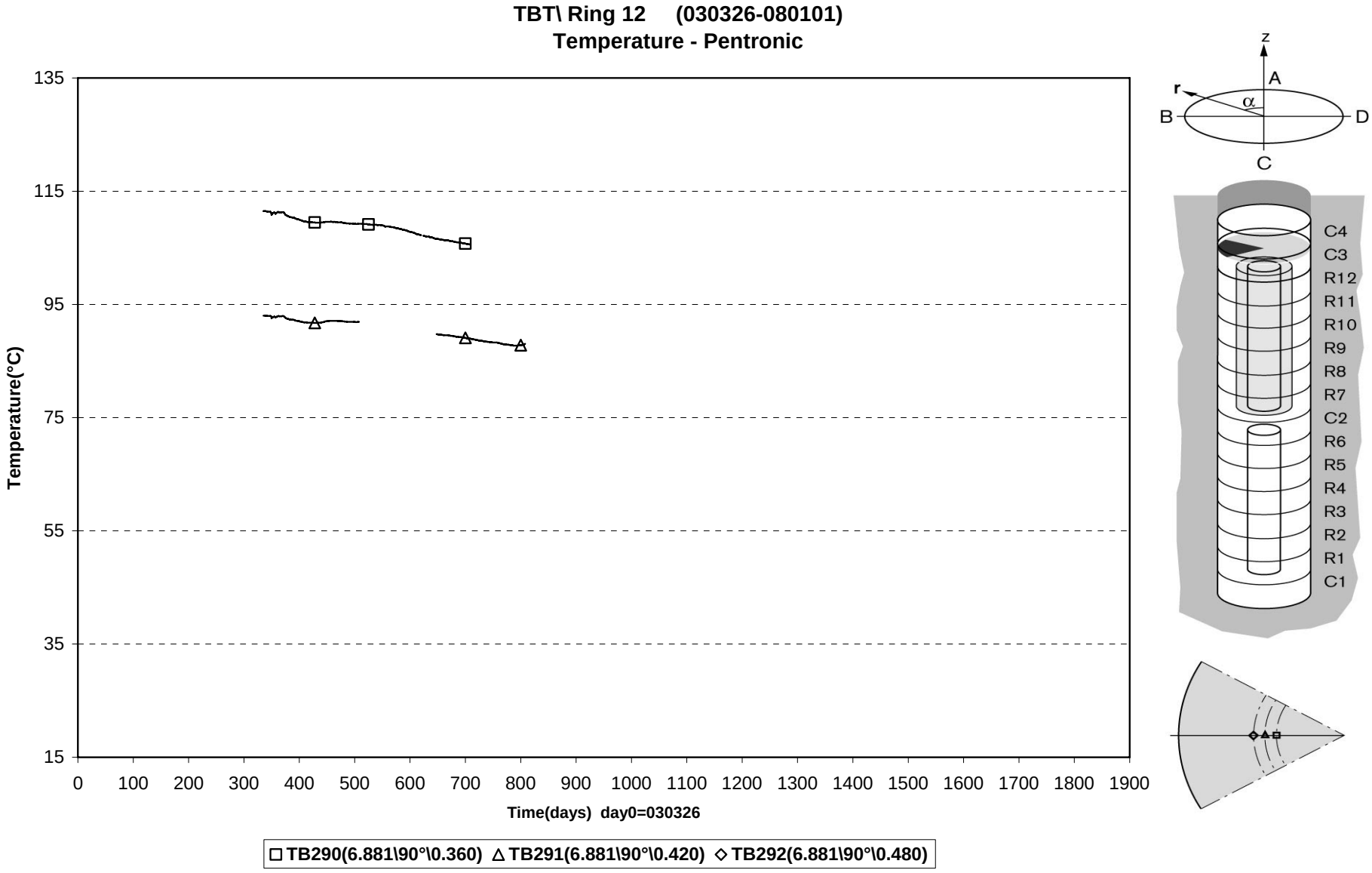
TBT\ Ring 12 (030326-080101)
Temperature - Pentronic
Temperature(°C)
135
115
95
75
55
35
15
0 100 200 300 400 500 600 700 800 900 1000 1100 1200 1300 1400 1500 1600 1700 1800 1900
Time(days) day0=030326
TB290(6.881\90°\0.360) TB291(6.881\90°\0.420) TB292(6.881\90°\0.480)
z
A
r
α
B
D
C
C4
C3
R12
R11
R10
R9
R8
R7
C2
R6
R5
R4
R3
R2
R1
C1

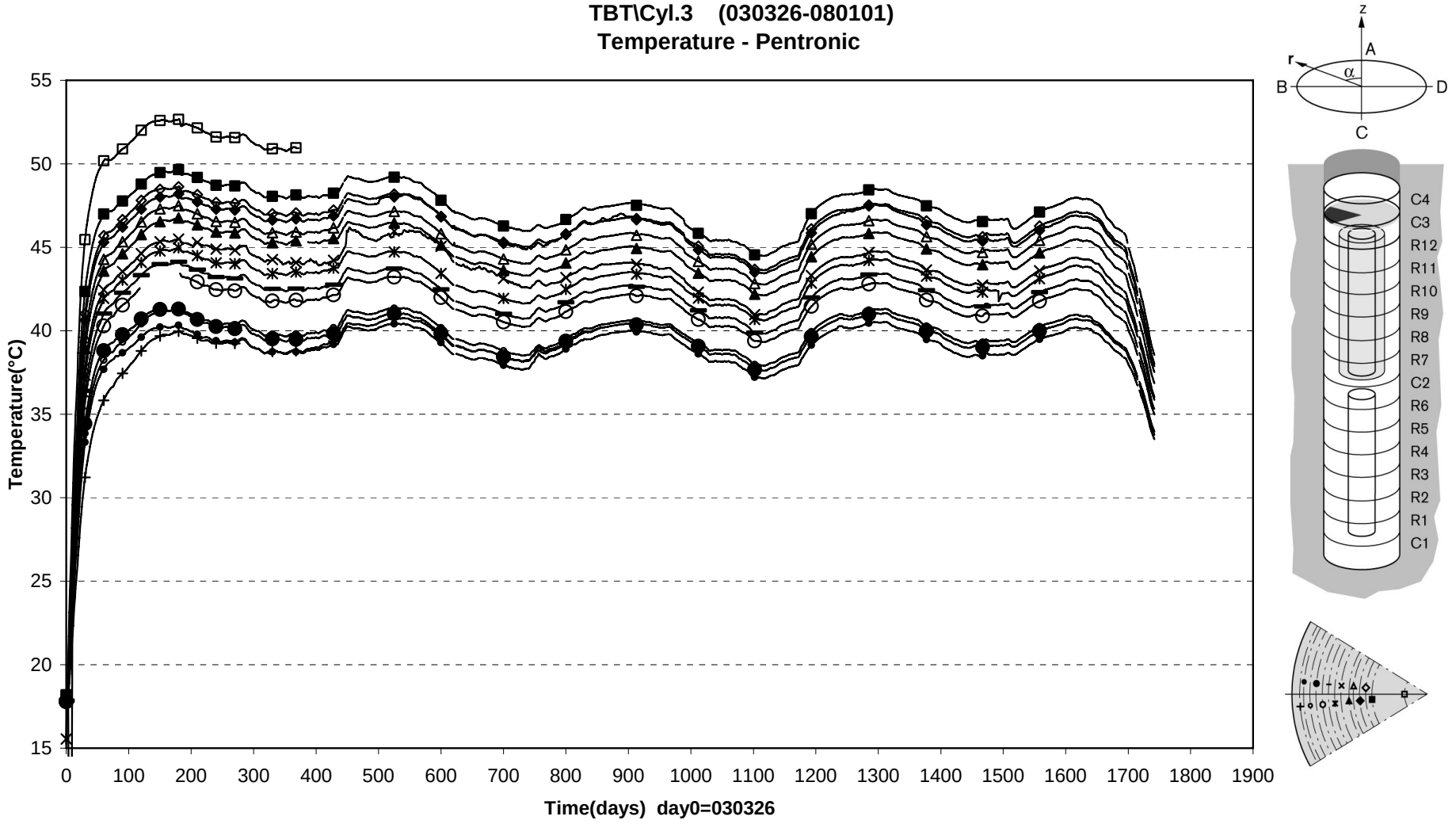
TBT\Cyl.3 (030326-080101)
Temperature - Pentronic
Temperature(°C)
Time(days) day0=030326
55
50
45
40
35
30
25
20
15
0
100
200
300
400
500
600
700
800
900
1000
1100
1200
1300
1400
1500
1600
1700
1800
1900
z
A
r
α
B
D
C
C4
C3
R12
R11
R10
R9
R8
R7
C2
R6
R5
R4
R3
R2
R1
C1
TB276(7450\90°\150)
TB277(7450\95°\360)
TB278(7450\85°\400)
TB279(7450\95°\440)
TB280(7450\85°\480)
TB281(7450\95°\520)
TB282(7450\85°\560)
TB283(7450\95°\600)
TB284(7450\85°\640)
TB285(7450\95°\680)
TB286(7450\85°\720)
TB287(7450\95°\760)
TB288(7450\85°\800)
TB289(7450\95°\825)

TBT\ Temperature in the rock-below the dep.hole (030326-080101)
Temperature - Pentronic

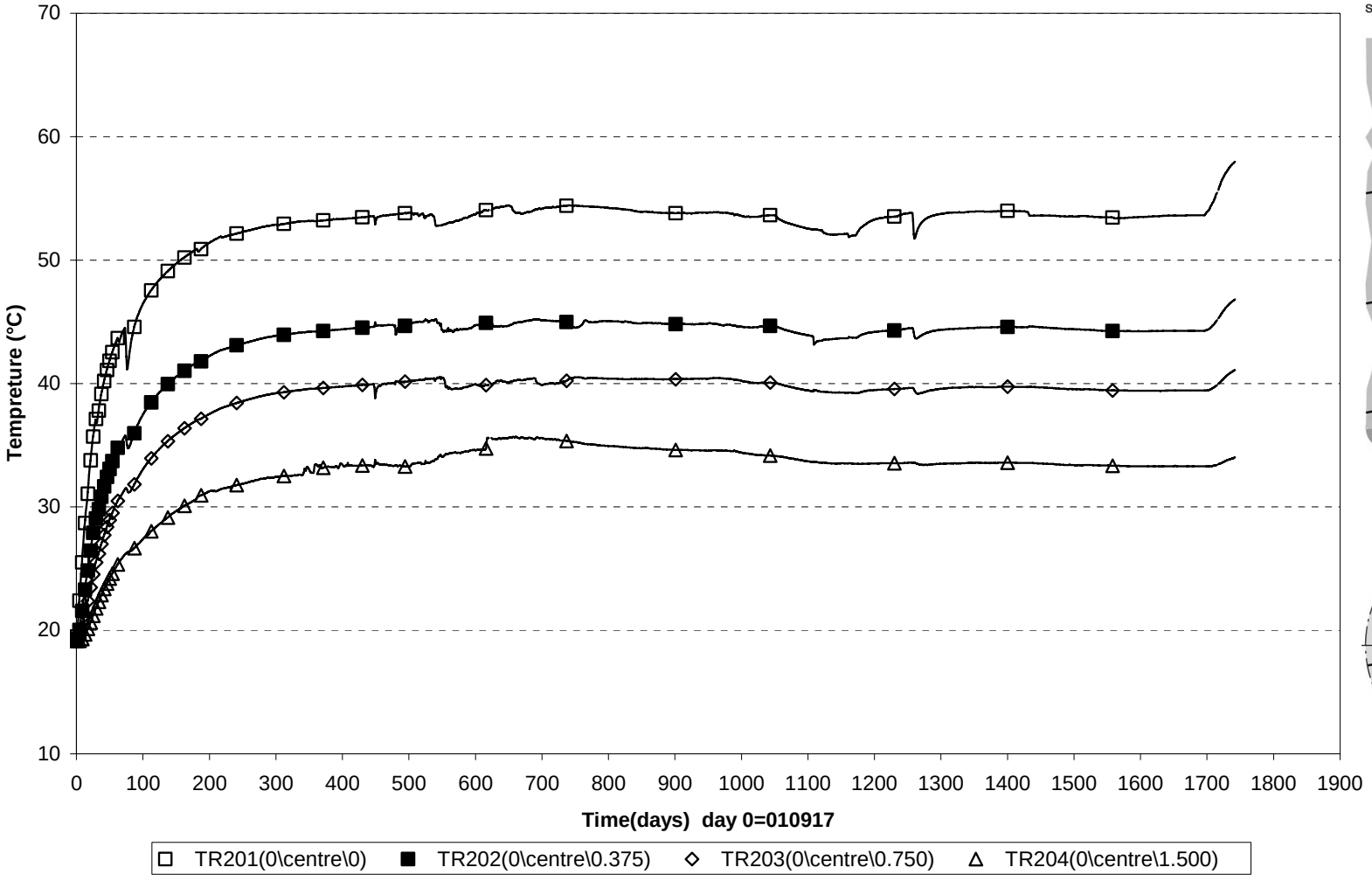

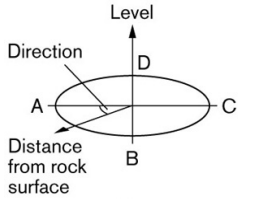

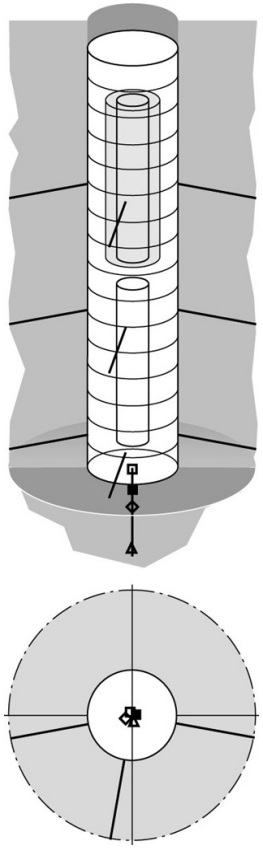

TBT\ Temperature in the rock-level 0,61 m (030326-080101)
Temperature - Pentronic

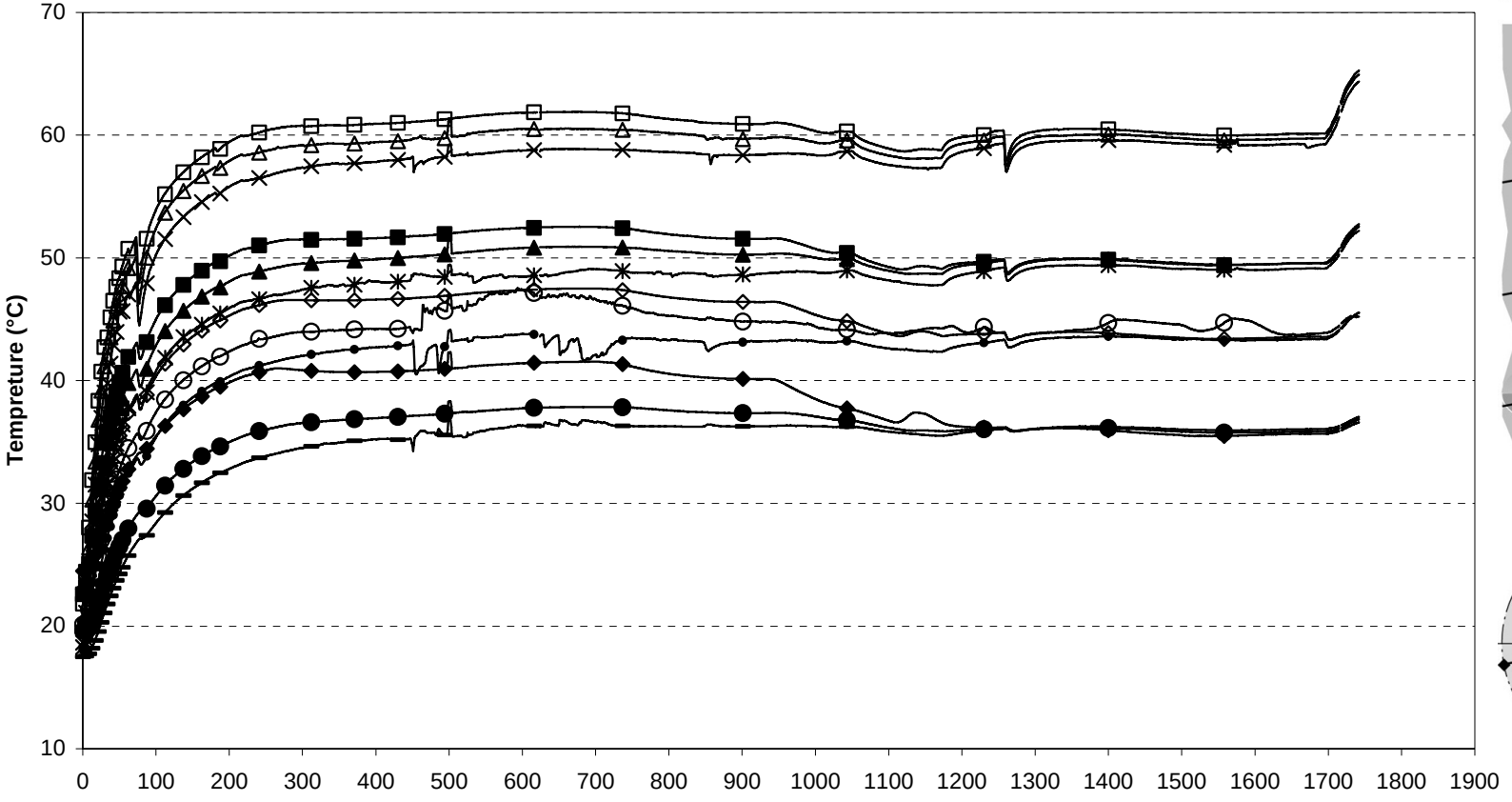

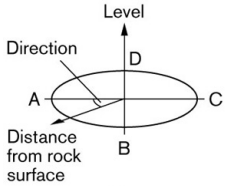

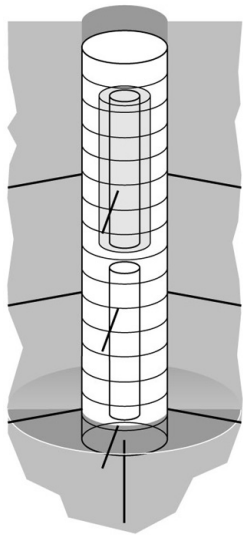

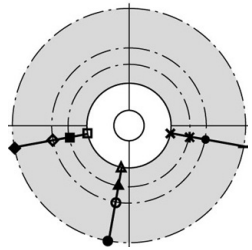

TBT\ Temperature in the rock-level 3,01 m (030326-080101)
Temperature - Pentronic

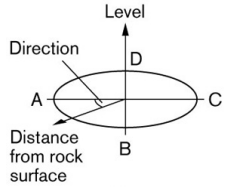

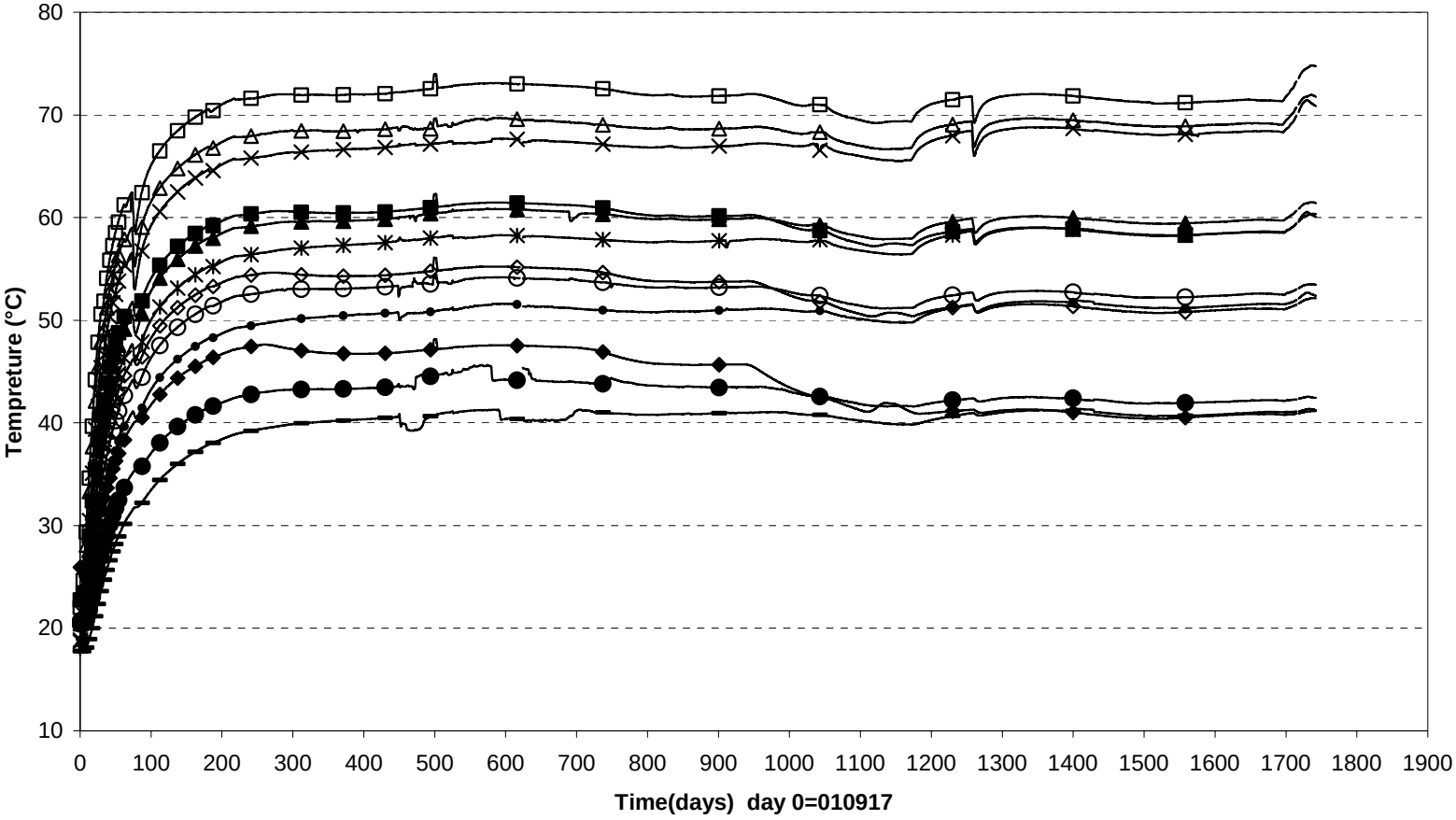

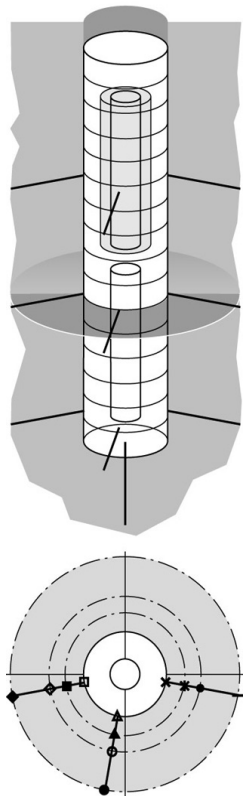

TBT\ Temperature in the rock-level 5,41 m (030326-080101)
Temperature - Pentronic

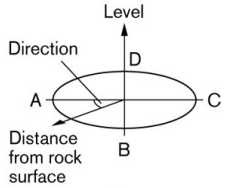

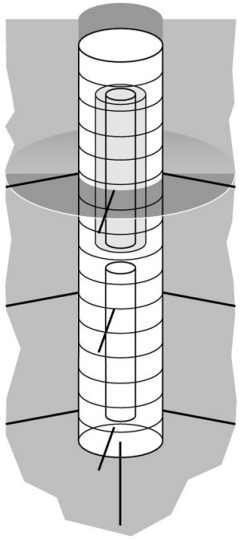

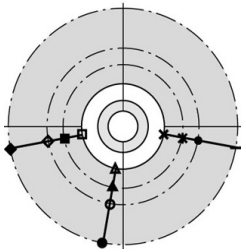

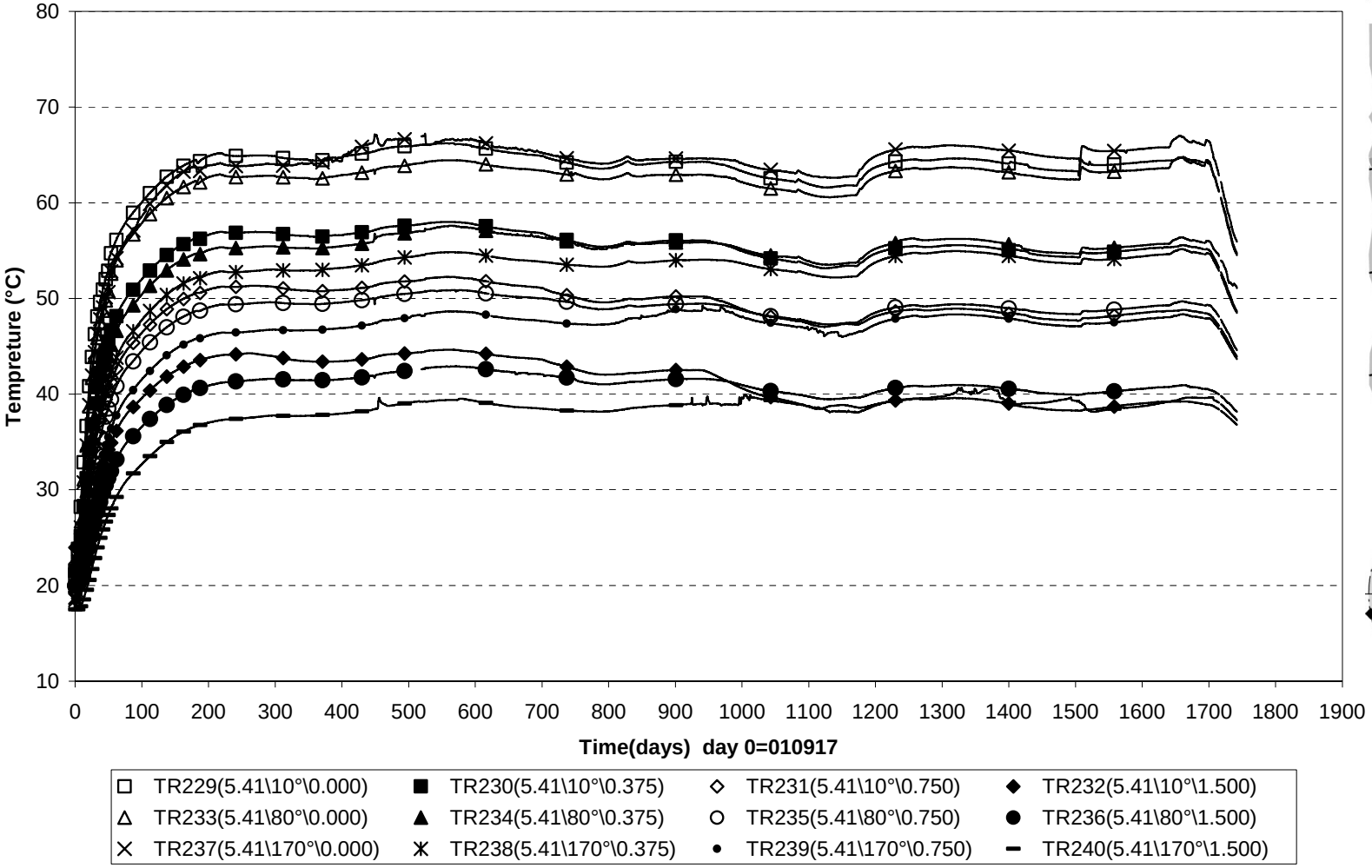

External temperatures Heater 1 (030326-080101)

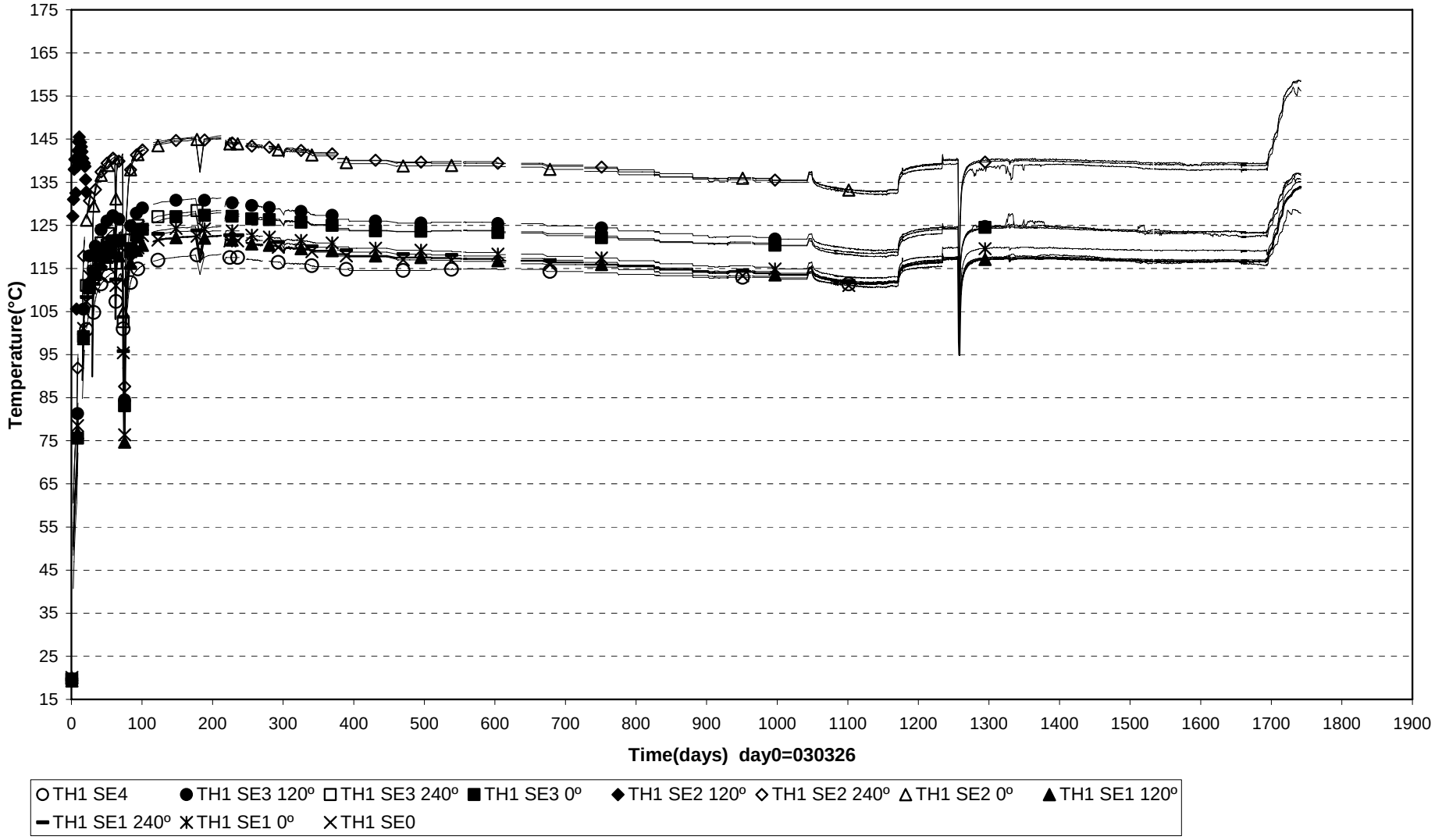

External temperatures Heater 2 (070504-080101)

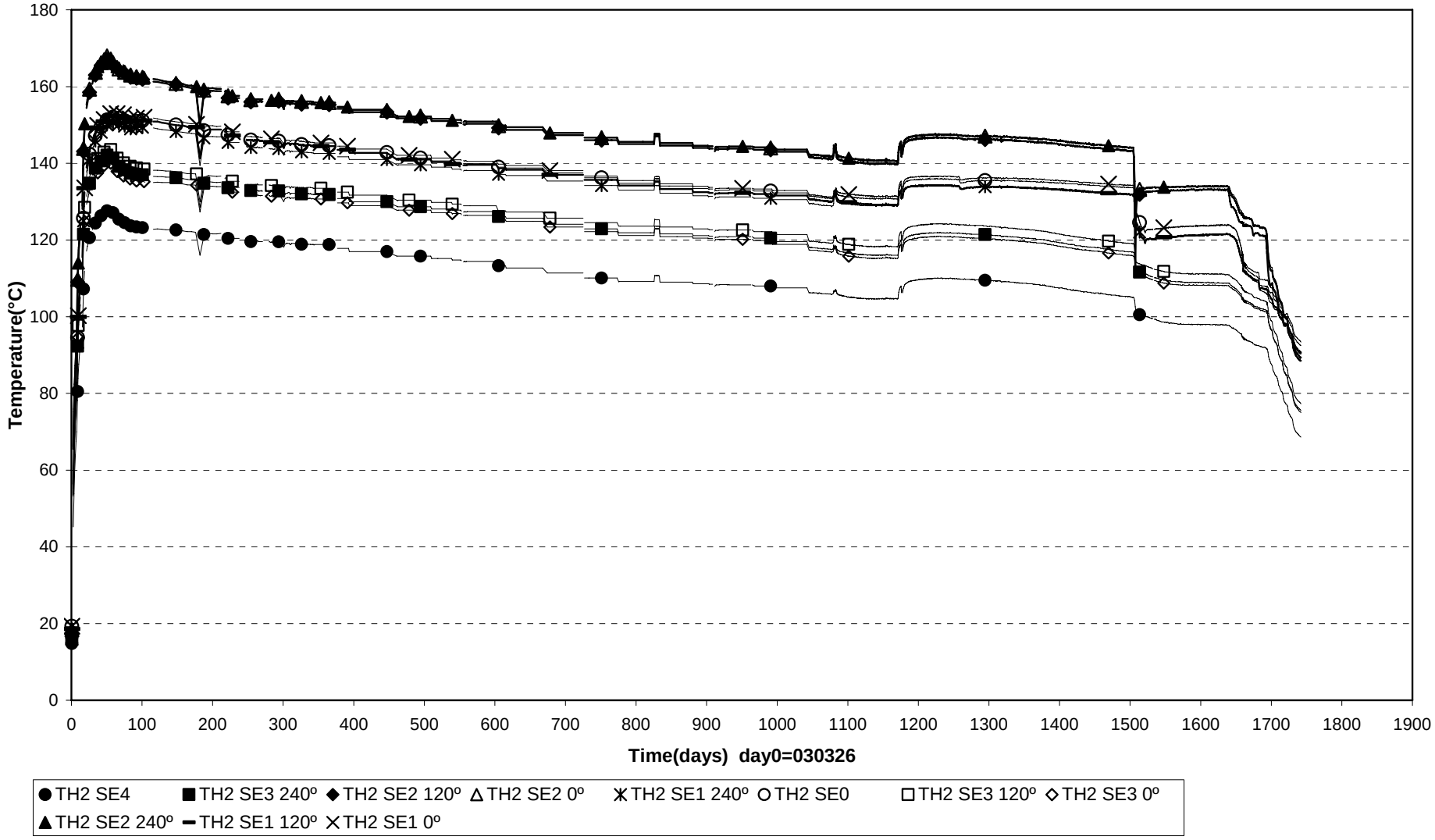

Internal temperatures Heater 1 (030326-080101)

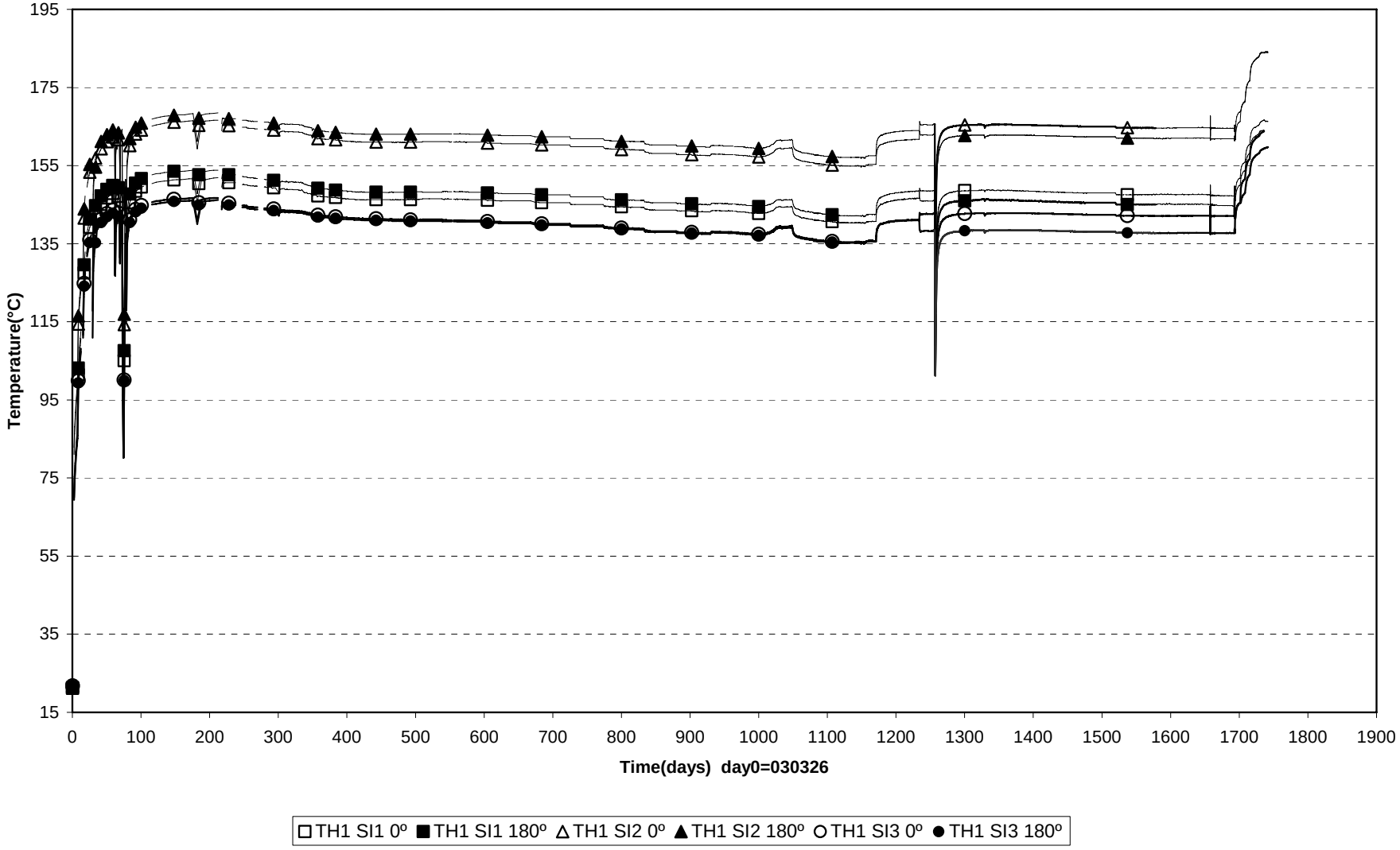

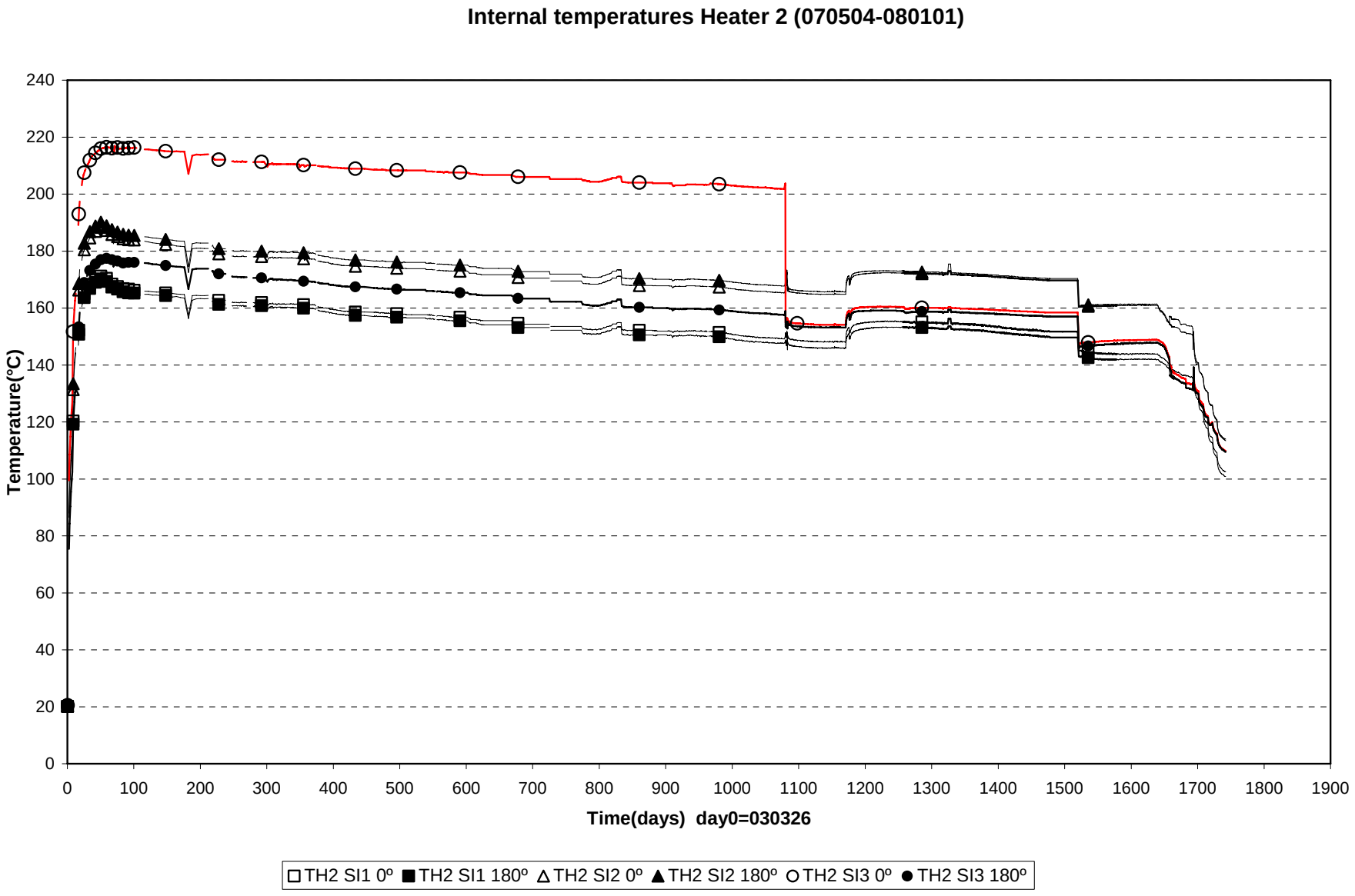
Internal temperatures Heater 2 (070504-080101)
Temperature(°C)
240
220
200
180
160
140
120
100
80
60
40
20
0
0
100
200
300
400
500
600
700
800
900
1000
1100
1200
1300
1400
1500
1600
1700
1800
1900
Time(days) day0=030326
TH2 SI1 0º
TH2 SI1 180º
TH2 SI2 0º
TH2 SI2 180º
TH2 SI3 0º
TH2 SI3 180º

Appendix B

Measurement from optiska sensors

DBE.Technology

Fiber Optic sensors in TBT

The high temperatures and the corrosive environment yield extreme requirements on the sensor material. Never before fiber optic sensors from DBE have been implemented under these conditions and thus a few optical pressure and temperature sensors have been installed for evaluation purposes.

Two pressure sensors and two pore water pressure sensors have been installed each including a low resolution temperature grating for compensation purposes. Figure 1 and 2 show the location of each sensor in addition to all the other sensors.

Data from PB231 has presented in this report .The other three sensors are out of order.

Table 1. Numbering and position of the instruments referred to in this report.

Instrument number	Measuring section	Block	α [deg]	r [mm]	z [mm]	Remark
PB204	2	Ring3	250	420	1950	Total pressure radial
PB205	2	Ring 3	290	420	2000	Total pressure axial
PB206	2	Ring 3	0	535	1950	Total pressure radial
PB207	2	Ring 3	20	535	1950	Total pressure tangential
PB208	2	Ring 3	45	585	2000	Total pressure axial
PB209	2	Ring 3	100	635	1950	Total pressure tangential
PB210	2	Ring 3	170	710	1950	Total pressure tangential
PB211	2	Ring3	180	710	1950	Total pressure radial
PB212	2	Ring 3	260	770	2000	Total pressure axial
PB213	2	Ring 3	270	875	1950	Total pressure radial on the rock
PB230a	**2**	**Ring 3**	**180**	**376**	**1950**	**Fiber Optic total pressure radial**
PB230b	**2**	**Ring 3**	**180**	**428**	**950**	**Fiber Optic temperature**
PB217	5	Ring 9	270	535	5450	Total pressure radial against sand
PB218	5	Ring 9	340	635	5500	Total pressure axial
PB219	5	Ring 9	0	635	5450	Total pressure radial
PB220	5	Ring 9	20	635	5450	Total pressure tangential
PB221	5	Ring 9	70	710	5500	Total pressure axial
PB222	5	Ring 9	110	710	5450	Total pressure radial
PB223	5	Ring 9	160	770	5500	Total pressure axial
PB 224	5	Ring 9	180	770	5450	Total pressure radial
PB225	5	Ring 9	200	770	5450	Total pressure tangential
PB226	5	Ring 9	270	875	5450	Total pressure radial on the rock
PB231a	**5**	**Ring 9**	**180**	**573**	**5450**	**Fiber Optic total pressure radial**
PB231b	**5**	**Ring 9**	**180**	**608**	**5450**	**Fiber Optic temperature**

Instrument number	**Measuring section**	**Block**	**α [deg]**	**r [mm]**	**z [mm]**	**Remark**
UB201	2	Ring 3	270	420	1750	Pore pressure
UB202	2	Ring 3	350	535	1750	Pore pressure
UB203	2	Ring 3	90	635	1750	Pore pressure
UB204	2	Ring 3	280	785	1750	Pore pressure
UB209a	**2**	**Ring 3**	**190**	**495**	**1750**	**Fiber Optic pore pressure**
UB209b	**2**	**Ring 3**	**190**	**555**	**1750**	**Fiber Optic temperature**
UB205	5	Ring 9	270	420	5250	Pore pressure
UB206	5	Ring 9	315	635	5250	Pore pressure
UB207	5	Ring 9	90	710	5250	Pore pressure
UB208	5	Ring 9	225	785	5250	Pore pressure
UB210	**5**	**Ring 9**	**160**	**420**	**5250**	**Fiber Optic pore pressure and temp.**
TB215	3	Ring 4	97.5	320	2450	Pentronic thermocouple thermometer
TB216	3	Ring 4	82.5	360	2450	Pentronic thermocouple thermometer
TB217	3	Ring 4	97.5	390	2450	Pentronic thermocouple thermometer
TB218	3	Ring 4	92.5	420	2450	Pentronic thermocouple thermometer
TB222	3	Ring 4	92.5	480	2450	Pentronic thermocouple thermometer
TB229	3	Ring 4	97.5	585	2450	Pentronic thermocouple thermometer
TB235	3	Ring 4	87.5	690	2450	Pentronic thermocouple thermometer
TB239	3	Ring 4	87.5	810	2450	Pentronic thermocouple thermometer
TB254	6	Ring 10	90	360	5950	Pentronic thermocouple thermometer
TB255	6	Ring 10	90	420	5950	Pentronic thermocouple thermometer
TB256	6	Ring 10	90	480	5950	Pentronic thermocouple thermometer
TB260	6	Ring 10	82.5	585	5950	Pentronic thermocouple thermometer
TB267	6	Ring 10	87.5	690	5950	Pentronic thermocouple thermometer
TB275	6	Ring 10	87.5	810	5950	Pentronic thermocouple thermometer

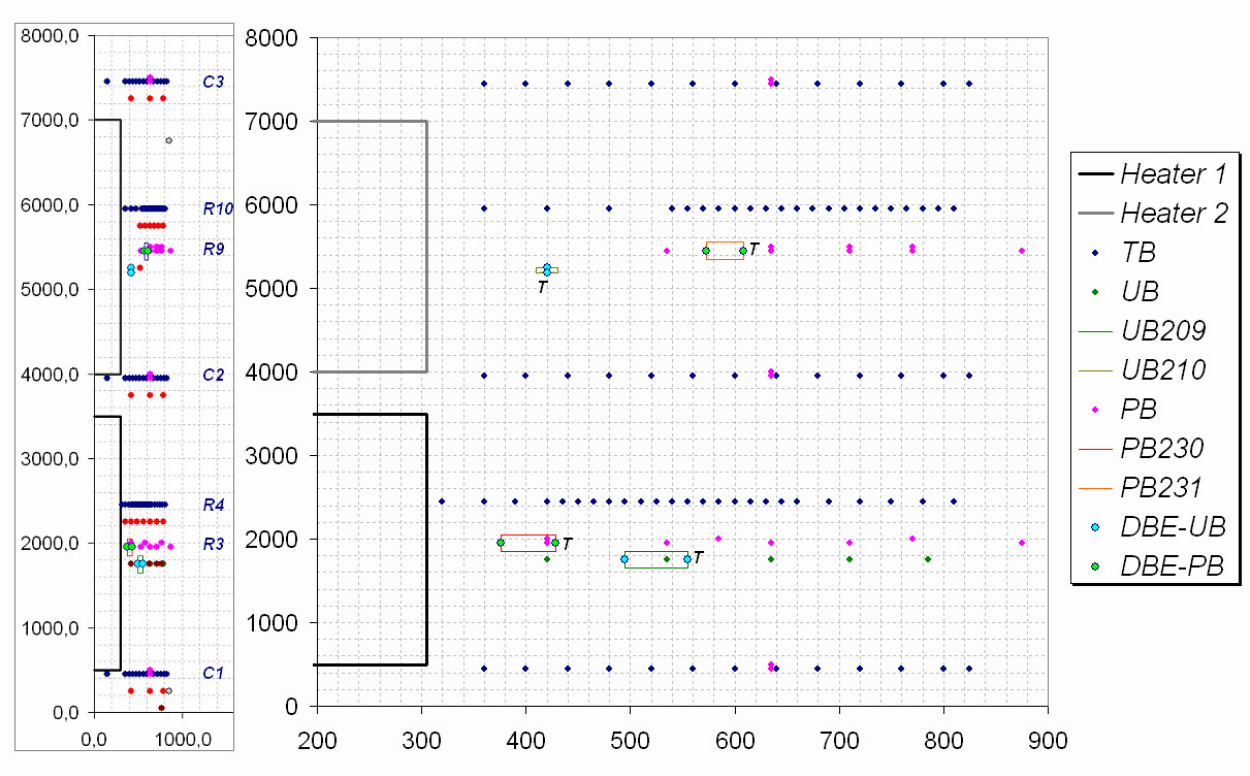

Fig. 1. *Vertical location and radial distance of each sensor in mm.*

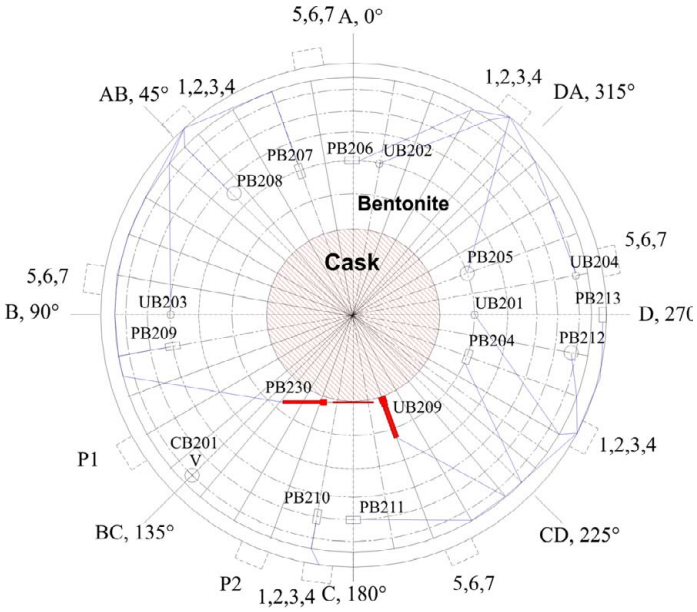

Fig. 2a. *Radial location of sensors in Ring 3 horizontal cross-sections of the lower canister.*

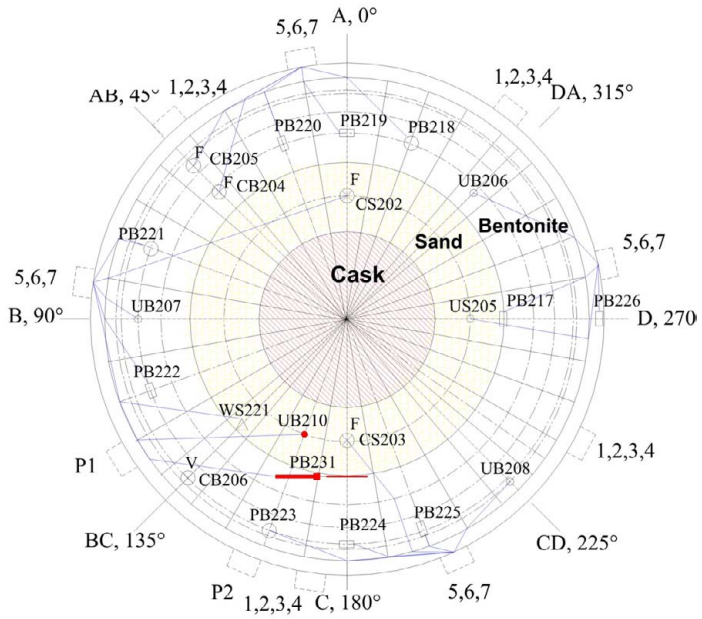

Fig. 2b. *Radial location of sensors in Ring 9 horizontal cross-sections of the upper canister.*

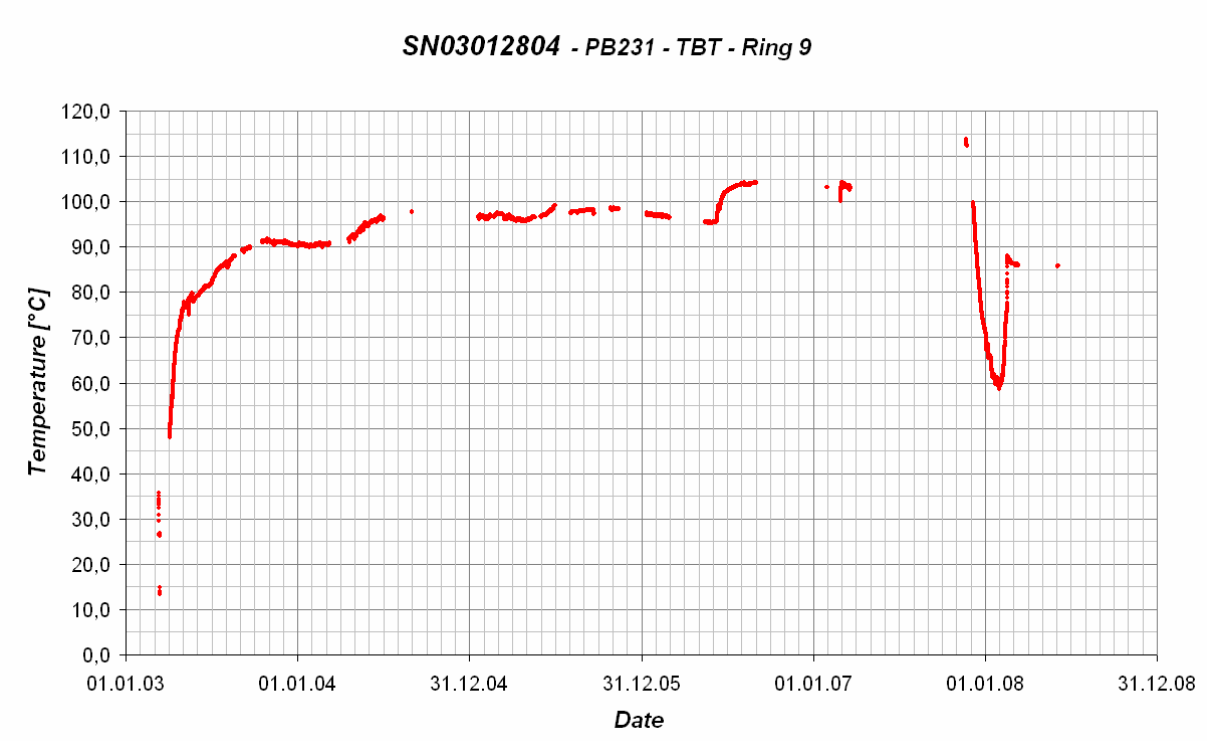

Data update of FO-sensor PB231 (the other three sensors failed)

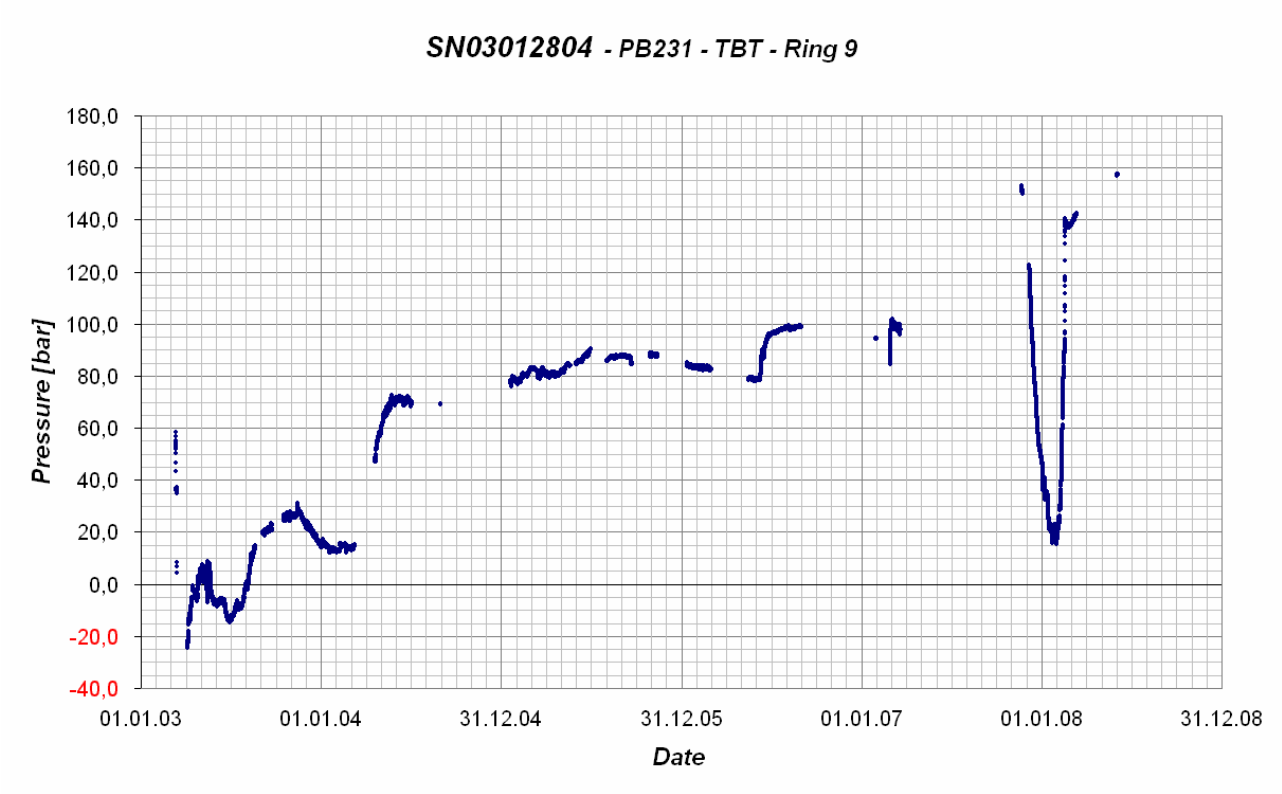
SN03012804 - PB231 - TBT - Ring 9
Pressure [bar]
180,0
160,0
140,0
120,0
100,0
80,0
60,0
40,0
20,0
0,0
-20,0
-40,0
01.01.03
01.01.04
31.12.04
31.12.05
01.01.07
01.01.08
31.12.08
Date